Multigrid Hirsch-Fye quantum Monte Carlo method for dynamical mean-field theory

Nils Blümer, Univ. Mainz

Outline

Introduction: Hubbard model, DMFT, HF-QMC

Unbiased Green functions and spectra from HF-QMC

Multigrid Hirsch-Fye quantum Monte Carlo algorithm

Spectral weight transfer at the Mott transition

Breakdown of a Fermi liquid

Summary and outlook

Introduction

Hubbard model

(i) Single band: $\hat{H} = \sum_{(i,j),\sigma} t_{ij} \, (\hat{c}^{\dagger}_{i\sigma} \hat{c}_{j\sigma} + \text{h.c.}) + U \sum_{i} \hat{n}_{i\uparrow} \hat{n}_{i\downarrow}$

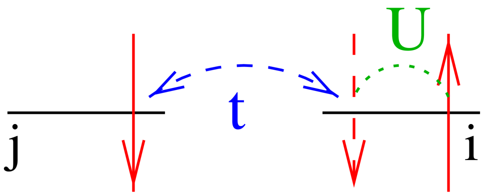

Captures important strong-correlation phenomena: Mott metal-insulator transition, (anti-) ferromagnetism, heavy fermions, high-T_c superconductivity (?), . . .

Few parameters: interaction U/W, temperature T/W, filling n, dispersion $\epsilon_{\boldsymbol{k}}$

Introduction

Hubbard model

(i) Single band: $\hat{H} = \sum_{(i,j),\sigma} t_{ij} (\hat{c}^\dagger_{i\sigma} \hat{c}_{j\sigma} + \text{h.c.}) + U \sum_i \hat{n}_{i\uparrow} \hat{n}_{i\downarrow}$

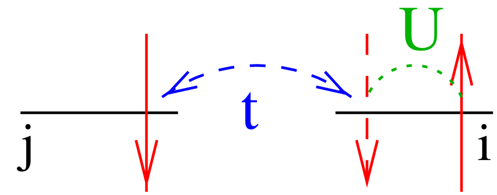

Captures important strong-correlation phenomena: Mott metal-insulator transition, (anti-) ferromagnetism, heavy fermions, high-T_c superconductivity (?), . . .

Few parameters: interaction U/W, temperature T/W, filling n, dispersion $\epsilon_{\boldsymbol{k}}$

(ii) Multi-band model, e.g., 2-band model with inequivalent bands:

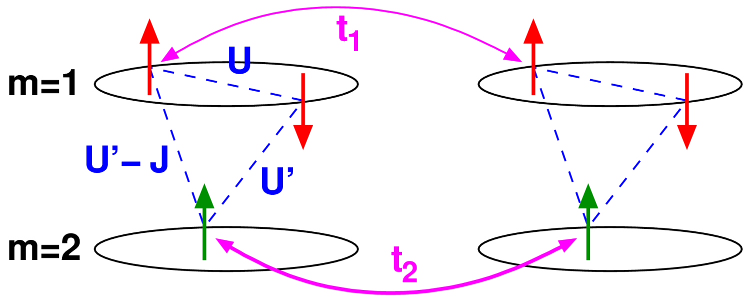

Introduction

Hubbard model

(i) Single band: $\hat{H} = \sum_{(i,j),\sigma} t_{ij} \, (\hat{c}^\dagger_{i\sigma} \hat{c}_{j\sigma} + \text{h.c.}) + U \sum_i \hat{n}_{i\uparrow} \hat{n}_{i\downarrow}$

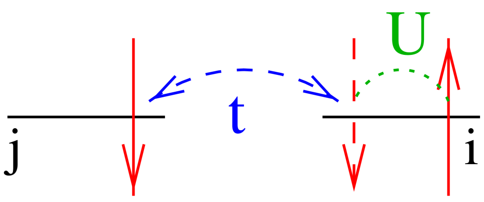

Captures important strong-correlation phenomena: Mott metal-insulator transition, (anti-) ferromagnetism, heavy fermions, high-T_c superconductivity (?), . . .

Few parameters: interaction U/W, temperature T/W, filling n, dispersion $\epsilon_{\boldsymbol{k}}$

(ii) Multi-band model, e.g., 2-band model with inequivalent bands:

$$
\begin{aligned}
H \; = \; & \sum_{m=1}^{2} \Big[- \sum_{\langle ij \rangle \sigma} t_m \, c^\dagger_{im\sigma} c_{jm\sigma} + U \sum_i n_{im\uparrow} n_{im\downarrow} \Big] \\
+ \; & \sum\nolimits_{i\sigma\sigma'} (U' - \delta_{\sigma\sigma'} J_z) \, n_{i1\sigma} \, n_{i2\sigma'} \\
+ \; & \tfrac{1}{2} J_\perp \sum\nolimits_{i\sigma} \Big[c^\dagger_{i1\sigma} \Big(c^\dagger_{i2\bar{\sigma}} c_{i1\bar{\sigma}} + c^\dagger_{i1\bar{\sigma}} c_{i2\bar{\sigma}} \Big) c_{i2\sigma} + \text{h.c.} \Big]
\end{aligned}
$$

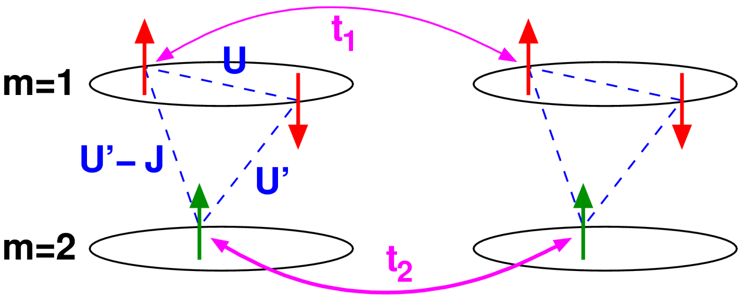

Introduction

Hubbard model

(i) Single band: $\hat{H} = \sum_{(i,j),\sigma} t_{ij} (\hat{c}^\dagger_{i\sigma} \hat{c}_{j\sigma} + \text{h.c.}) + U \sum_i \hat{n}_{i\uparrow} \hat{n}_{i\downarrow}$

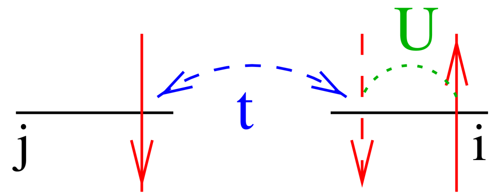

Captures important strong-correlation phenomena: Mott metal-insulator transition, (anti-) ferromagnetism, heavy fermions, high-T_c superconductivity (?), . . .

Few parameters: interaction U/W, temperature T/W, filling n, dispersion $\epsilon_{\boldsymbol{k}}$

(ii) Multi-band model, e.g., 2-band model with inequivalent bands:

$$H = \sum_{m=1}^{2} \Big[- \sum_{\langle ij \rangle \sigma} t_m c^\dagger_{im\sigma} c_{jm\sigma} + U \sum_i n_{im\uparrow} n_{im\downarrow} \Big] + \sum_{i\sigma\sigma'} (U' - \delta_{\sigma\sigma'} J_z)\, n_{i1\sigma}\, n_{i2\sigma'} + \tfrac{1}{2} J_\perp \sum_{i\sigma} \Big[c^\dagger_{i1\sigma} \Big(c^\dagger_{i2\bar{\sigma}} c_{i1\bar{\sigma}} + c^\dagger_{i1\bar{\sigma}} c_{i2\bar{\sigma}} \Big) c_{i2\sigma} + \text{h.c.} \Big]$$

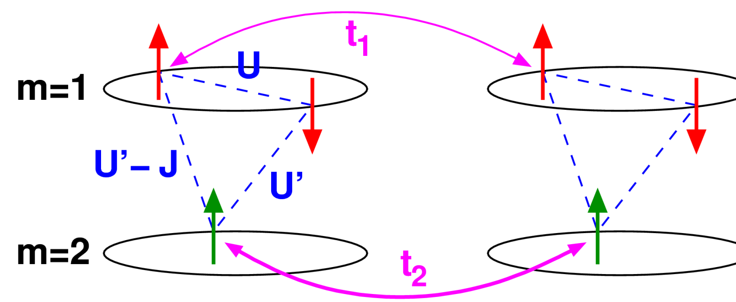

More complexity, more realistic: OSMT, spin+orbital order, LDA+DMFT, . . .

Approaches for Hubbard-type models

$$\hat{H} = \sum_{(i,j),\sigma} t_{ij}\,(\hat{c}^{\dagger}_{i\sigma}\hat{c}_{j\sigma} + \text{h.c.}) + U \sum_{i} \hat{n}_{i\uparrow}\hat{n}_{i\downarrow}$$

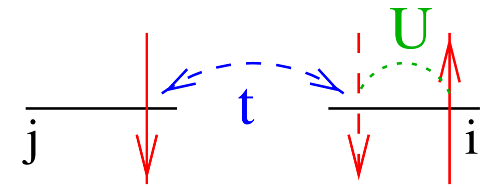

Perturbation theory

- $U \longrightarrow 0$: Hartree-Fock
  2nd order PT, . . .
- $t/U \longrightarrow 0$ (for $n = 1$)
  $\rightsquigarrow$ Heisenberg model

finite clusters: ED, QMC

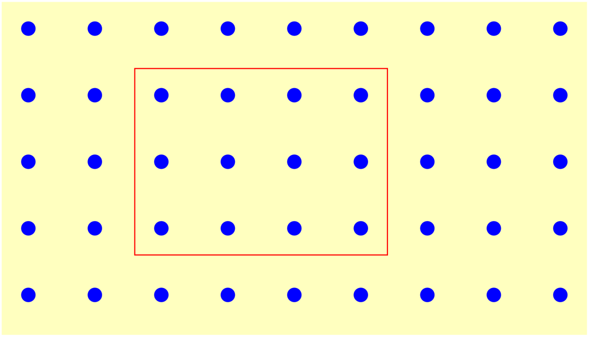

$d \longrightarrow 1$: Bethe ansatz, DMRG

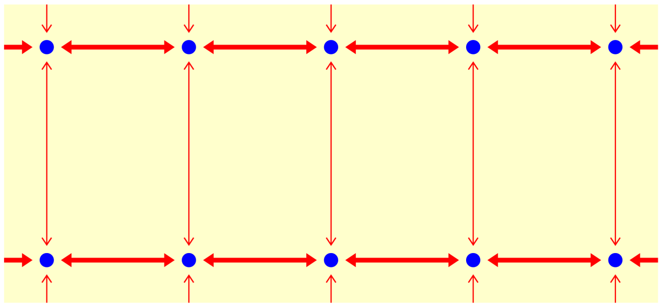

Approaches for Hubbard-type models

$$\hat{H} = \sum_{(i,j),\sigma} t_{ij} \, (\hat{c}^{\dagger}_{i\sigma} \hat{c}_{j\sigma} + \text{h.c.}) + U \sum_{i} \hat{n}_{i\uparrow} \hat{n}_{i\downarrow}$$

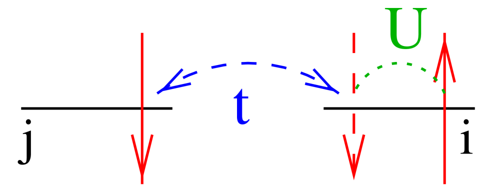

Perturbation theory

- $U \longrightarrow 0$: Hartree-Fock
  2nd order PT, . . .
- $t/U \longrightarrow 0$ (for $n = 1$)
  $\rightsquigarrow$ Heisenberg model

finite clusters: ED, QMC

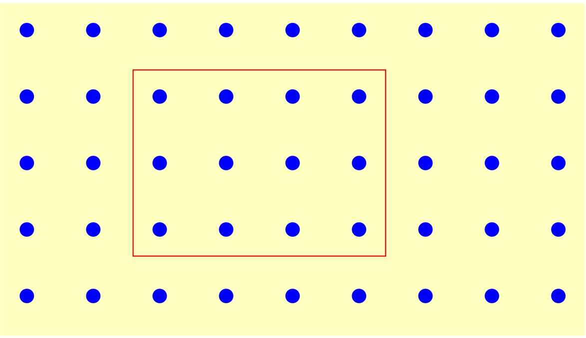

$d \rightarrow 1$: Bethe ansatz, DMRG

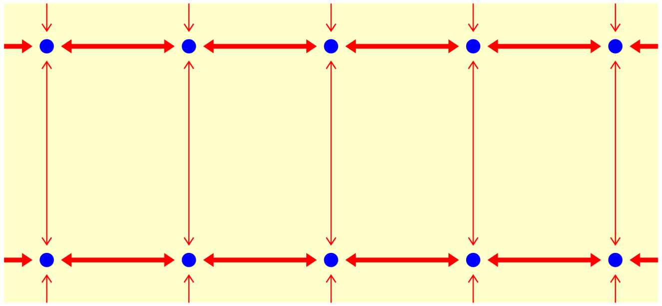

Dynamical mean-field theory (DMFT): local self-energy $\Sigma(\boldsymbol{k}, \omega) \equiv \Sigma(\omega)$

[Metzner, Vollhardt, PRL (1989), Georges, Kotliar, PRL (1992), Jarrell, PRL (1992)]

+	non-perturbative $\rightsquigarrow$ valid at MIT
+	dynamical on-site correlations preserved
+	in thermodynamic limit
+/−	exact for coordination $Z \rightarrow \infty$

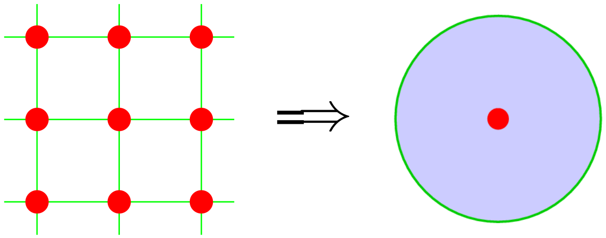

Iterative solution of DMFT equations

0. Initialize self-energy
1. Solve Dyson equation
2. Solve single impurity Anderson model (SIAM)

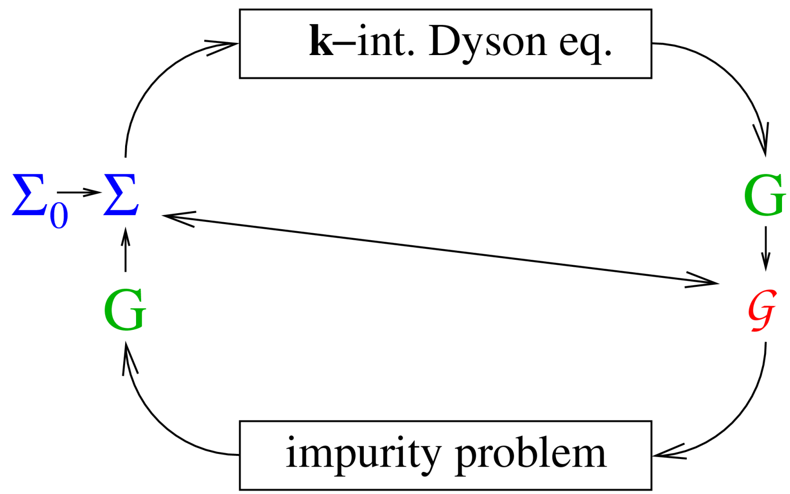

$\longleftarrow$ DOS / t_{ij} / $\varepsilon_{\nu\boldsymbol{k}}$

$\longleftarrow$ local interactions

Iterative solution of DMFT equations

0. Initialize self-energy
1. Solve Dyson equation
2. Solve single impurity Anderson model (SIAM)

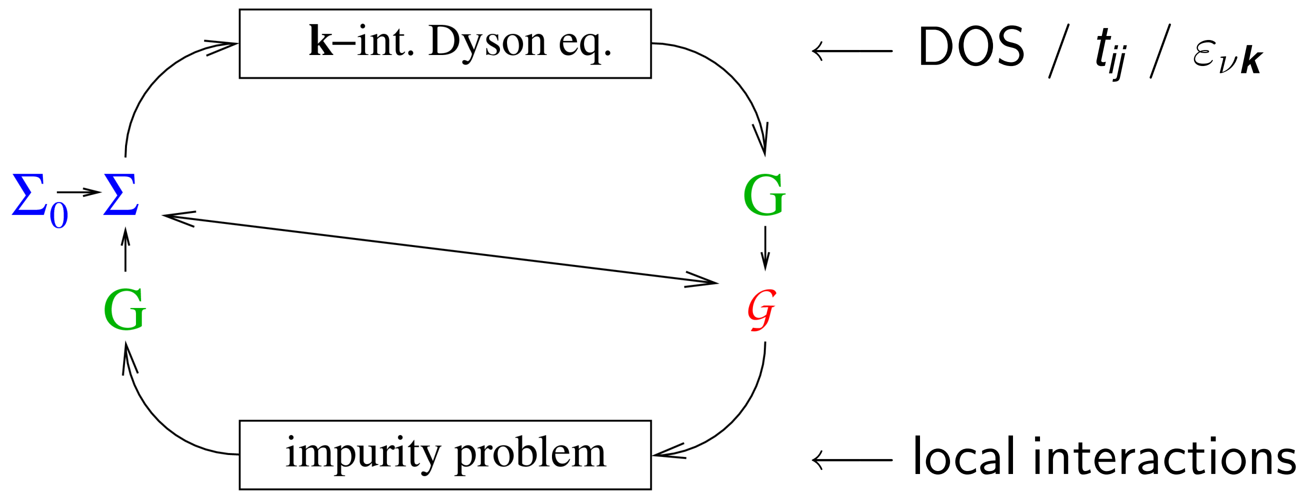

Impurity solver:

- Iterative perturbation theory (IPT; not controlled)
- Quantum Monte Carlo (QMC)

Iterative solution of DMFT equations

0. Initialize self-energy
1. Solve Dyson equation
2. Solve single impurity Anderson model (SIAM)

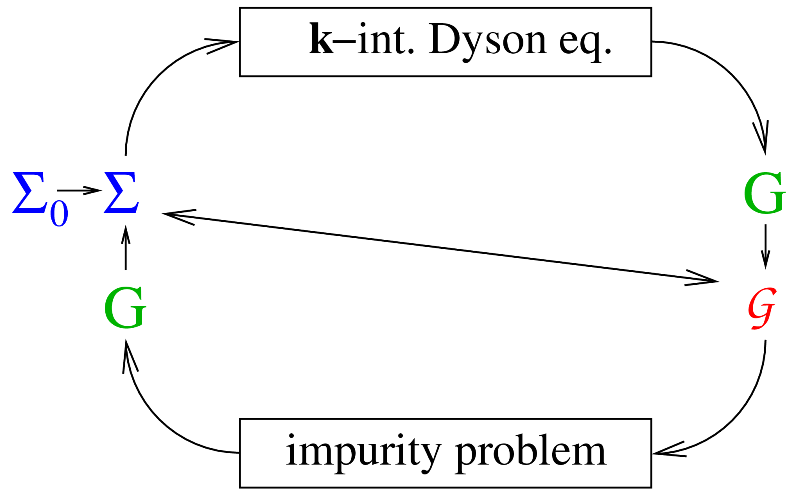

$\longleftarrow$ DOS / t_{ij} / $\varepsilon_{\nu \boldsymbol{k}}$

$\longleftarrow$ local interactions

Impurity solver:

- Iterative perturbation theory (IPT; not controlled)
- Quantum Monte Carlo (QMC)
- Exact diagonalization (ED; large finite-size errors)
- Numerical renormalization group (NRG; 1-2 bands)
- Density matrix renormalization group (DMRG)
- Self-energy functional theory (SFT) + ED

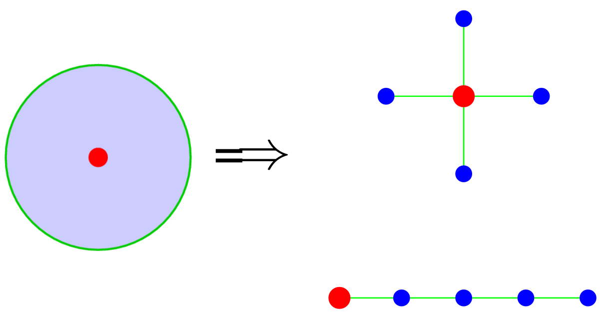

Auxiliary-field QMC algorithm [Hirsch, Fye (1986)]

Green function G in imaginary time (fermionic Grassmann variables ψ, ψ^*):

$$G_\sigma(\tau_2-\tau_1) = \frac{1}{\mathcal{Z}}\int \mathcal{D}[\psi]\,\mathcal{D}[\psi^*]\;\psi_\sigma(\tau_1)\psi^*_\sigma(\tau_2)\;\exp\left[\mathcal{A}_0 - U\sum_{\sigma\sigma'}\int_0^\beta d\tau\,\psi^*_\sigma\psi_\sigma\psi^*_{\sigma'}\psi_{\sigma'}\right]$$

Auxiliary-field QMC algorithm [Hirsch, Fye (1986)]

Green function G in imaginary time (fermionic Grassmann variables ψ, ψ^*):

$$G_\sigma(\tau_2-\tau_1) = \frac{1}{\mathcal{Z}} \int \mathcal{D}[\psi]\,\mathcal{D}[\psi^*]\;\; \psi_\sigma(\tau_1)\psi^*_\sigma(\tau_2)\;\exp\Big[\mathcal{A}_0 - U \sum_{\sigma\sigma'} \int_0^\beta d\tau\, \psi^*_\sigma\psi_\sigma\psi^*_{\sigma'}\psi_{\sigma'}\Big]$$

• Discretization $\beta = \Lambda\,\Delta\tau$, • Trotter decoupling $e^{-\beta(\hat{T}+\hat{V})} = \lim_{\Lambda\to\infty}\left[e^{-\Delta\tau\hat{T}}e^{-\Delta\tau\hat{V}}\right]^\Lambda$

Auxiliary-field QMC algorithm [Hirsch, Fye (1986)]

Green function G in imaginary time (fermionic Grassmann variables ψ, ψ^*):

$$G_\sigma(\tau_2-\tau_1)=\frac{1}{\mathcal{Z}}\int\mathcal{D}[\psi]\,\mathcal{D}[\psi^*]\;\psi_\sigma(\tau_1)\psi^*_\sigma(\tau_2)\;\exp\Big[\mathcal{A}_0-U\sum_{\sigma\sigma'}\int_0^\beta d\tau\,\psi^*_\sigma\psi_\sigma\psi^*_{\sigma'}\psi_{\sigma'}\Big]$$

- Discretization $\beta=\Lambda\,\Delta\tau$,
- Trotter decoupling $e^{-\beta(\hat{T}+\hat{V})}=\lim_{\Lambda\to\infty}\left[e^{-\Delta\tau\hat{T}}e^{-\Delta\tau\hat{V}}\right]^\Lambda$

- Discrete Hubbard-Stratonovich transformation $e^{\Delta\tau U(\hat{n}_\uparrow-\hat{n}_\downarrow)^2/2}=\frac{1}{2}\sum_{s=\pm1}e^{\lambda s\,(\hat{n}_\uparrow-\hat{n}_\downarrow)}$

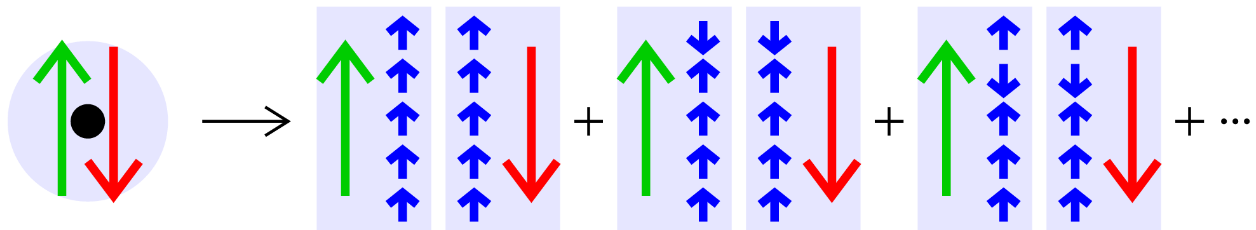

Wick theorem:

$$G=\frac{\sum M\det\{M\}}{\sum\det\{M\}}$$

Auxiliary-field QMC algorithm [Hirsch, Fye (1986)]

Green function G in imaginary time (fermionic Grassmann variables ψ, ψ^*):

$$G_\sigma(\tau_2 - \tau_1) = \frac{1}{\mathcal{Z}} \int \mathcal{D}[\psi]\,\mathcal{D}[\psi^*]\;\; \psi_\sigma(\tau_1)\psi^*_\sigma(\tau_2)\;\; \exp\left[\mathcal{A}_0 - U \sum_{\sigma\sigma'} \int_0^\beta d\tau\, \psi^*_\sigma \psi_\sigma \psi^*_{\sigma'} \psi_{\sigma'}\right]$$

- Discretization $\beta = \Lambda\,\Delta\tau$, • Trotter decoupling $e^{-\beta(\hat{T}+\hat{V})} = \lim_{\Lambda\to\infty} \left[e^{-\Delta\tau\hat{T}} e^{-\Delta\tau\hat{V}}\right]^\Lambda$

- Discrete Hubbard-Stratonovich transformation $e^{\Delta\tau U(\hat{n}_\uparrow - \hat{n}_\downarrow)^2/2} = \frac{1}{2} \sum_{s=\pm 1} e^{\lambda s\,(\hat{n}_\uparrow - \hat{n}_\downarrow)}$

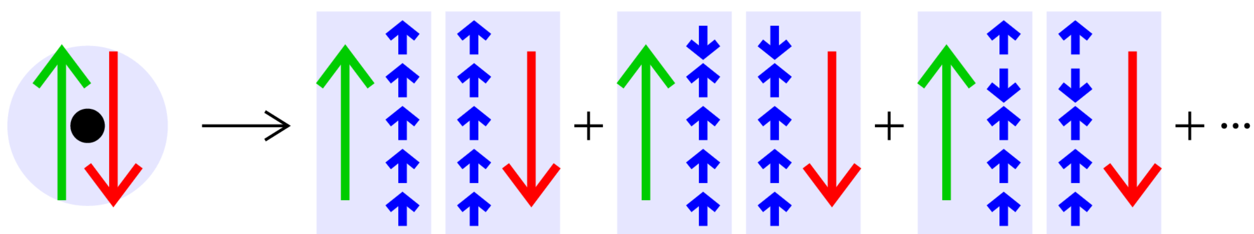

Wick theorem:

$$G = \frac{\sum M \det\{M\}}{\sum \det\{M\}}$$

Metropolis MC importance sampling over auxiliary Ising field $\{s\}$: 2^Λ configurations

+ numerically exact, + no sign problem, − effort scales as T^{-3}

Special issue: Fourier transformations in DMFT-QMC cycle

Iterative solution of DMFT equations (for imaginary-time impurity solver)

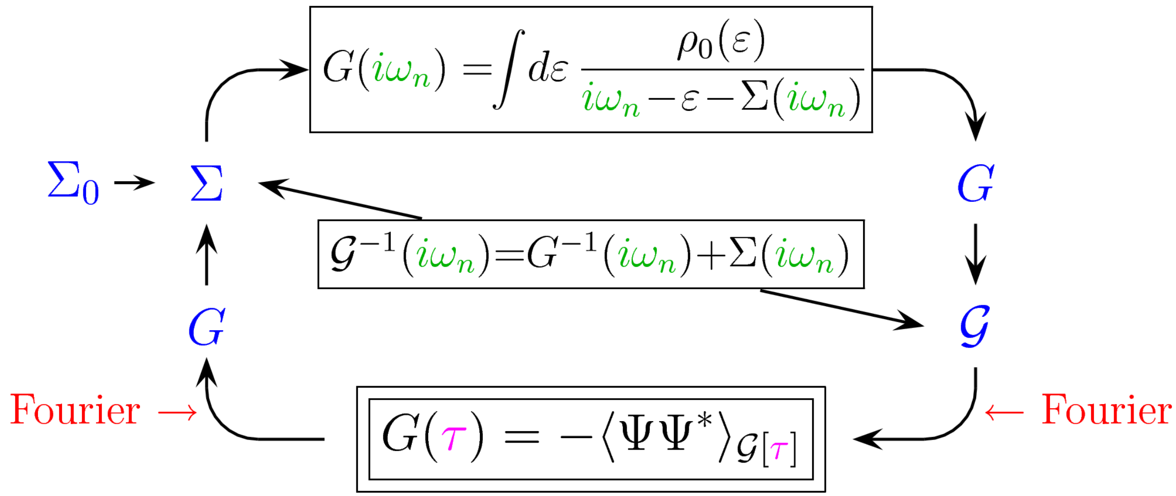

Special issue: Fourier transformations in DMFT-QMC cycle

Iterative solution of DMFT equations (for imaginary-time impurity solver)

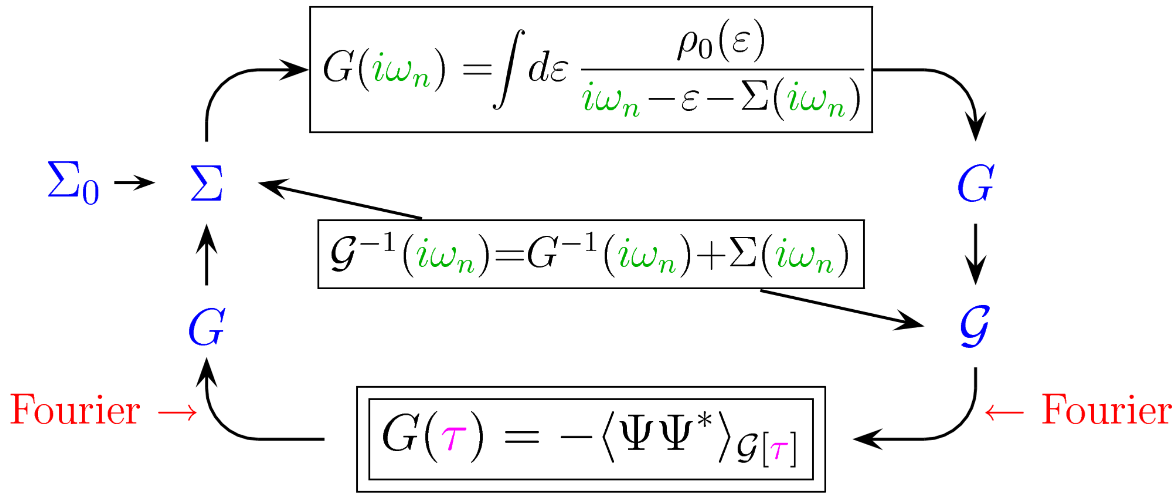

Naive discrete Fourier transformation $\rightsquigarrow$ oscillations (instead of $G(\omega) \stackrel{\omega\to\infty}{\longrightarrow} 1/\omega$)

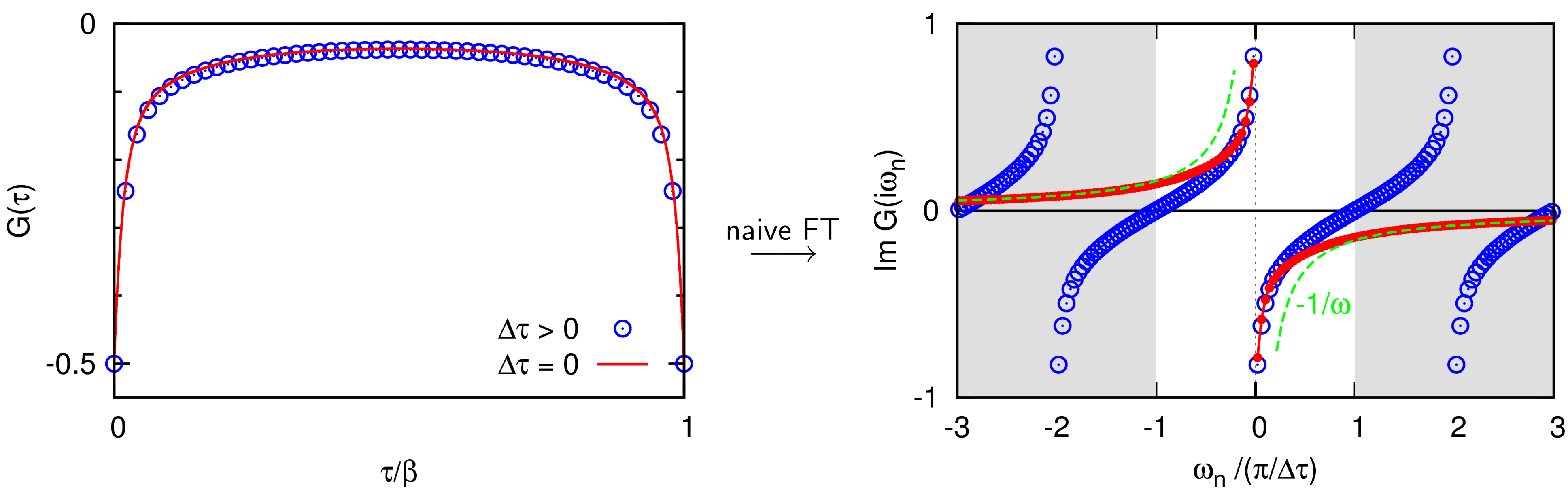

Best solution: interpolate $G_{\mathrm{QMC}}(\tau)$, e.g., by cubic splines [Jarrell, Krauth, Gull, ...]

But: $\dfrac{d^2G(\tau)}{d\tau^2}$ maximal for $\tau \rightarrow 0, \beta$ $\rightsquigarrow$ natural boundary conditions inappropriate

Best solution: interpolate $G_{\mathrm{QMC}}(\tau)$, e.g., by cubic splines [Jarrell, Krauth, Gull, . . .]

But: $\dfrac{d^2G(\tau)}{d\tau^2}$ maximal for $\tau \to 0, \beta$ $\rightsquigarrow$ natural boundary conditions inappropriate

- adjust boundary cond. [Oudovenko]
- spline-fit only difference w.r.t. reference problem:
  - IPT [Jarrell]

Best solution: interpolate $G_{\text{QMC}}(\tau)$, e.g., by cubic splines [Jarrell, Krauth, Gull, . . .]

But: $\dfrac{d^2G(\tau)}{d\tau^2}$ maximal for $\tau \to 0, \beta$ $\rightsquigarrow$ natural boundary conditions inappropriate

- adjust boundary cond. [Oudovenko]
- spline-fit only difference w.r.t. reference problem:
  - IPT [Jarrell]
  - high-frequency expansion for $\Sigma(\omega)$ + param. [Knecht, NB]

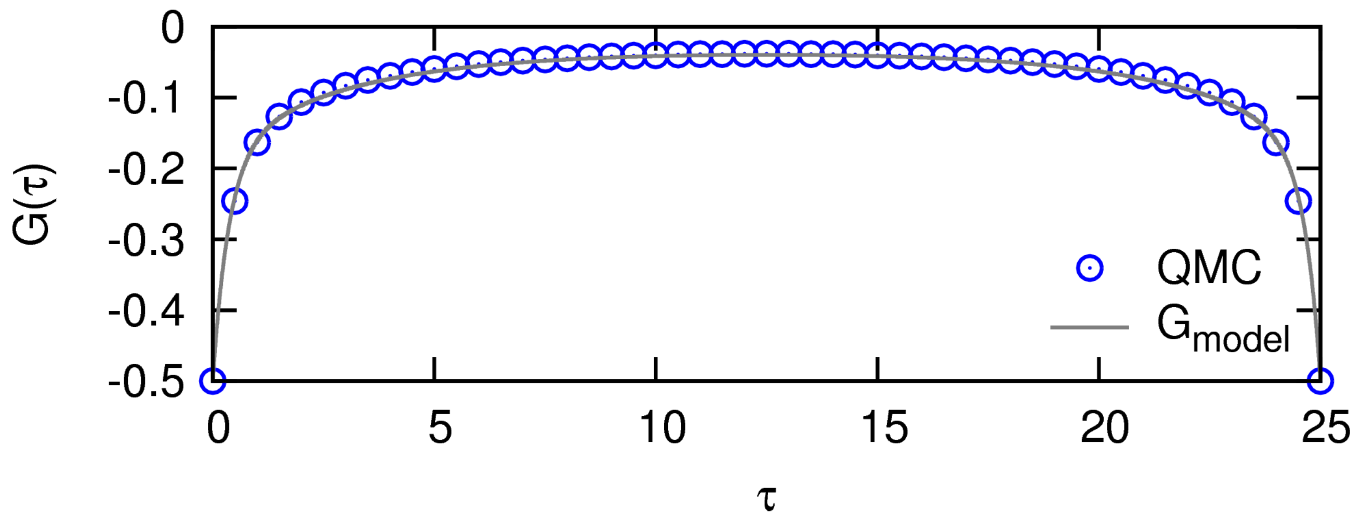

$$\Sigma_\sigma(\omega) = U\left(\langle \hat{n}_{-\sigma}\rangle - \tfrac{1}{2}\right)\omega^0 + U^2\langle \hat{n}_{-\sigma}\rangle\left(1 - \langle \hat{n}_{-\sigma}\rangle\right)\omega^{-1} + \mathcal{O}(\omega^{-2})$$

Best solution: interpolate $G_{\mathrm{QMC}}(\tau)$, e.g., by cubic splines [Jarrell, Krauth, Gull, . . .]

But: $\dfrac{d^2G(\tau)}{d\tau^2}$ maximal for $\tau \to 0, \beta$ $\rightsquigarrow$ natural boundary conditions inappropriate

- adjust boundary cond. [Oudovenko]
- spline-fit only difference w.r.t. reference problem:
  - IPT [Jarrell]
  - high-frequency expansion for $\Sigma(\omega)$ + param. [Knecht, NB]

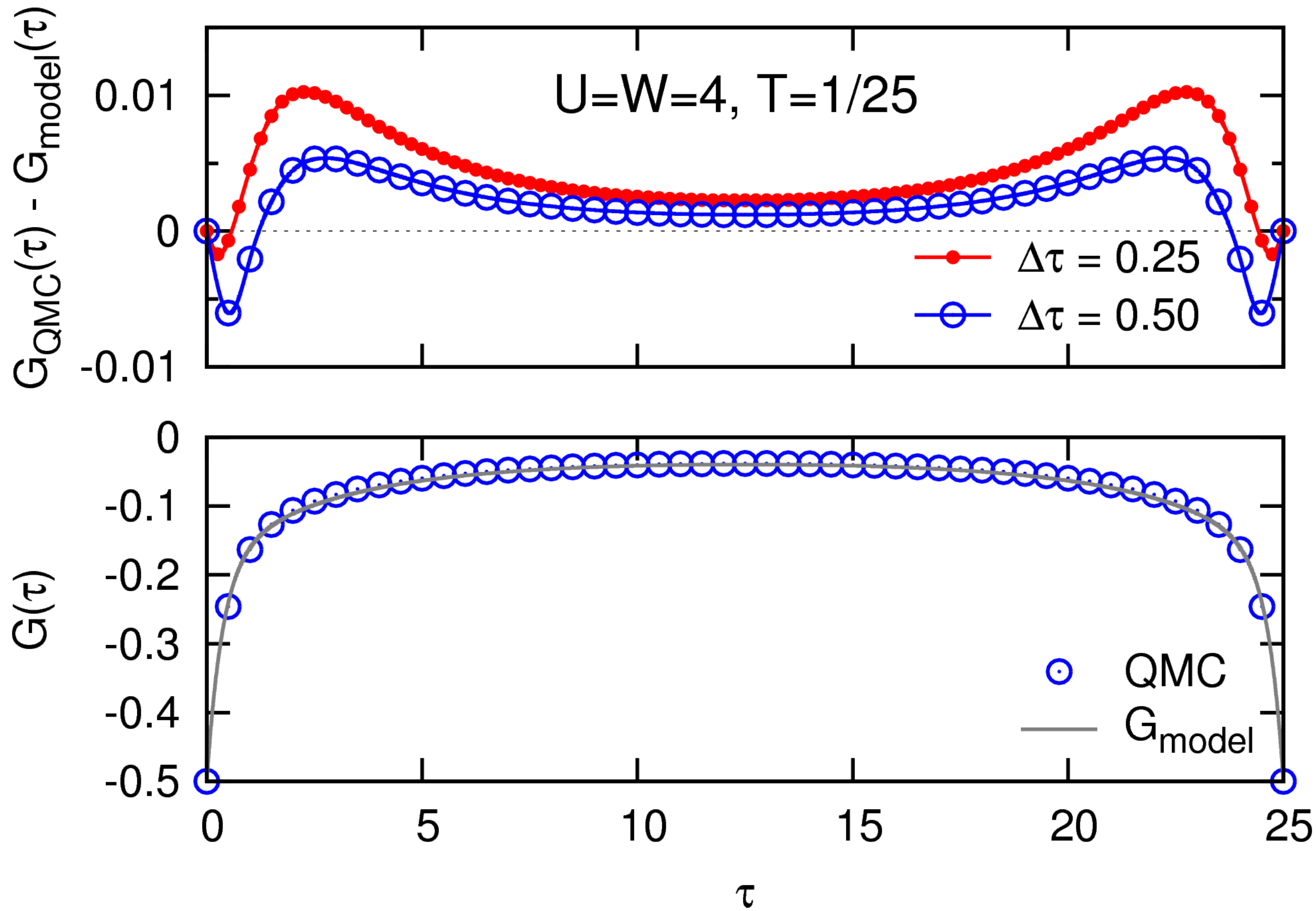

$$\Sigma_\sigma(\omega) = U\big(\langle \hat{n}_{-\sigma}\rangle - \tfrac{1}{2}\big)\,\omega^0 + U^2\langle \hat{n}_{-\sigma}\rangle\big(1 - \langle \hat{n}_{-\sigma}\rangle\big)\,\omega^{-1} + \mathcal{O}(\omega^{-2})$$

multi-band case: additional terms

Mott transition within DMFT

Fully frustrated 1-band model,
energy scale: bandwidth $W = 4$

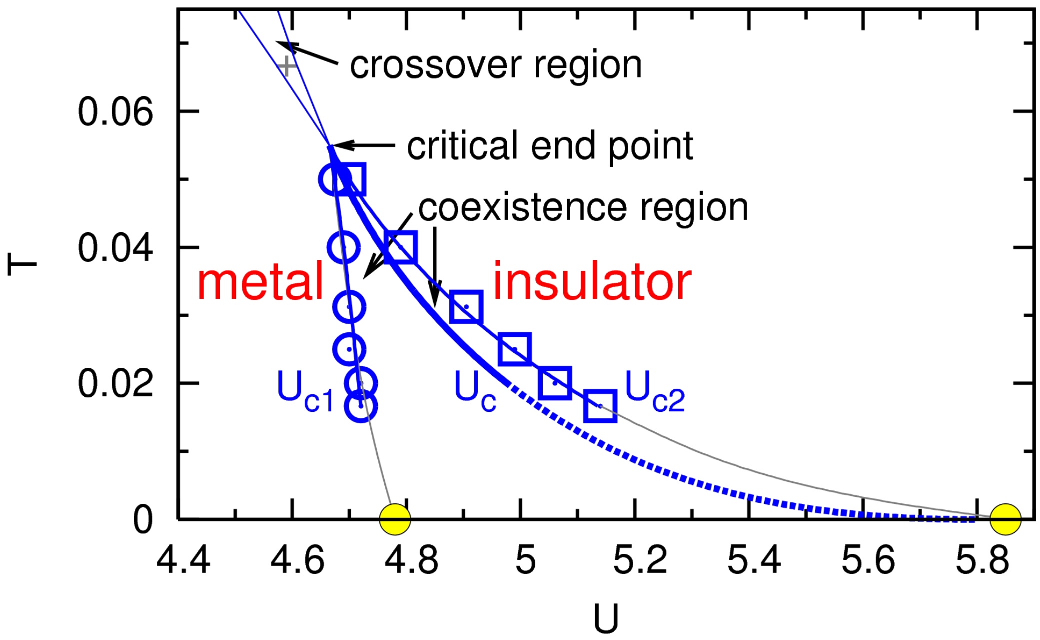

Mott transition within DMFT

Fully frustrated 1-band model,
energy scale: bandwidth $W = 4$

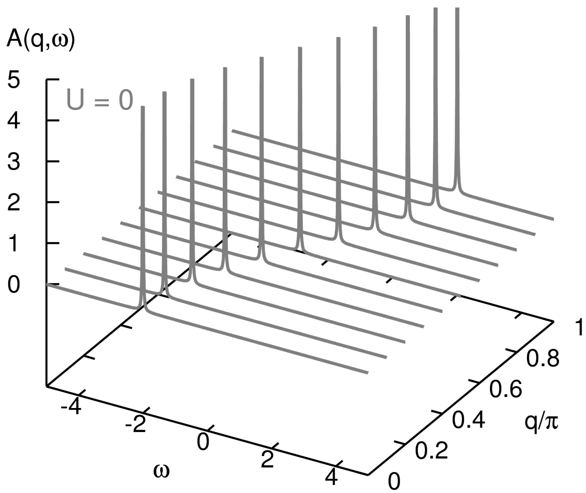

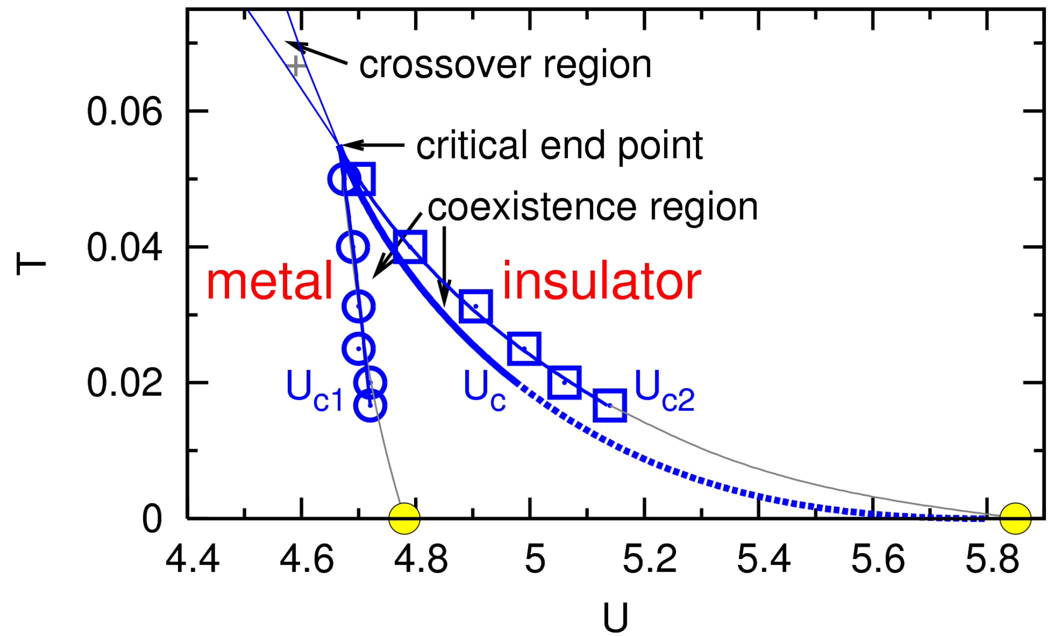

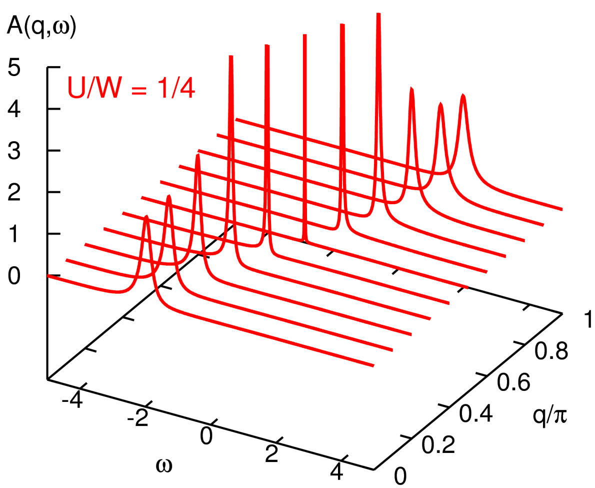

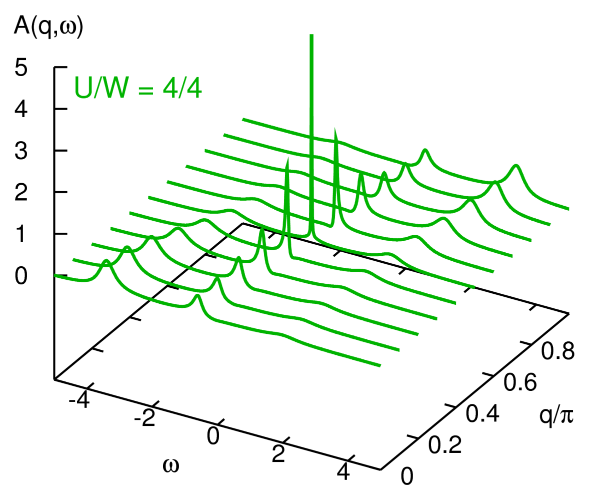

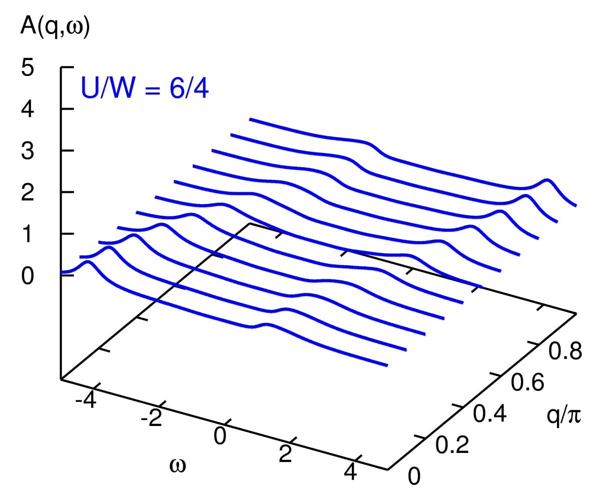

New development: continuous-time QMC algorithms

1. weak-coupling expansion

[Rubtsov, Savkin, Lichtenstein, PRB (2005)]

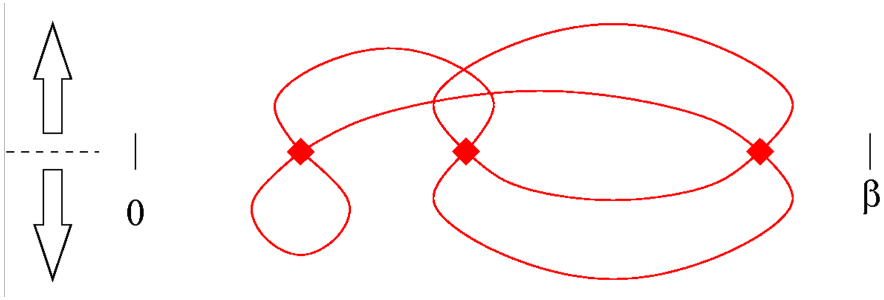

2. hybridization expansion

[Werner et al., PRL (2006)]

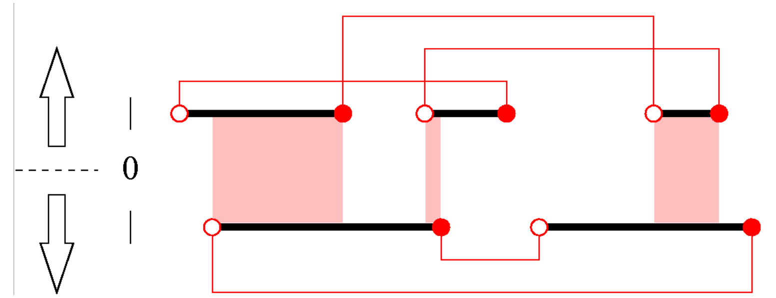

No systematic errors (in principle). Also more efficient than HF-QMC?

New development: continuous-time QMC algorithms

1. weak-coupling expansion
[Rubtsov, Savkin, Lichtenstein, PRB (2005)]

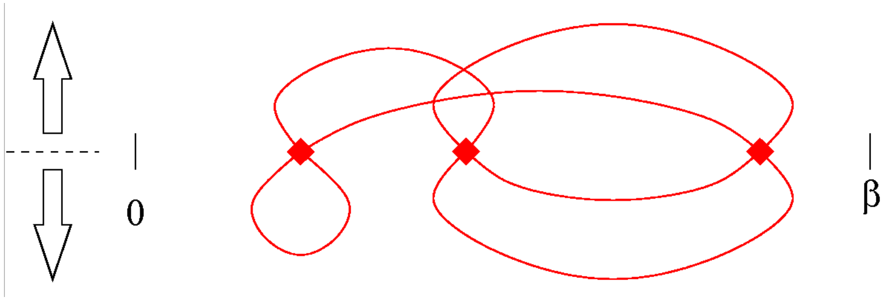

2. hybridization expansion
[Werner et al., PRL (2006)]

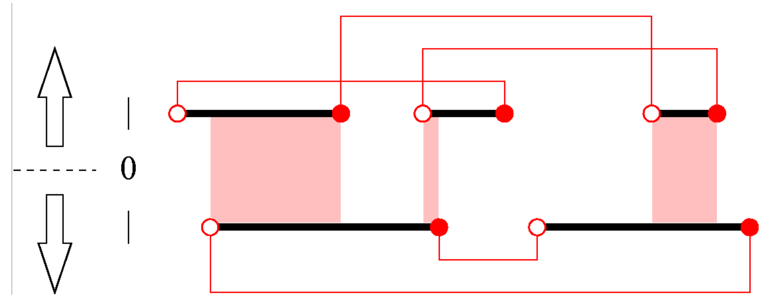

No systematic errors (in principle). Also more efficient than HF-QMC? No!

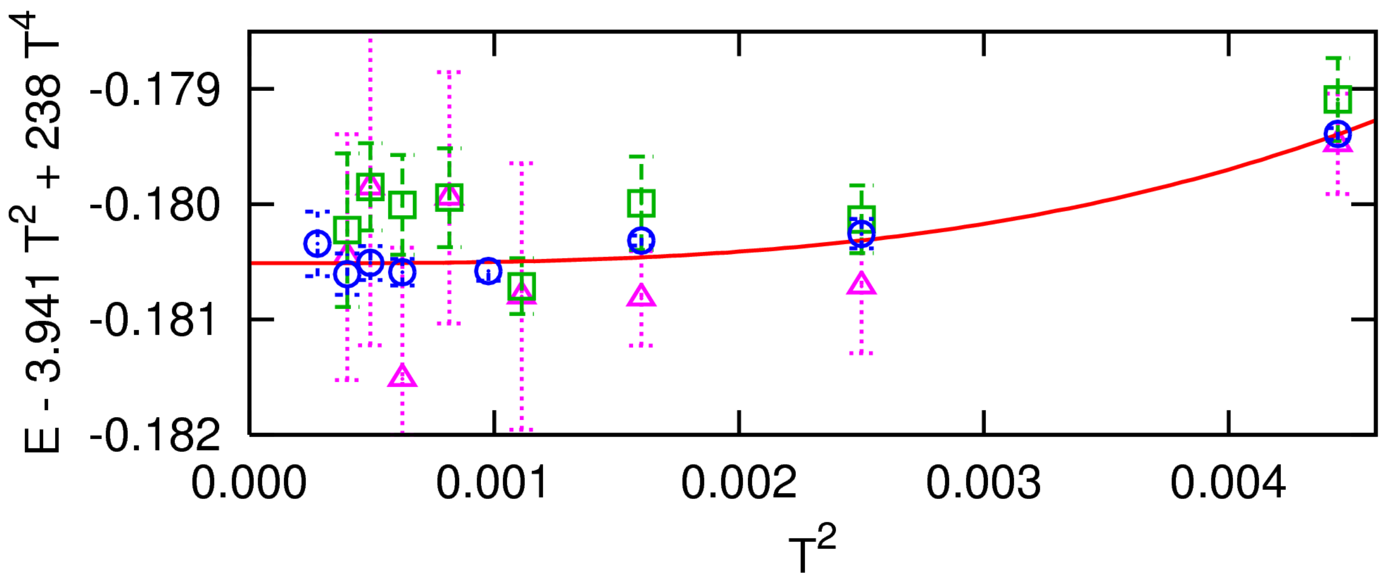

Test case:

1 band, $U = W = 4$

○ HF-QMC ($\Delta\tau \to 0$)

□ weak-coupling CT-QMC

△ hybridization CT-QMC

HF-QMC + extrapolation $\Delta\tau \to 0$ can be more efficient [NB, PRB **76**, 205120 (2007)]

Extrapolation $\Delta\tau \to 0$ can improve accuracy of observable estimates by several orders of magnitude!

Extrapolation $\Delta\tau \to 0$ can improve accuracy of observable estimates by several orders of magnitude!

Example: energy for $U = W = 4$ (Bethe DOS), $T = 1/45$
[NB, PRB (2007)]

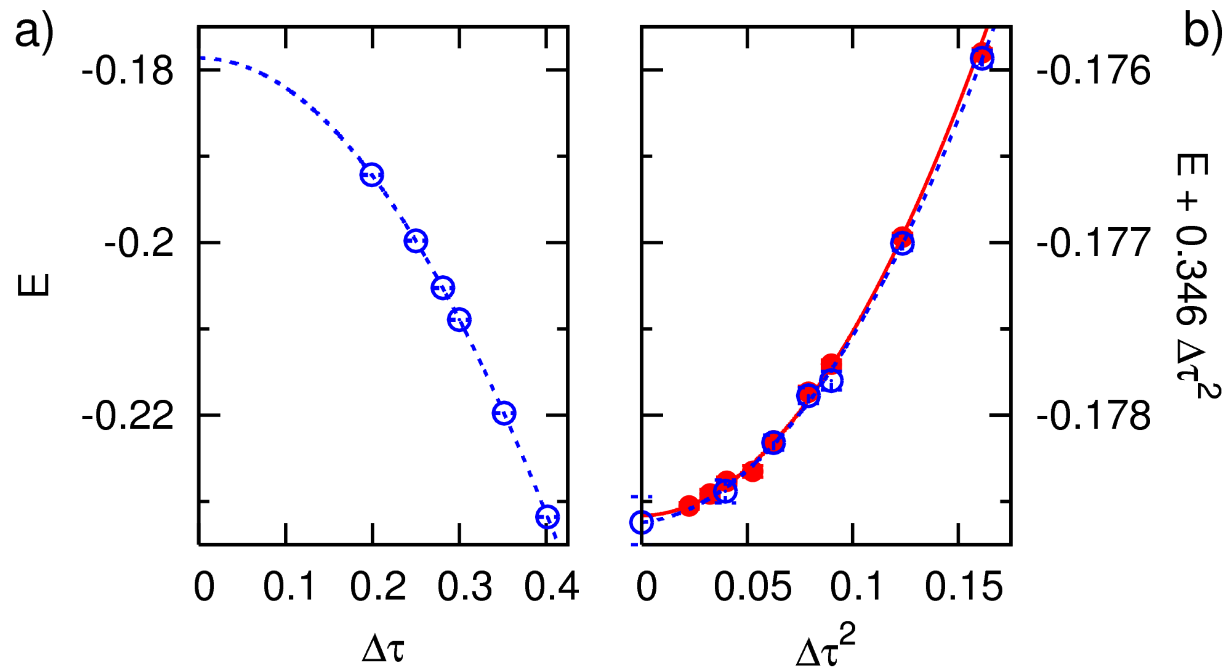

Extrapolation $\Delta\tau \to 0$ can improve accuracy of observable estimates by several orders of magnitude!

Example: energy for $U = W = 4$ (Bethe DOS), $T = 1/45$ [NB, PRB (2007)]

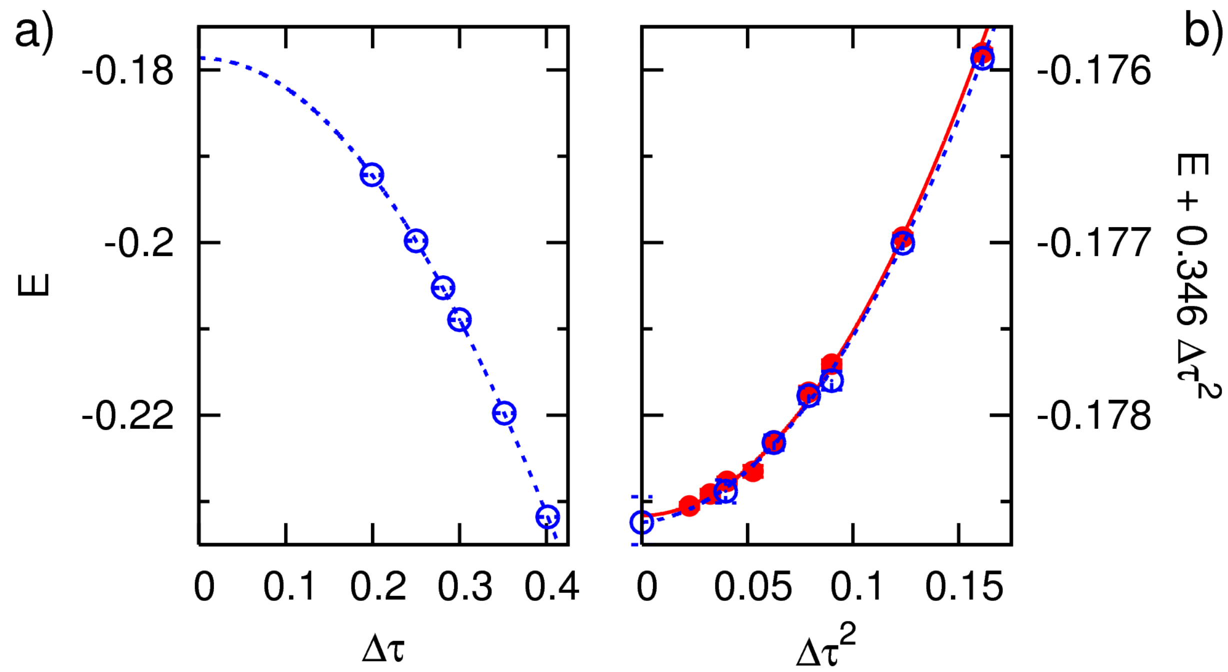

But (before 2007): extrapolation only for static observables (energy, double occupancy, qp weight)

care needed (suitable range of $\Delta\tau$)

may fail close to phase transitions

Extrapolation $\Delta\tau \to 0$ can improve accuracy of observable estimates by several orders of magnitude!

Example: energy for $U = W = 4$ (Bethe DOS), $T = 1/45$ [NB, PRB (2007)]

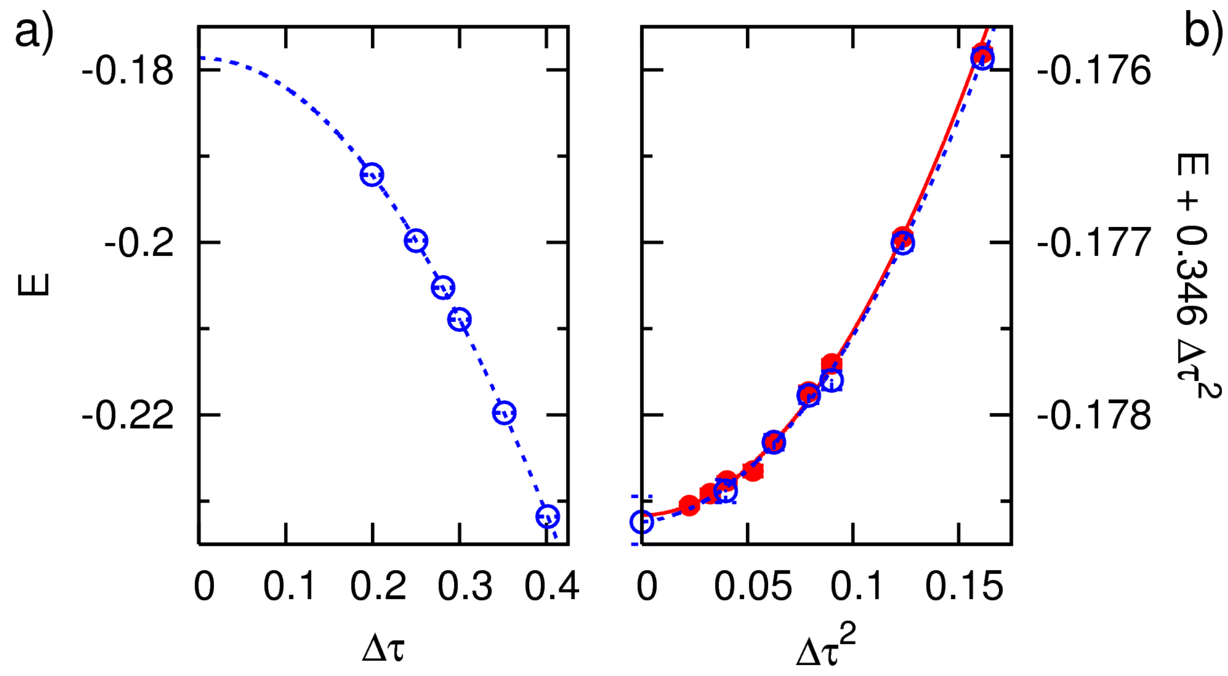

But (before 2007): extrapolation only for static observables (energy, double occupancy, qp weight)

care needed (suitable range of $\Delta\tau$)

may fail close to phase transitions

no extrapolation for Green functions + spectra

Unbiased Green functions and spectra from HF-QMC

State of the art: analytic continuation (using MEM) of imaginary-time Green function at fixed finite (often large) $\Delta\tau$ $\rightsquigarrow$ bias

Unbiased Green functions and spectra from HF-QMC

State of the art: analytic continuation (using MEM) of imaginary-time Green function at fixed finite (often large) $\Delta\tau$ $\rightsquigarrow$ bias

Reason: no obvious extrapolation scheme for $G(\tau)$

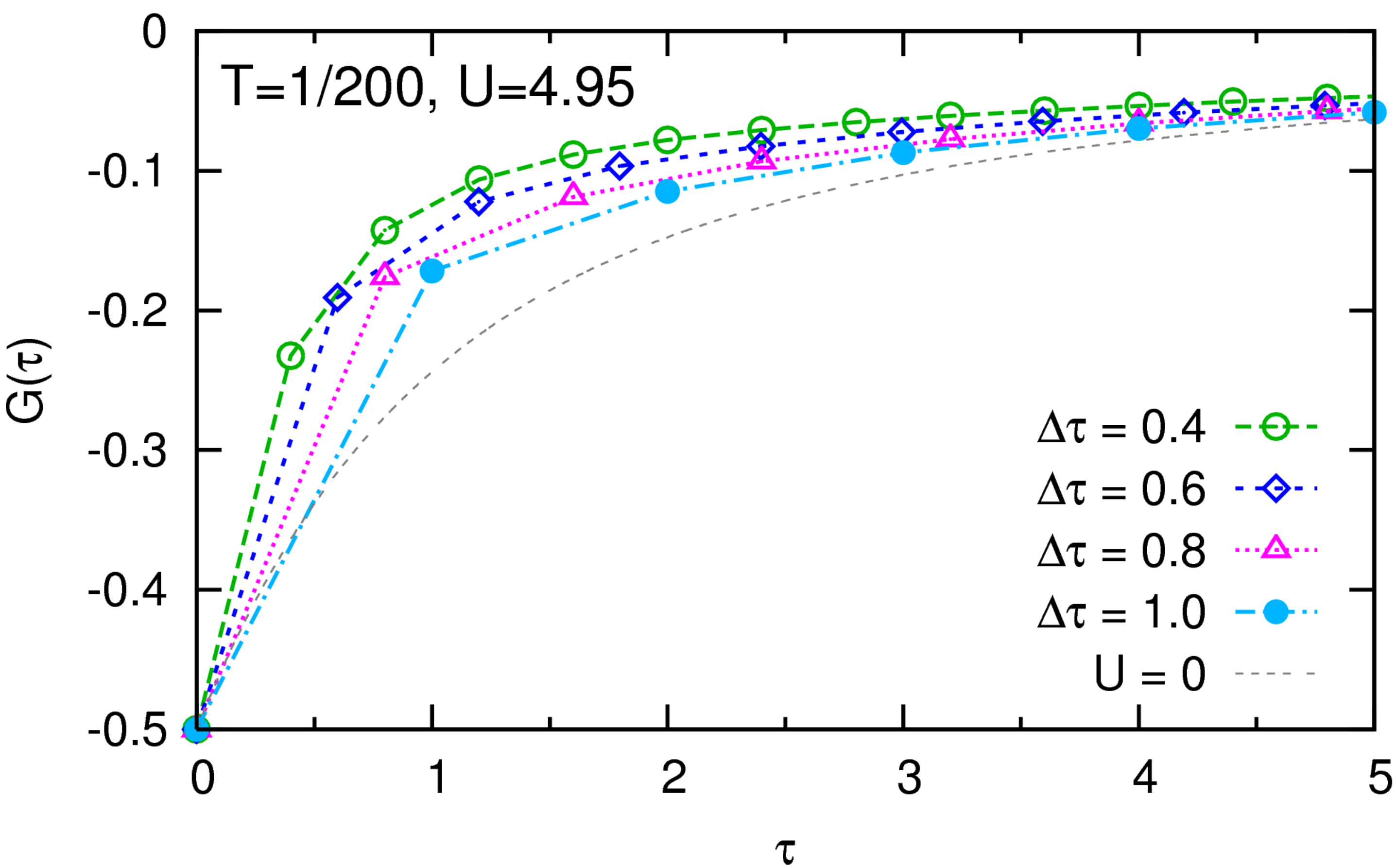

Low temperature ("beyond HF-QMC"): large $\Delta\tau$ $\rightsquigarrow$ large biases [NB, arXiv:0712.1290]

Unbiased Green functions and spectra from HF-QMC

State of the art: analytic continuation (using MEM) of imaginary-time Green function at fixed

Reason: no obvious extrapolatic

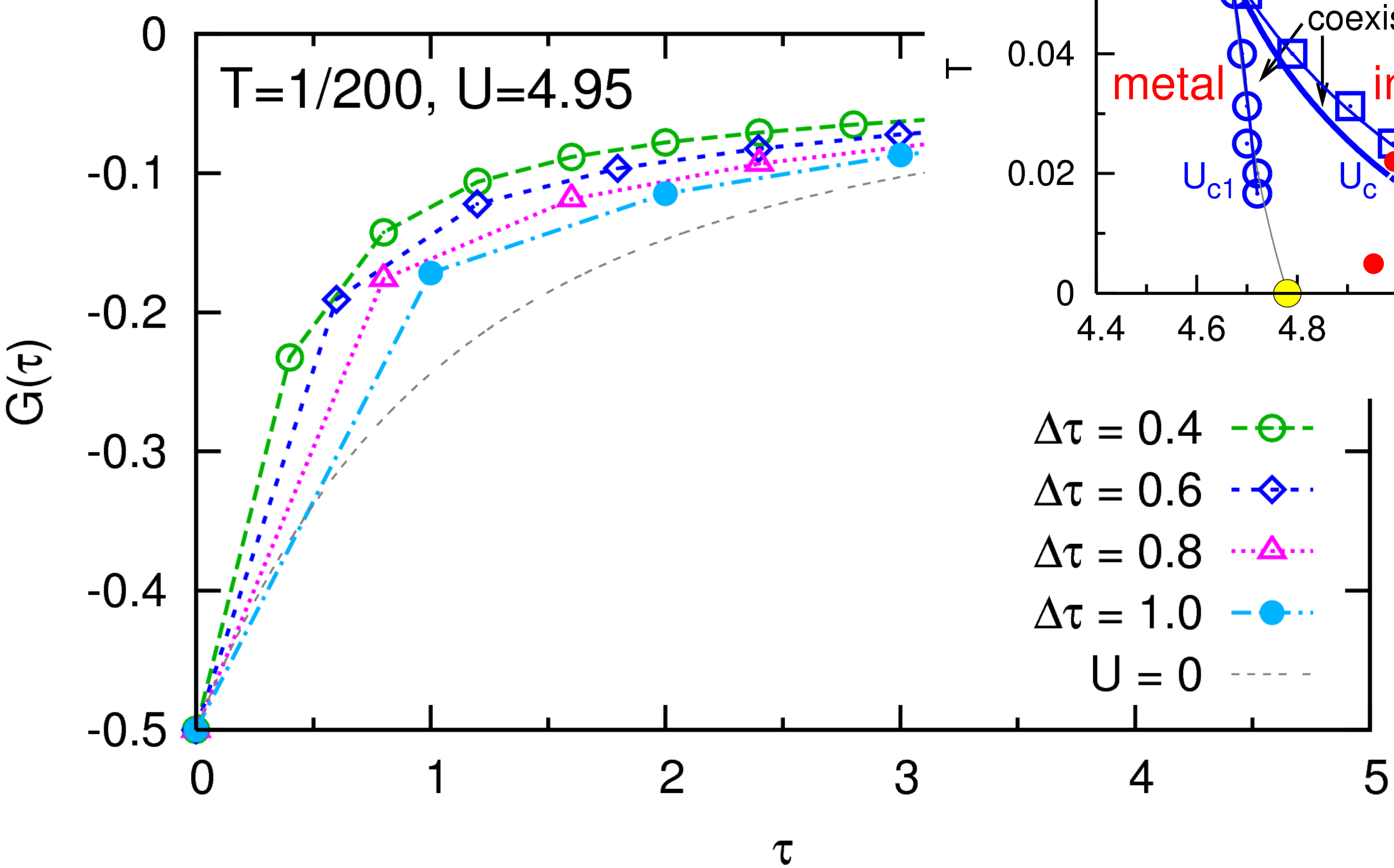

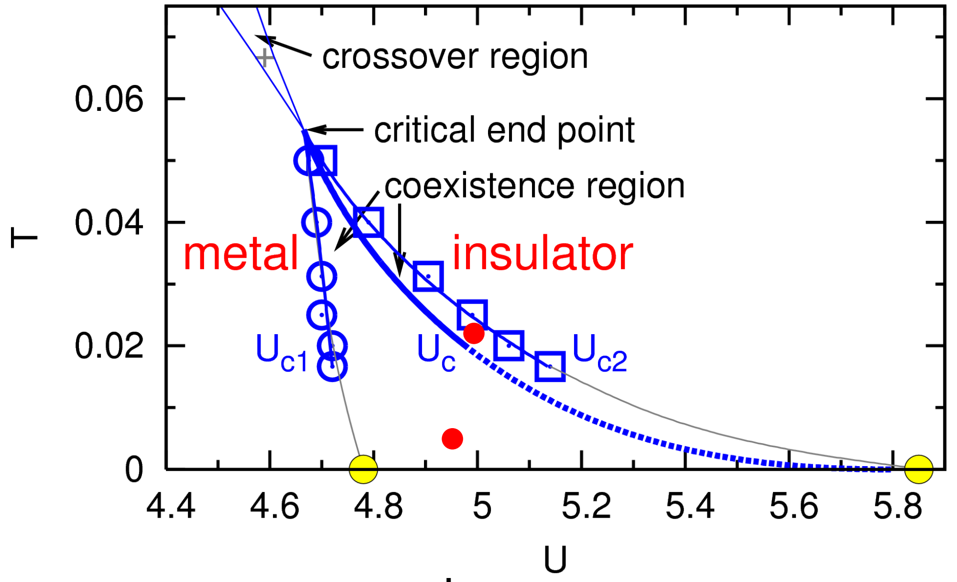

Low temperature ("beyond HF-QMC"): large $\Delta\tau \rightsquigarrow$ large biases [NB, arXiv:0712.1290]

Unbiased Green functions and spectra from HF-QMC

State of the art: analytic continuation (using MEM) of imaginary-time Green function at fixed finite (often large) $\Delta\tau$ $\rightsquigarrow$ bias

Reason: no obvious extrapolation scheme for $G(\tau)$

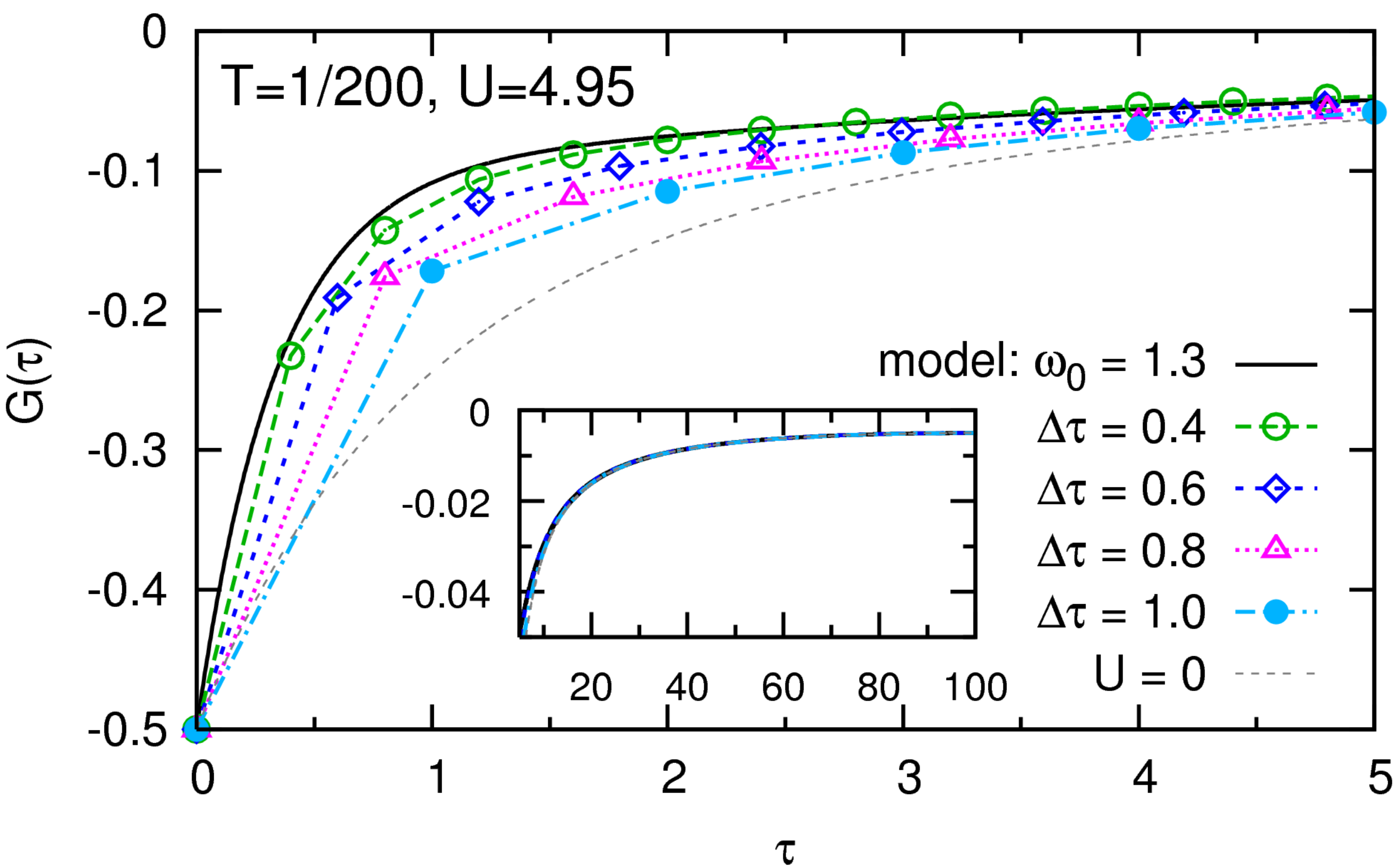

Low temperature ("beyond HF-QMC"): large $\Delta\tau$ $\rightsquigarrow$ large biases [NB, arXiv:0712.1290]

New Green function extrapolation scheme

For each $\Delta\tau$:

- average $G_{\Delta\tau}(\tau)$ over parallel runs for same impurity model
- average $\log[-G_{\Delta\tau}(\tau)]$ over iterations ($\sim$ geometric av. for $G_{\Delta\tau}(\tau)$)
- interpolate via difference Green function $G_{\Delta\tau}(\tau) - G_{\text{model}}(\tau)$

$\rightsquigarrow$ $G_{\Delta\tau_1}$, $G_{\Delta\tau_2}$, . . . $G_{\Delta\tau_n}$ (with error bars) on common fine τ grid

New Green function extrapolation scheme

For each $\Delta\tau$: • average $G_{\Delta\tau}(\tau)$ over parallel runs for same impurity model

• average $\log[-G_{\Delta\tau}(\tau)]$ over iterations ($\sim$ geometric av. for $G_{\Delta\tau}(\tau)$)

• interpolate via difference Green function $G_{\Delta\tau}(\tau) - G_{\text{model}}(\tau)$

$\rightsquigarrow$ $G_{\Delta\tau_1}$, $G_{\Delta\tau_2}$, . . . $G_{\Delta\tau_n}$ (with error bars) on common fine τ grid

• Extrapolate $\log[-G(\tau)]$ using cubic least-squares fits, overweighting low $\Delta\tau$

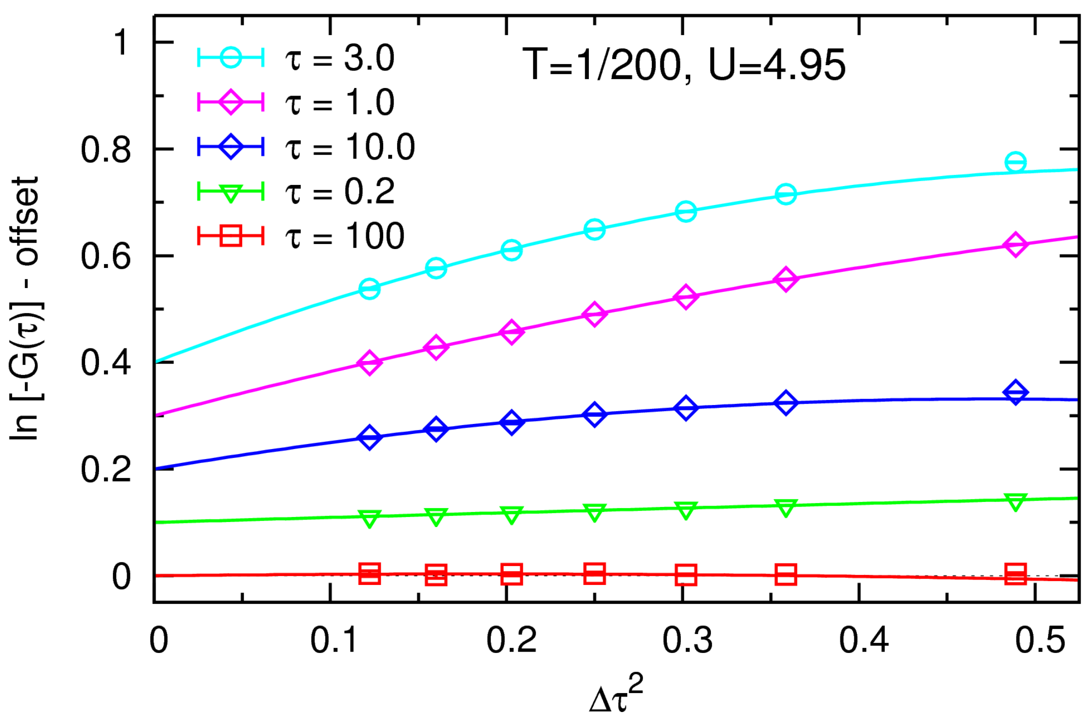

Result: unbiased, numerically exact Green function

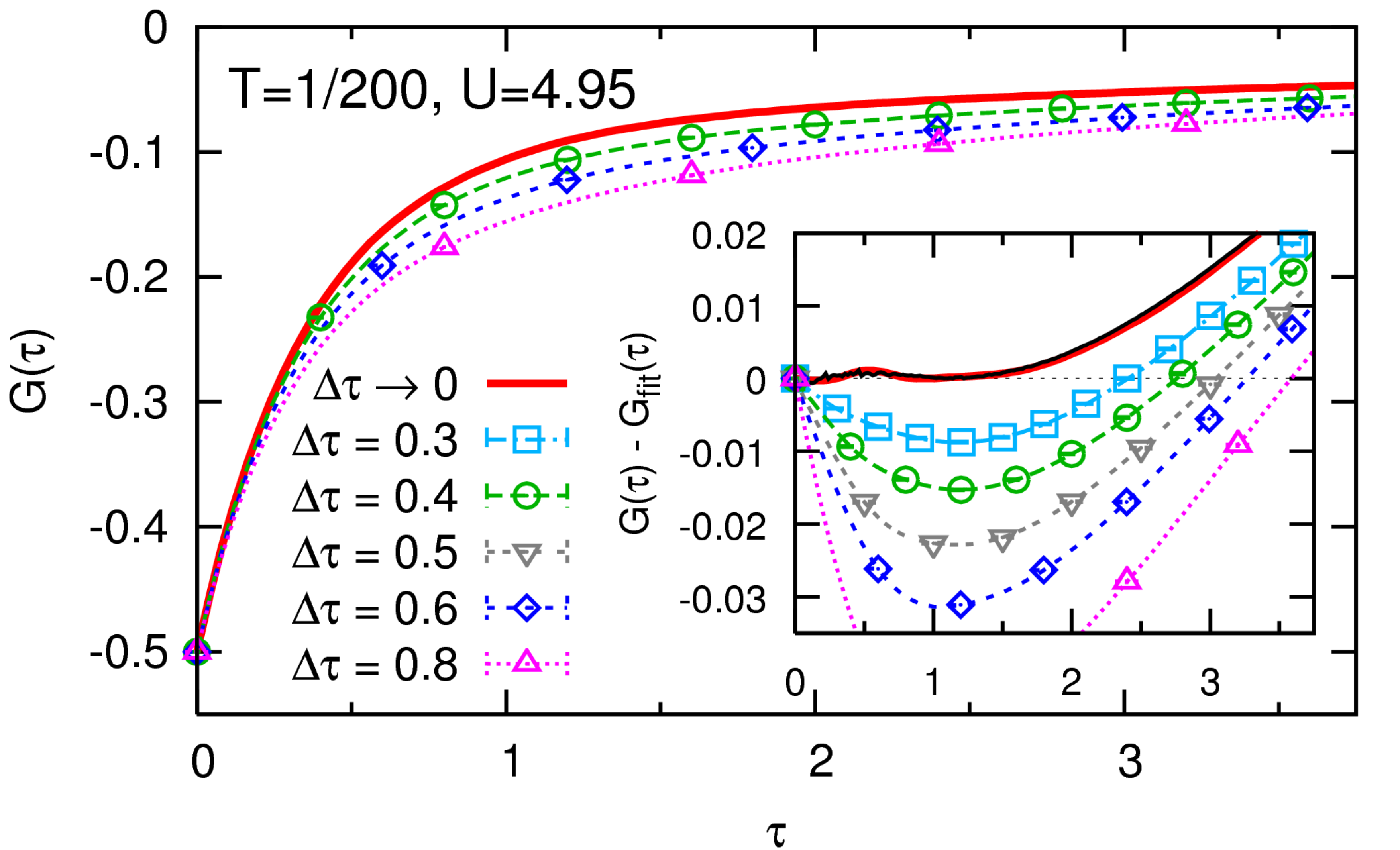

[NB, arXiv:0712.1290]

Excellent agreement with hybridization expansion CT-QMC [Werner et al., PRL (2006)]

2^{nd} and 1^{st} order derivatives of Green function

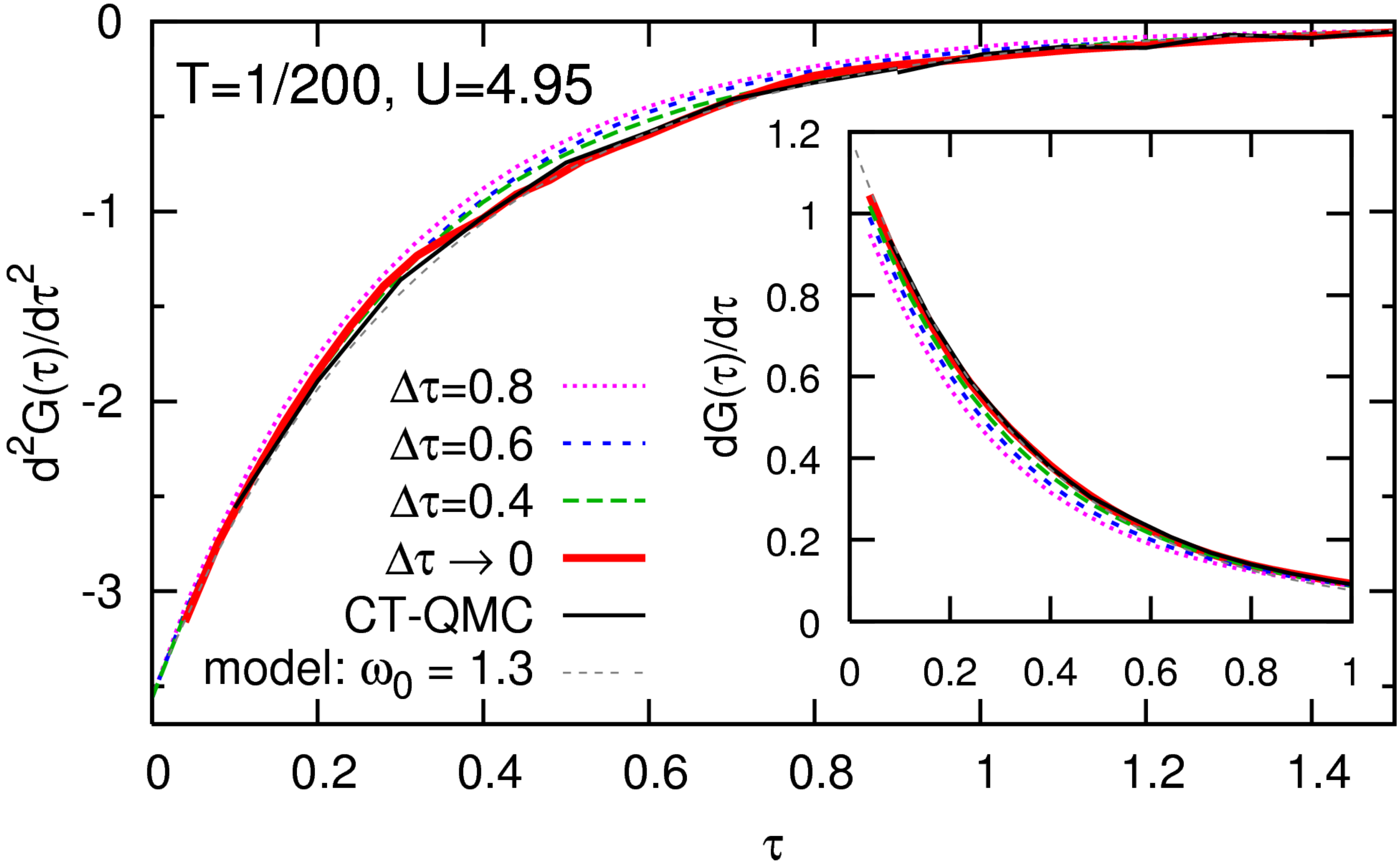

Exact asymptotics $\left.\dfrac{d^2G(\tau)}{d\tau^2}\right|_{\tau=0+} = -\dfrac{1}{2}\left(1+\dfrac{U^2}{4}\right);$ $\left.\dfrac{dG(\tau)}{d\tau}\right|_{\tau=0+}$ nonuniversal

Why average and extrapolation on logarithmic scale?

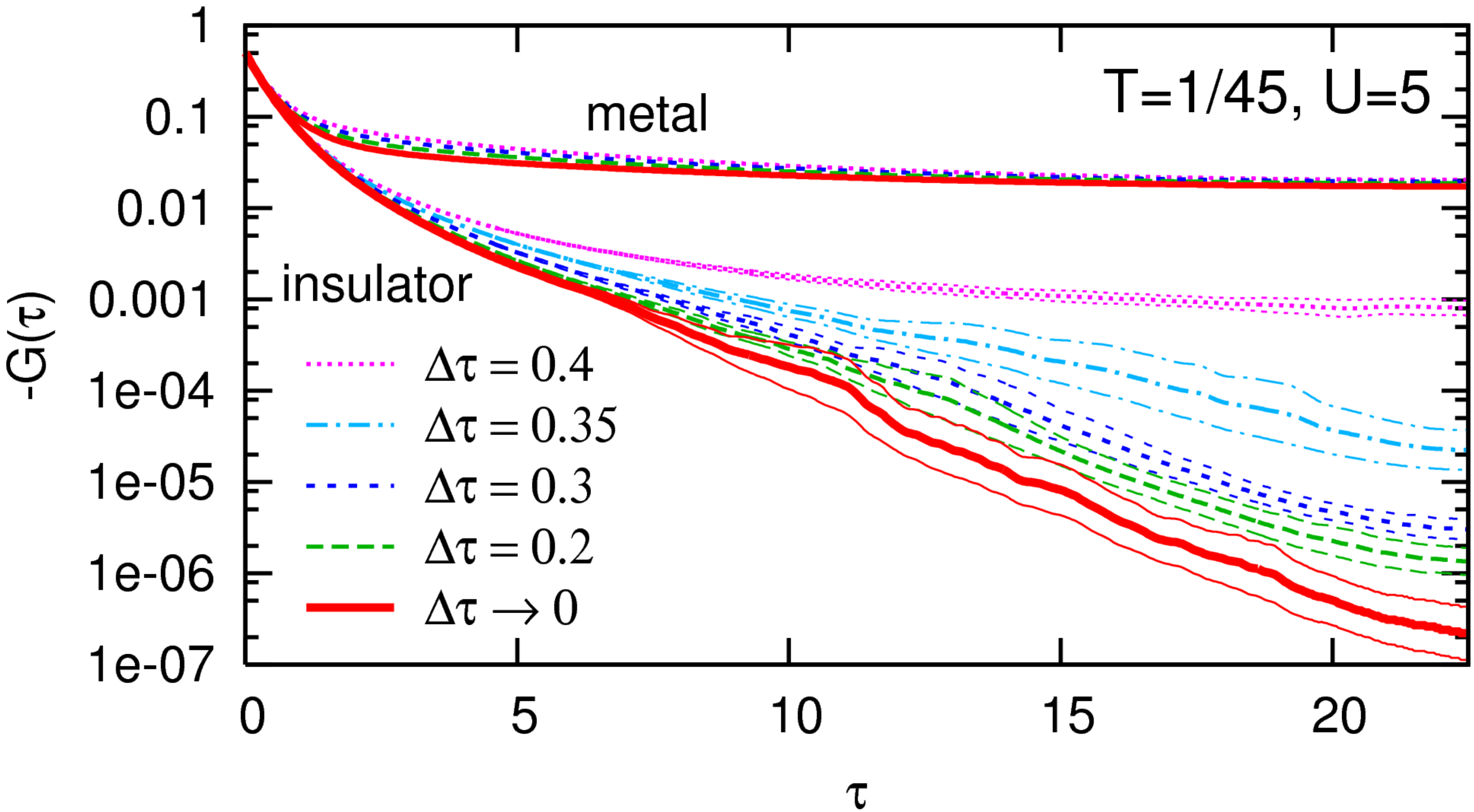

Difference metal–insulator and $\Delta\tau$ dependence involve orders of magnitude!

Even maximum statistical/iteration errors nearly order of magnitude

Low-τ resolution limited by $\Delta\tau$? No!

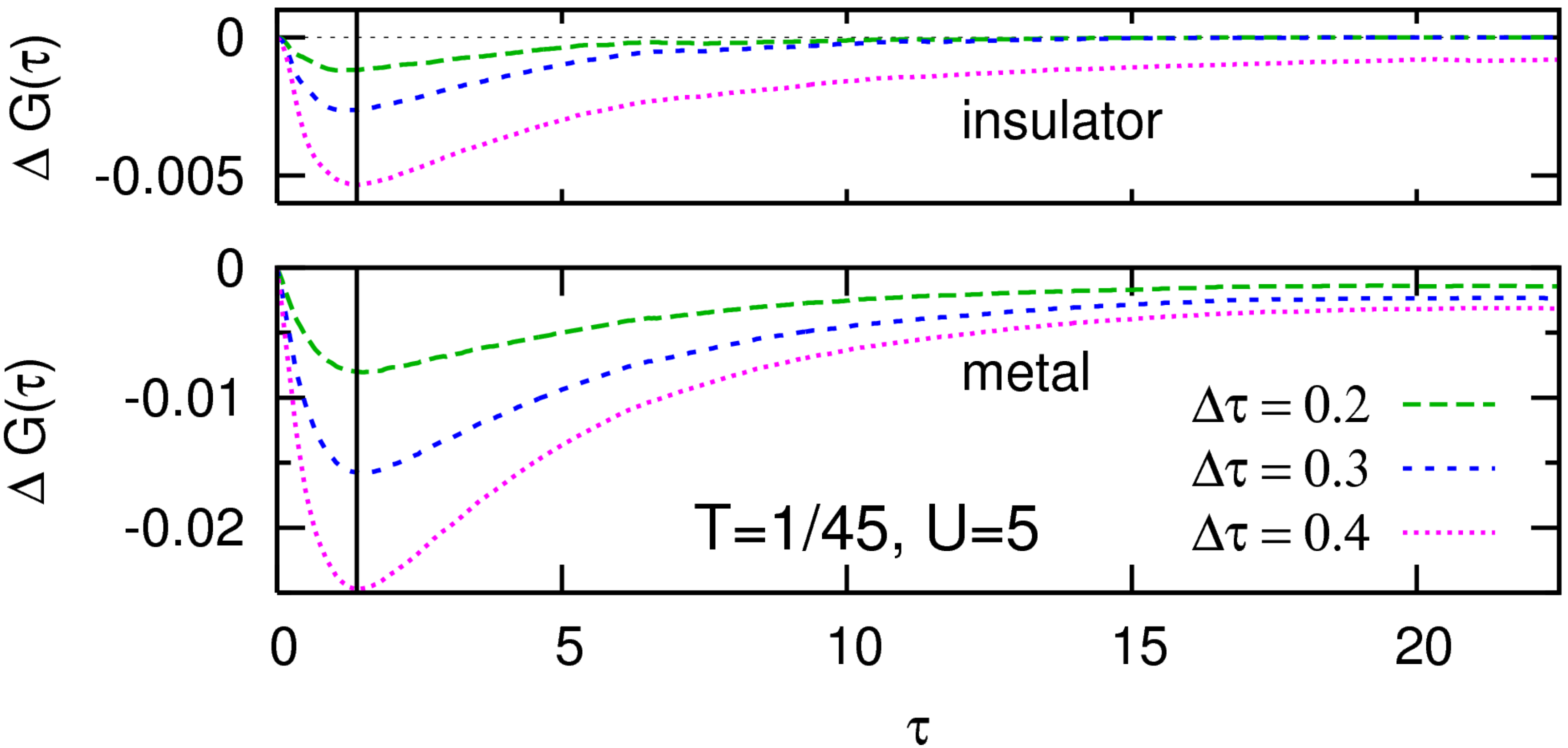

Uniform $\Delta\tau$ dependence, position of max. error independent of $\Delta\tau$ and phase!

Analytic continuation using Padé approximant for self-energy

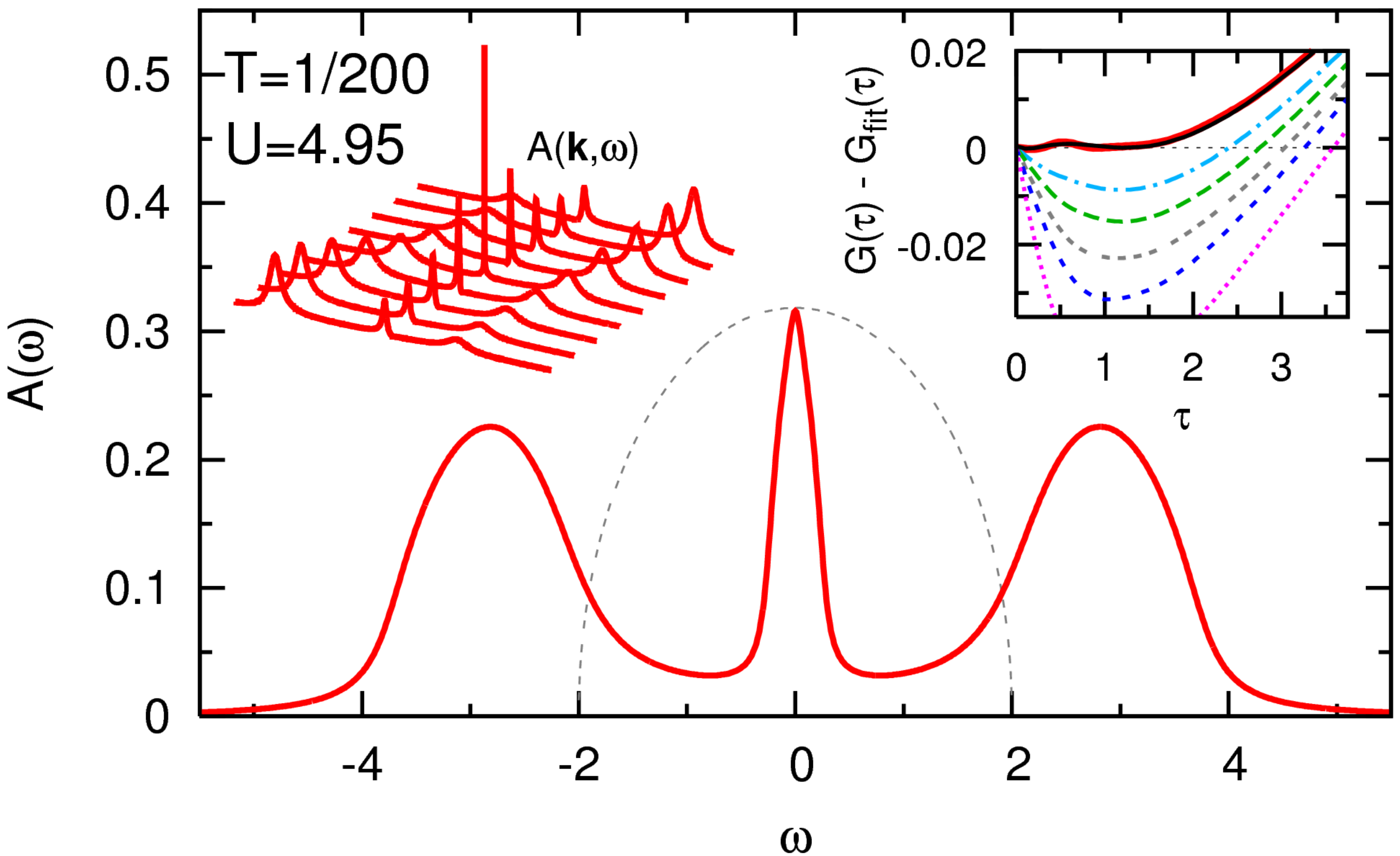

First spectra without discretization error from HF-QMC, at ultra-low T

Method directly applicable, e.g., to LDA+DMFT calculations [NB, arXiv:0712.1290]

Multigrid Hirsch-Fye quantum Monte Carlo algorithm

State of the art: (a) conventional HF-QMC

(b) *a posteriori* extrapolation of selected observables

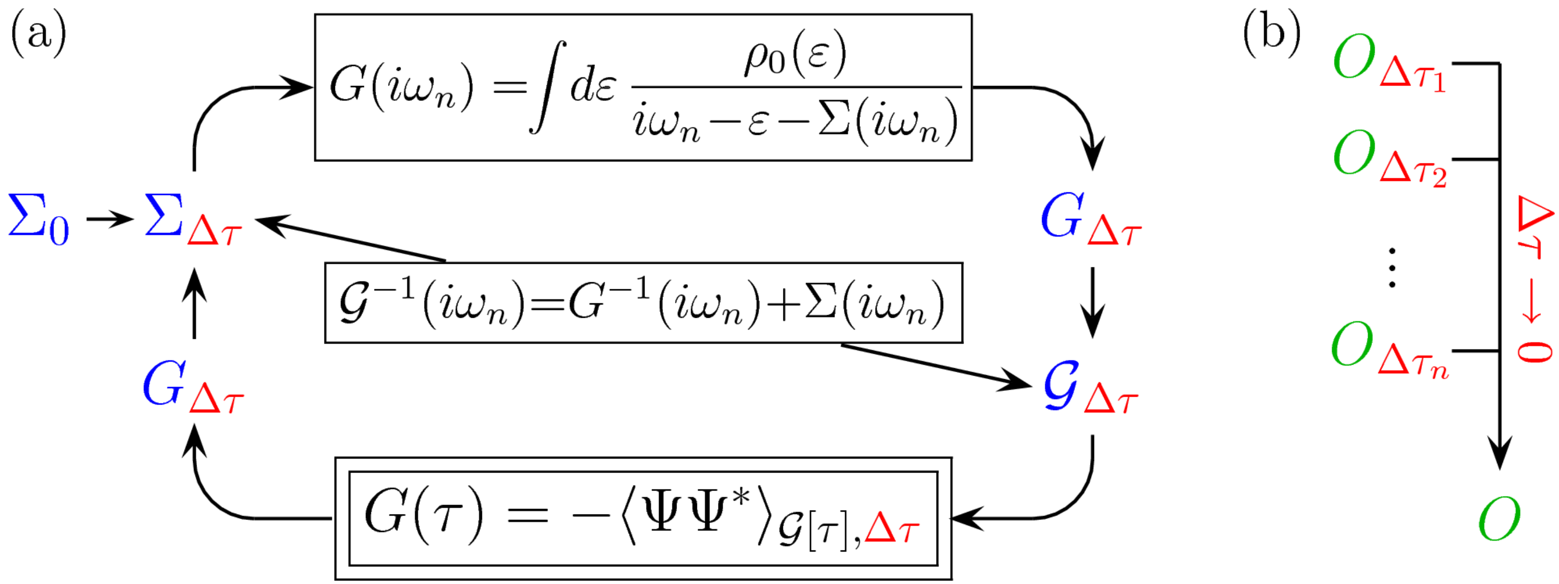

Multigrid Hirsch-Fye quantum Monte Carlo algorithm

State of the art: (a) conventional HF-QMC

(b) *a posteriori* extrapolation of selected observables

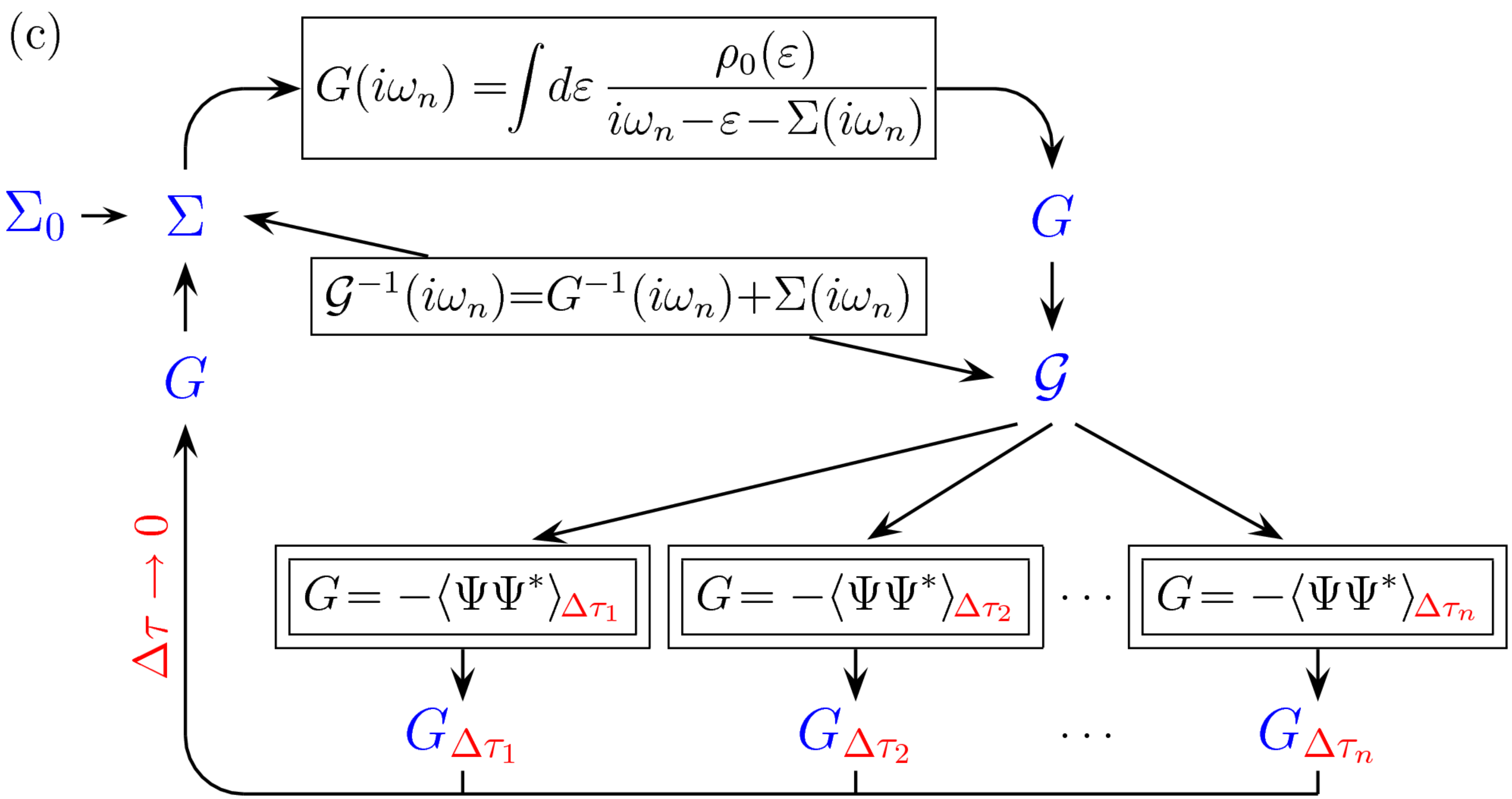

(c) Multigrid HF-QMC: internal elimination of Trotter error

$\rightsquigarrow$ quasi continuous time algorithm [NB, arXiv:0801.1222]

Schematic comparison via generalized Ginzburg-Landau functionals

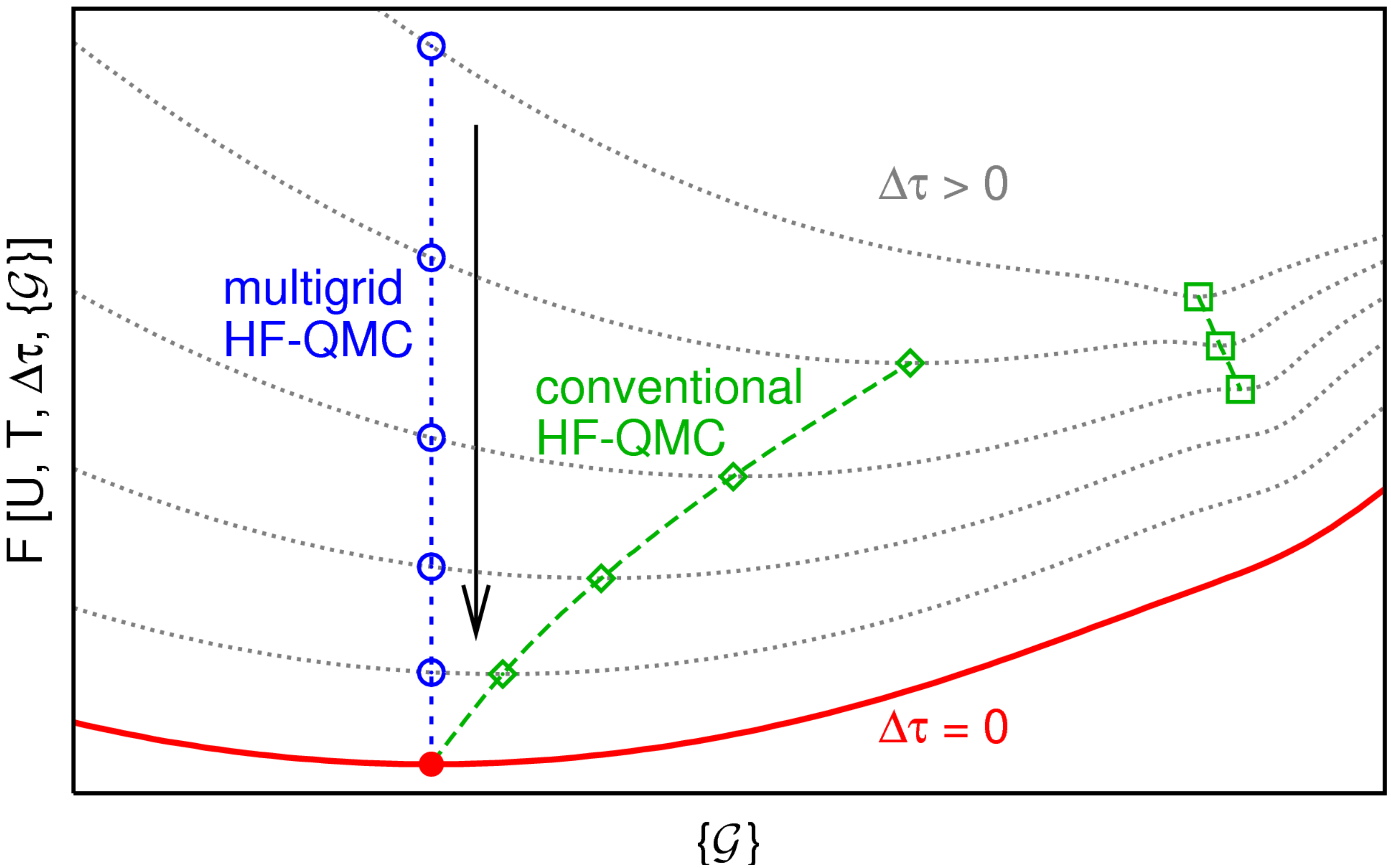

Conventional Hirsch-Fye QMC: DMFT fixed point shifts with $\Delta\tau$

Multigrid Hirsch-Fye QMC: DMFT iteration towards exact fixed point

Schematic comparison via generalized Ginzburg-Landau functionals

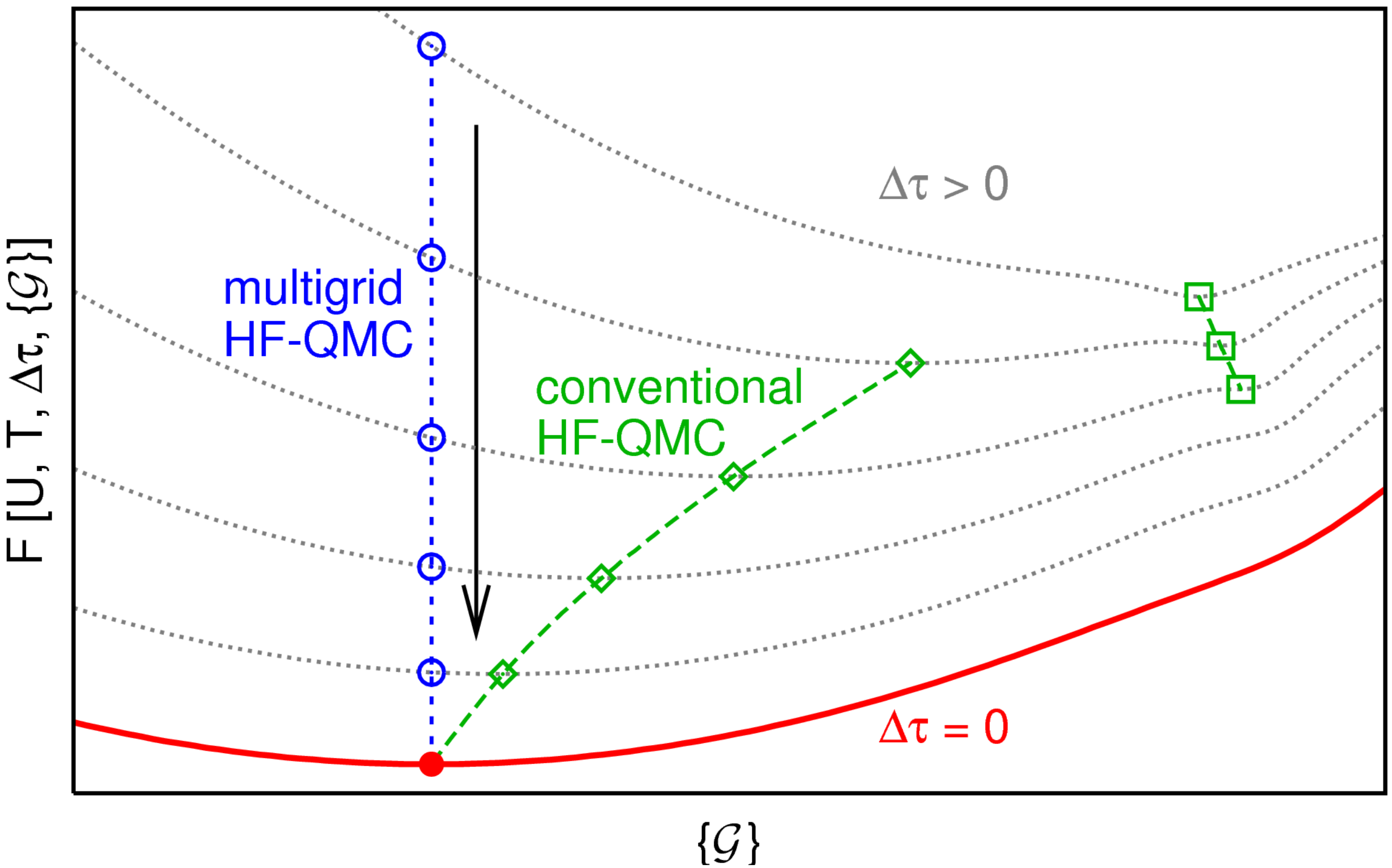

Conventional Hirsch-Fye QMC: DMFT fixed point shifts with $\Delta\tau$

Multigrid Hirsch-Fye QMC: DMFT iteration towards exact fixed point

Implementation: Green function extrapolation, hierarchy of frequency scales

Comparison: double occupancy $D = \langle n_{i\uparrow} n_{i\downarrow} \rangle$ near Mott transition

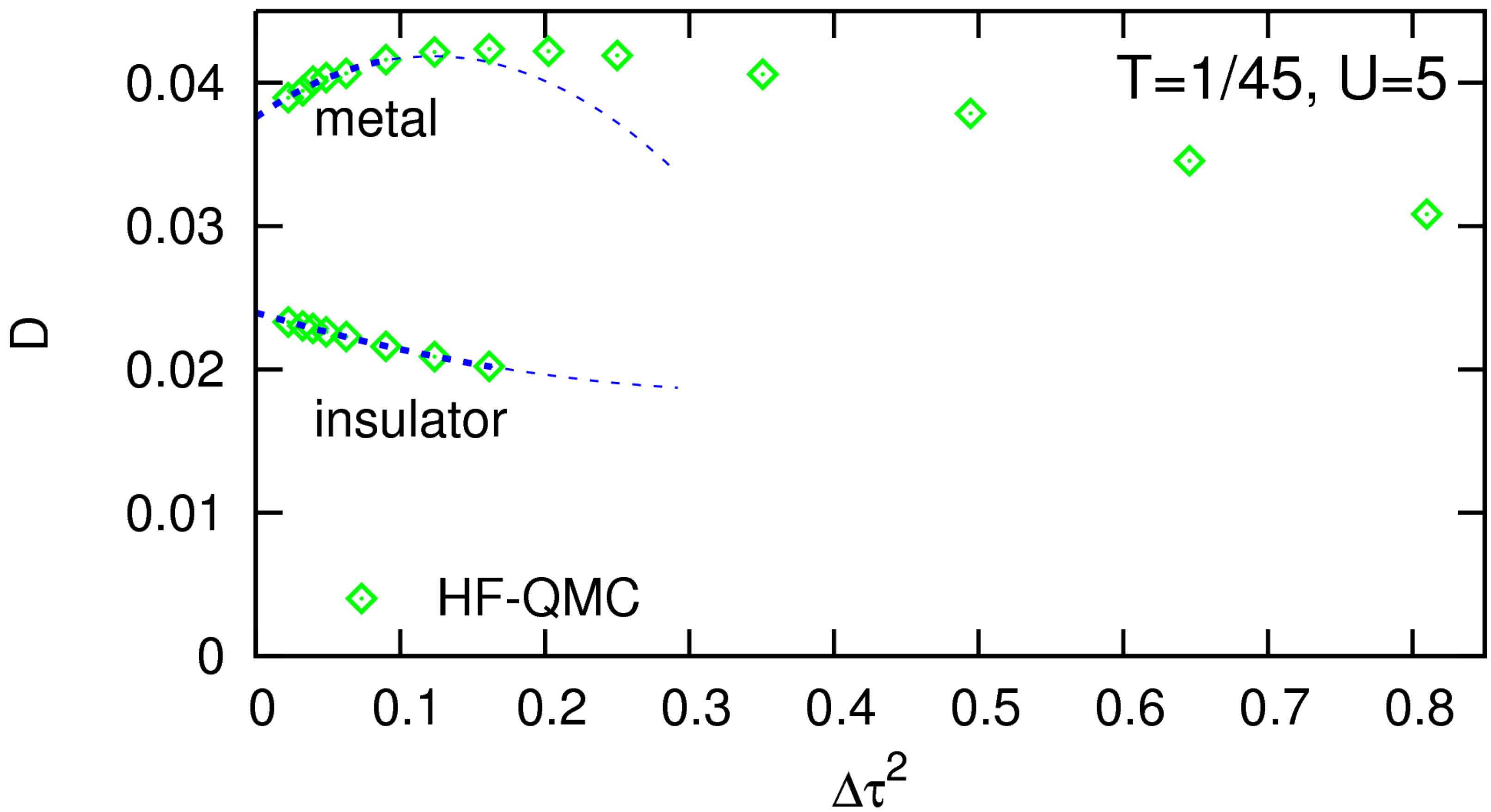

Conventional HF-QMC: no insulating solution for $\Delta\tau \gtrsim 0.4$

very irregular $\Delta\tau$ dependence beyond $\Delta\tau \approx 0.3$

Comparison: double occupancy $D = \langle n_{i\uparrow} n_{i\downarrow} \rangle$ near Mott transition

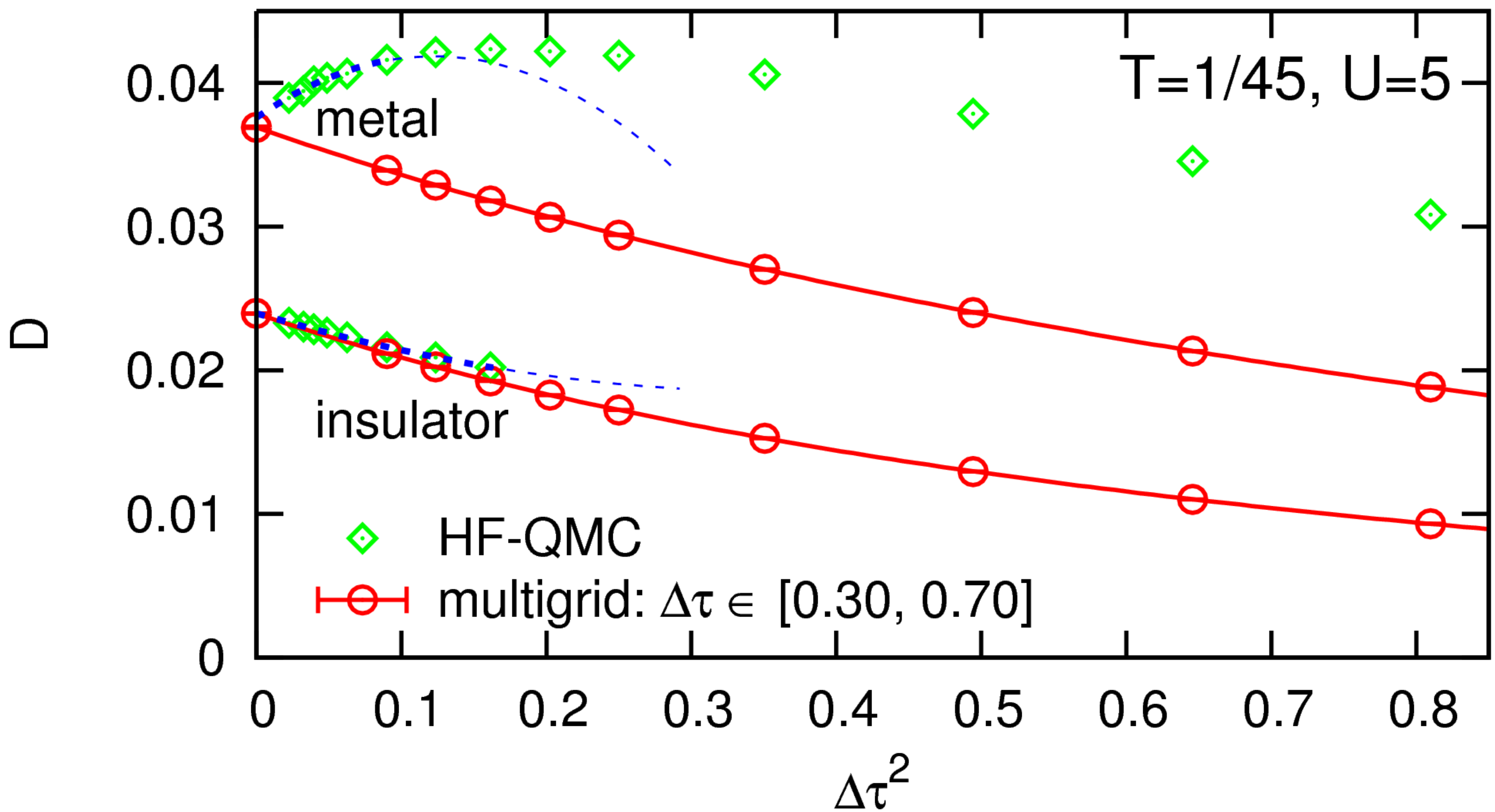

Conventional HF-QMC: no insulating solution for $\Delta\tau \gtrsim 0.4$

very irregular $\Delta\tau$ dependence beyond $\Delta\tau \approx 0.3$

Multigrid HF-QMC: vastly larger useful range of $\Delta\tau$

Systematic study: impact of grid range (on double occupancy)

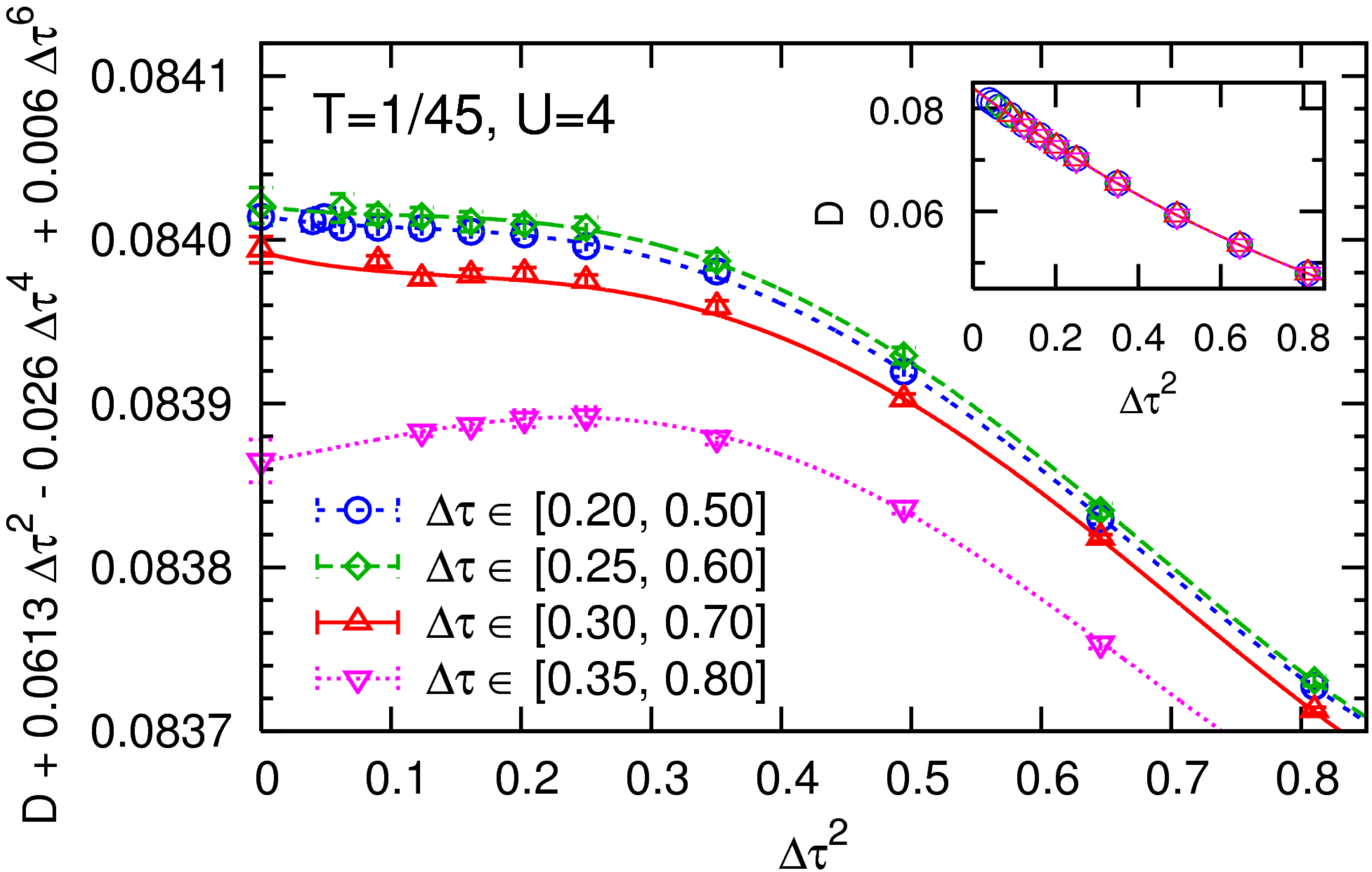

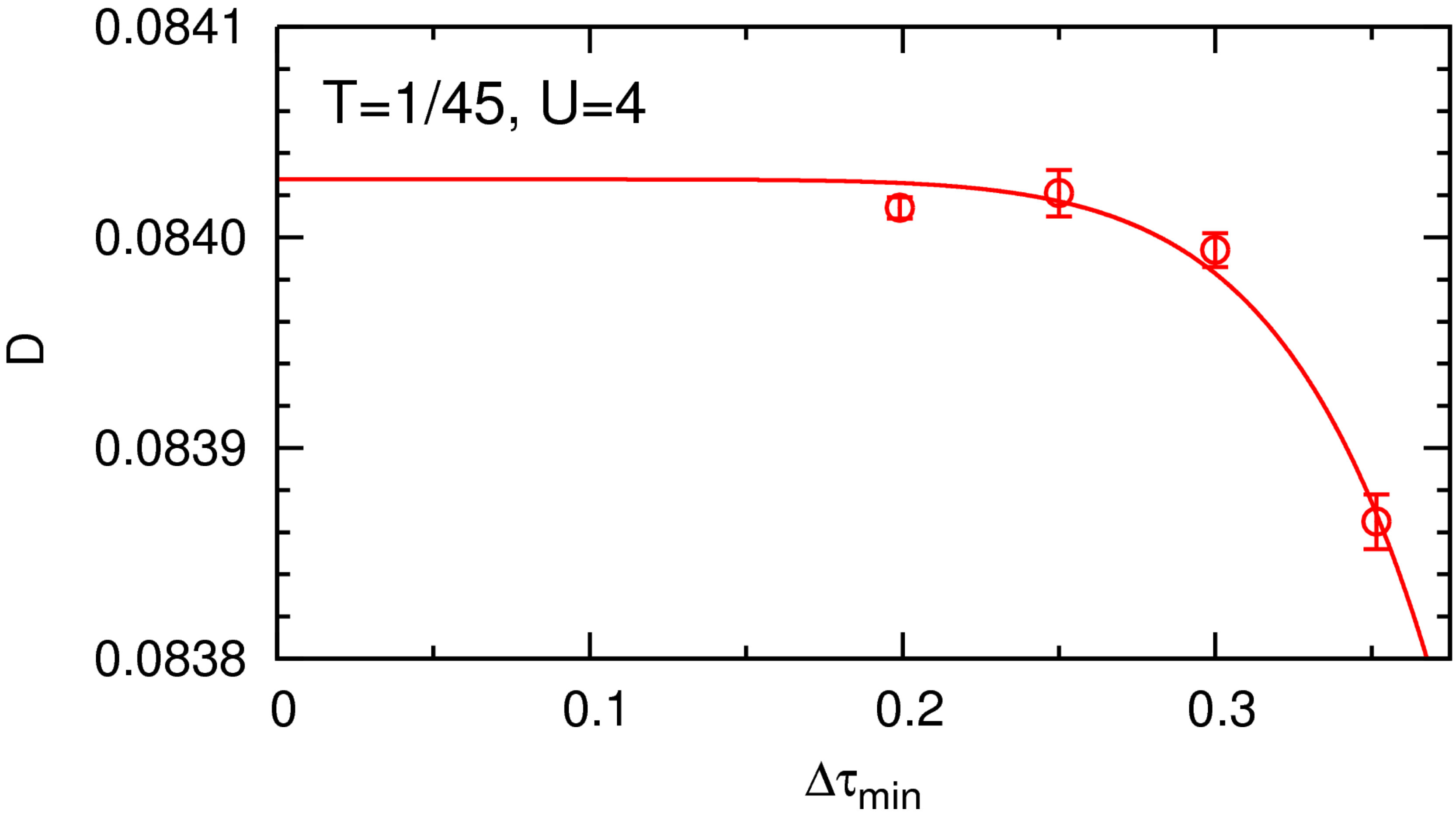

Multigrid HF-QMC usually “numerically exact” for $\tau_{\mathrm{min}} \lesssim 0.3$

Efficiency: potential energy $E_{pot} = UD$ (at $U = W = 4$)

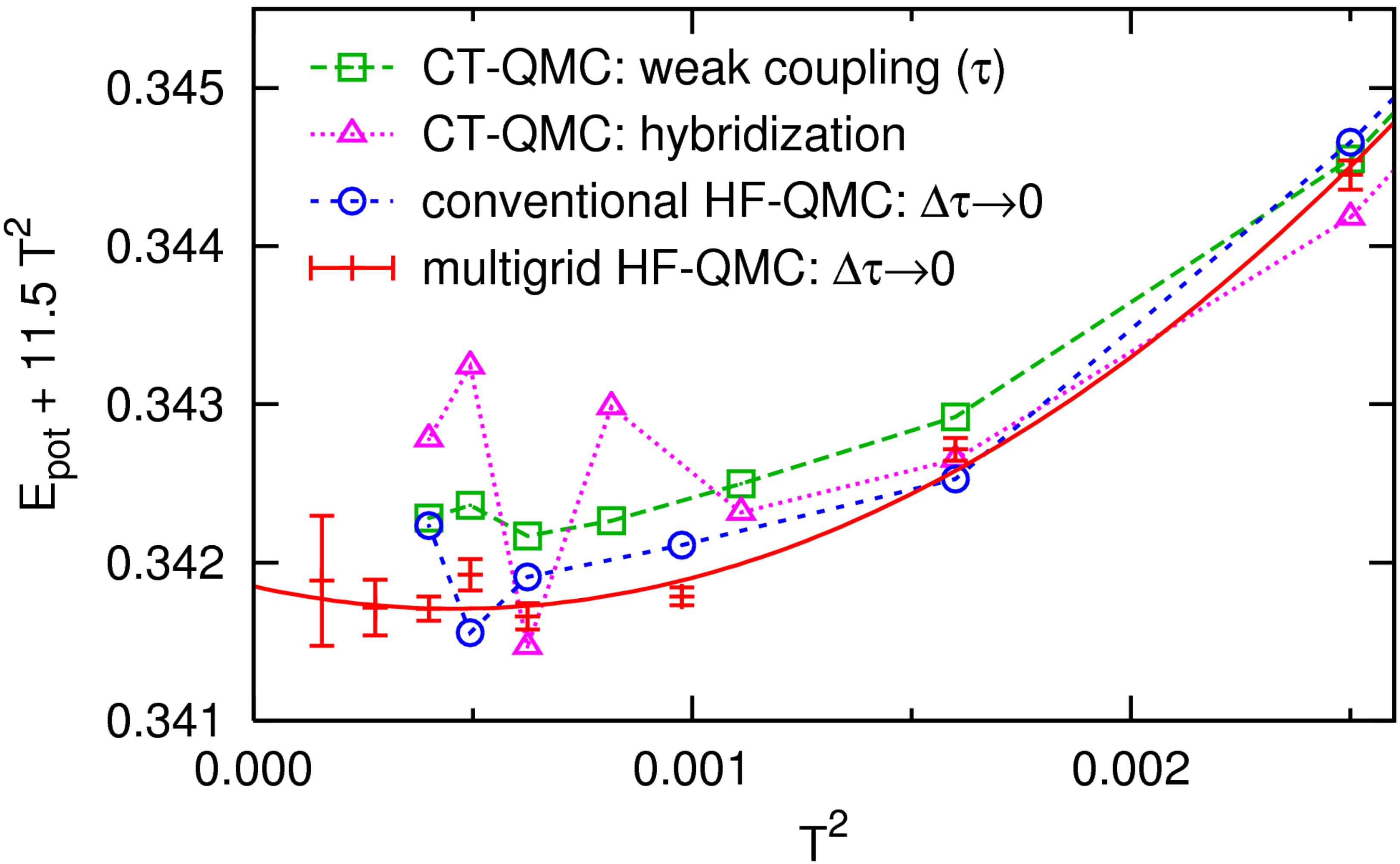

No more “difficult observables” for multigrid HF-QMC

Higher precision than CT-QMC methods at same effort

Spectral weight transfer at the Mott transition

Question: how does the Mott metal-insulator transition take place, precisely?

Spectral weight transfer at the Mott transition

Question: how does the Mott metal-insulator transition take place, precisely?

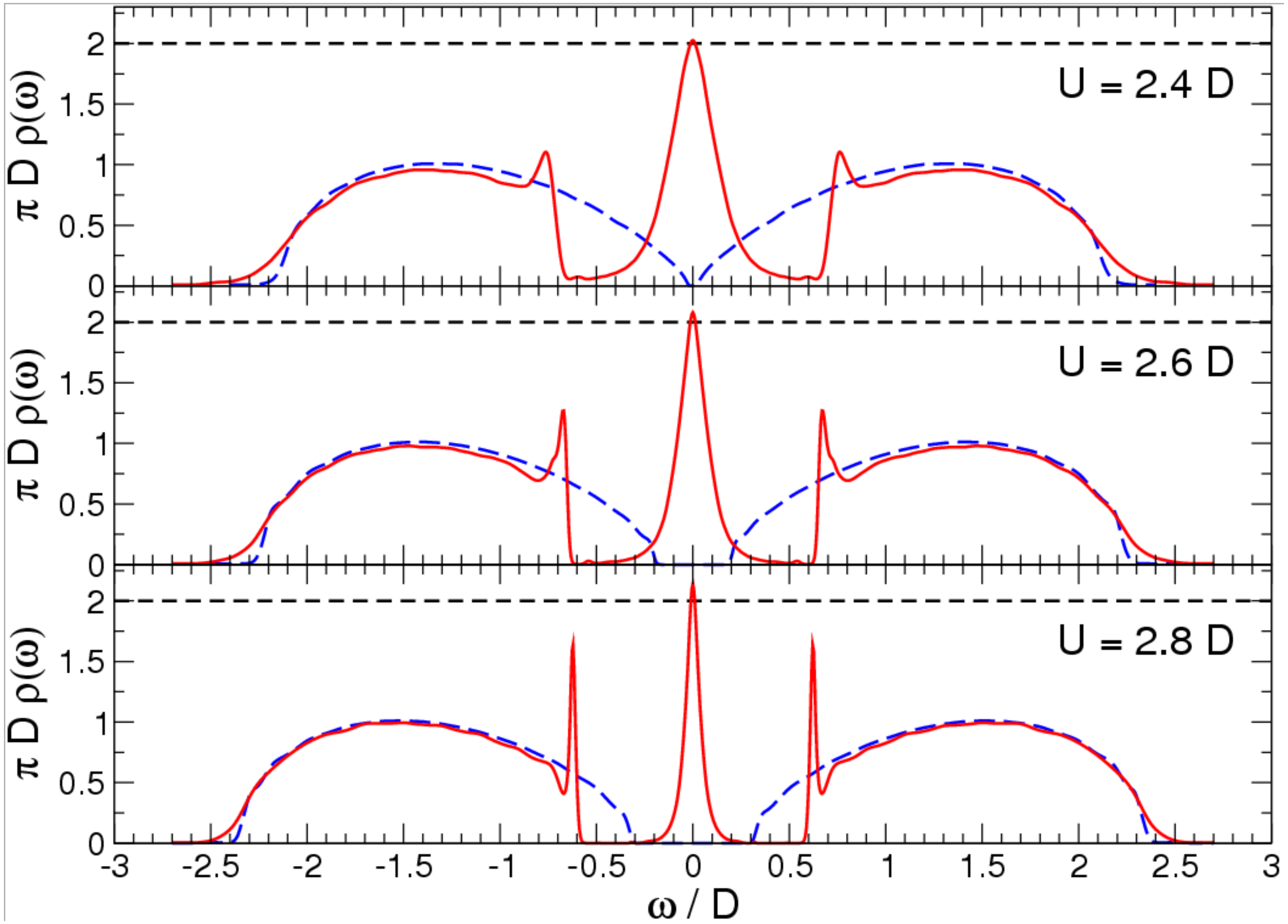

Dynamical DMRG ⇝ Hubbard band subpeaks in metallic phase (at $T = 0$)

[Karski, Raas, Uhrig, PRB (2005)]

Spectral weight transfer at the Mott transition

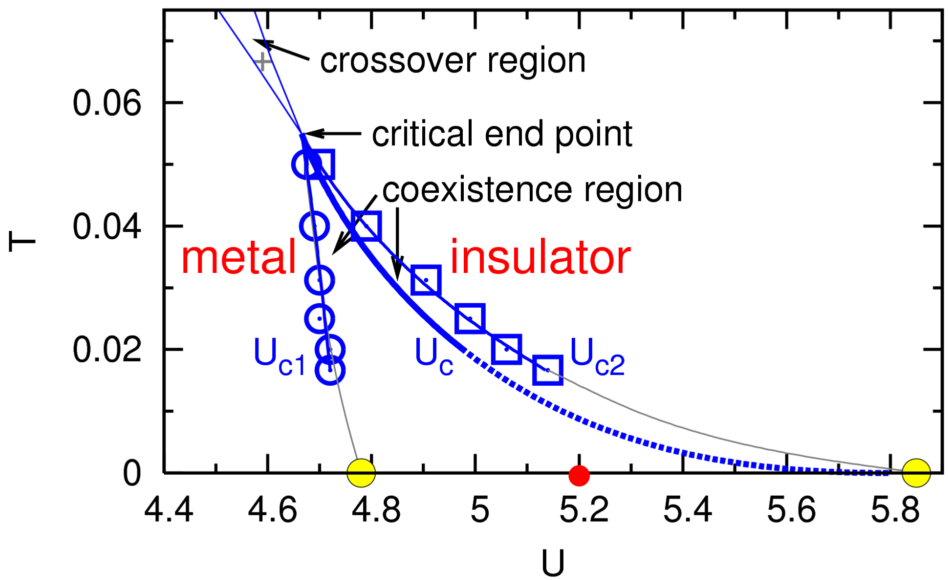

tor transition take place, precisely?

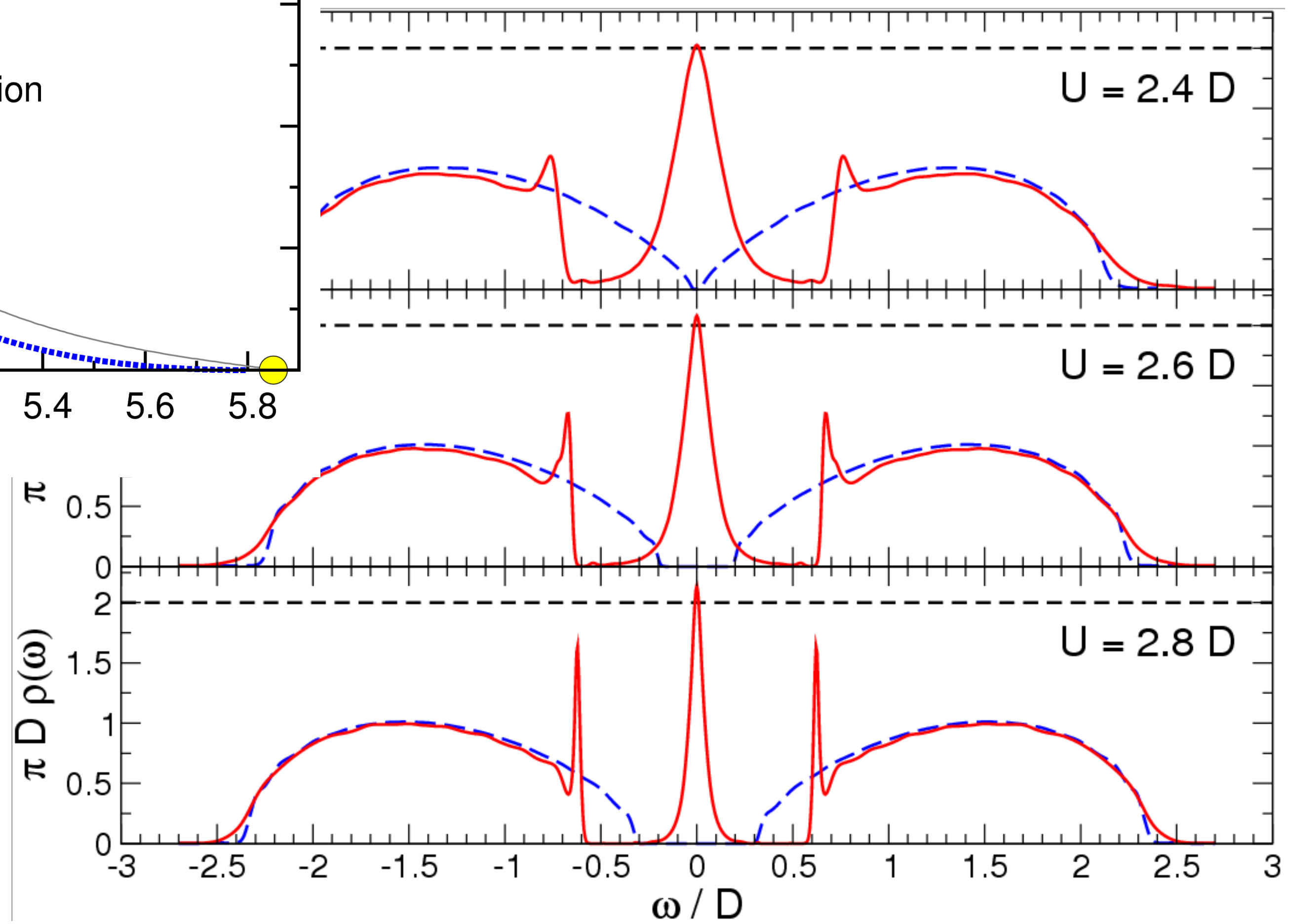

Dynamical DMRG ⇝ Hubbard band subpeaks in metallic phase (at $T = 0$)

[Karski, Raas, Uhrig, PRB (2005)]

Spectral weight transfer at the Mott transition

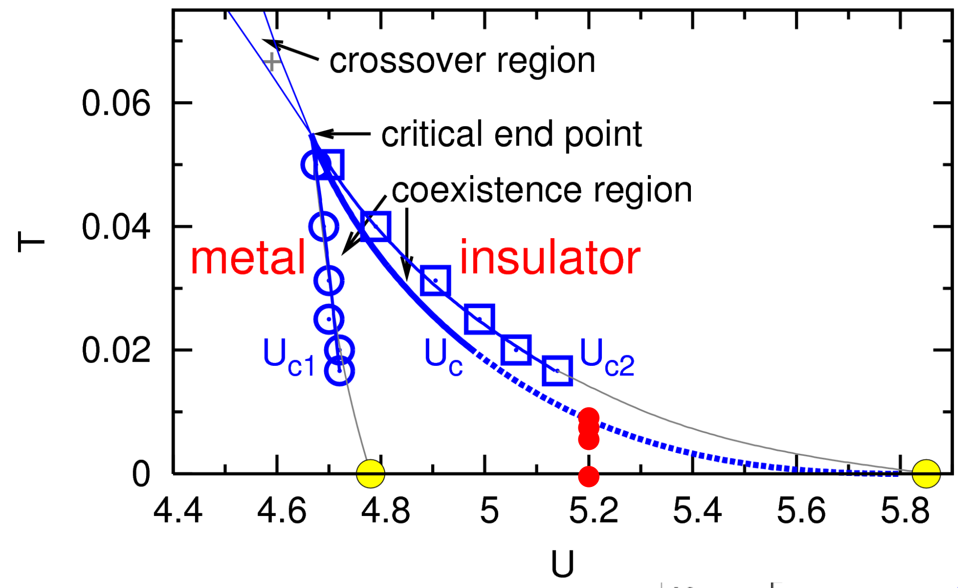

tor transition take place, precisely?

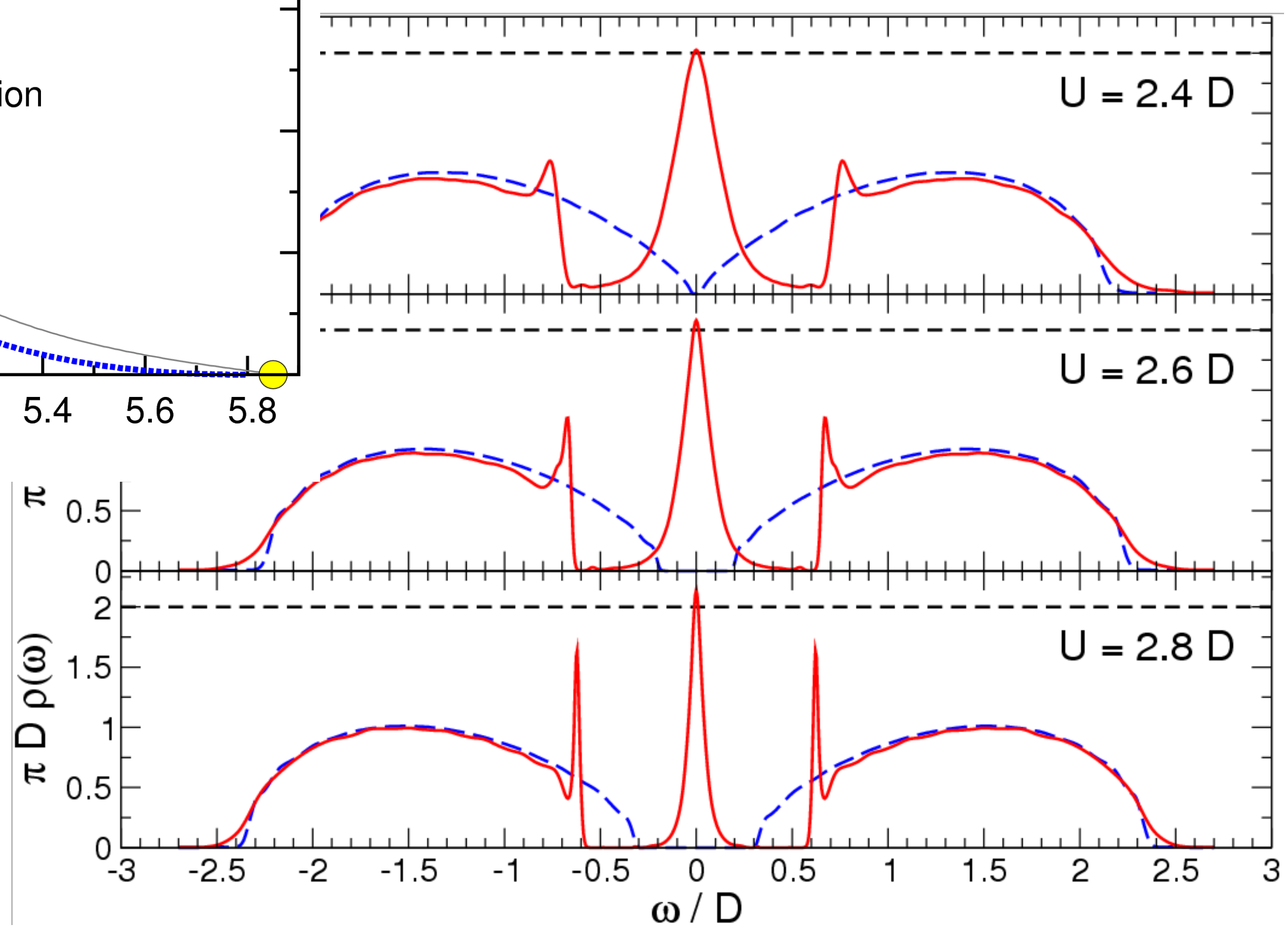

Dynamical DMRG ⇝ Hubbard band subpeaks in metallic phase (at $T = 0$)

[Karski, Raas, Uhrig, PRB (2005)]

Verify using multigrid HF-QMC. . .

Analysis via difference of spectral functions (symmetric in ω) at $U = 5.2$

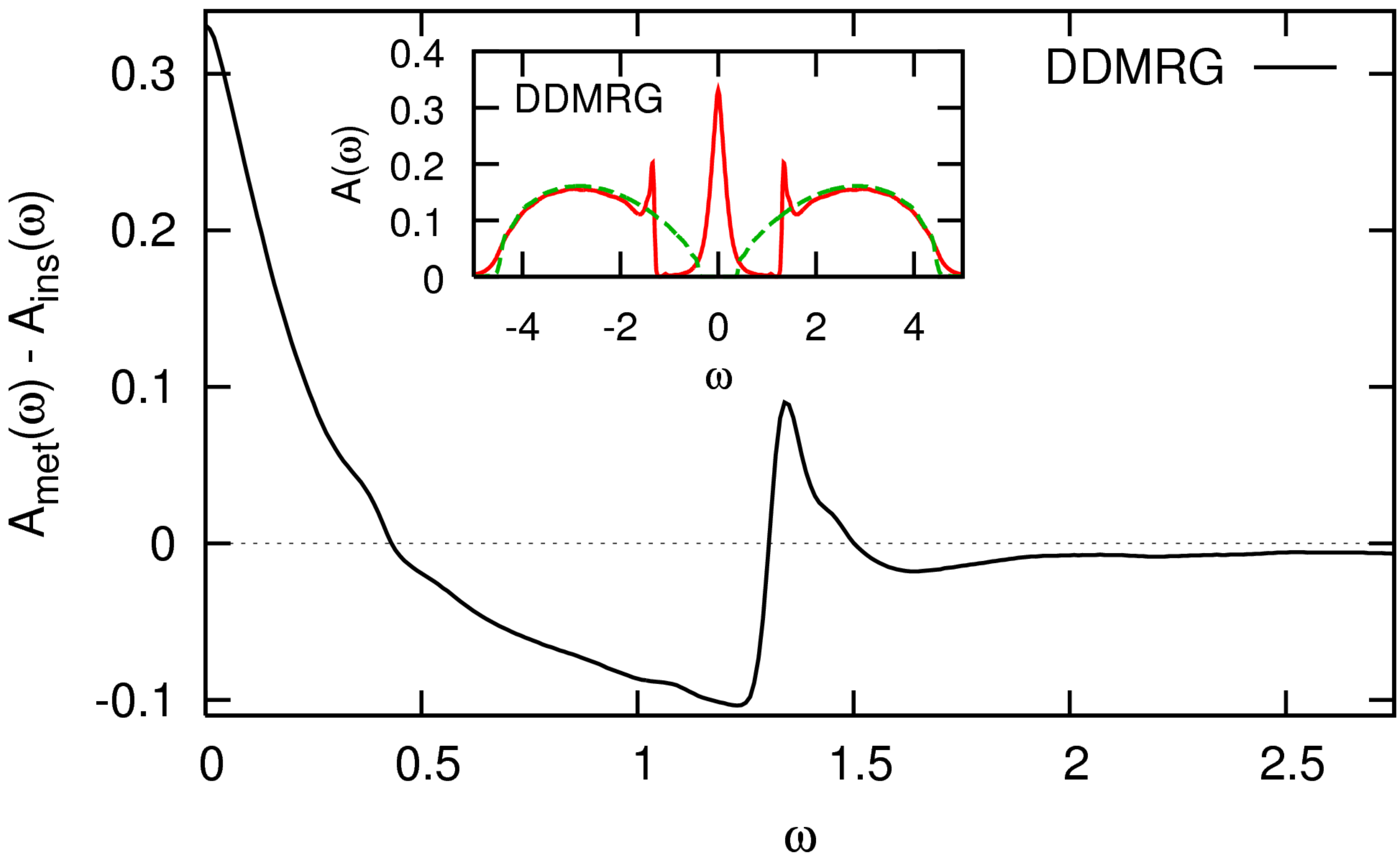

Problems for QMC: (i) analytic continuation of QMC data ill-conditioned

(ii) no $T \rightarrow 0$ extrapolation of spectra

Difference Green functions in imaginary time

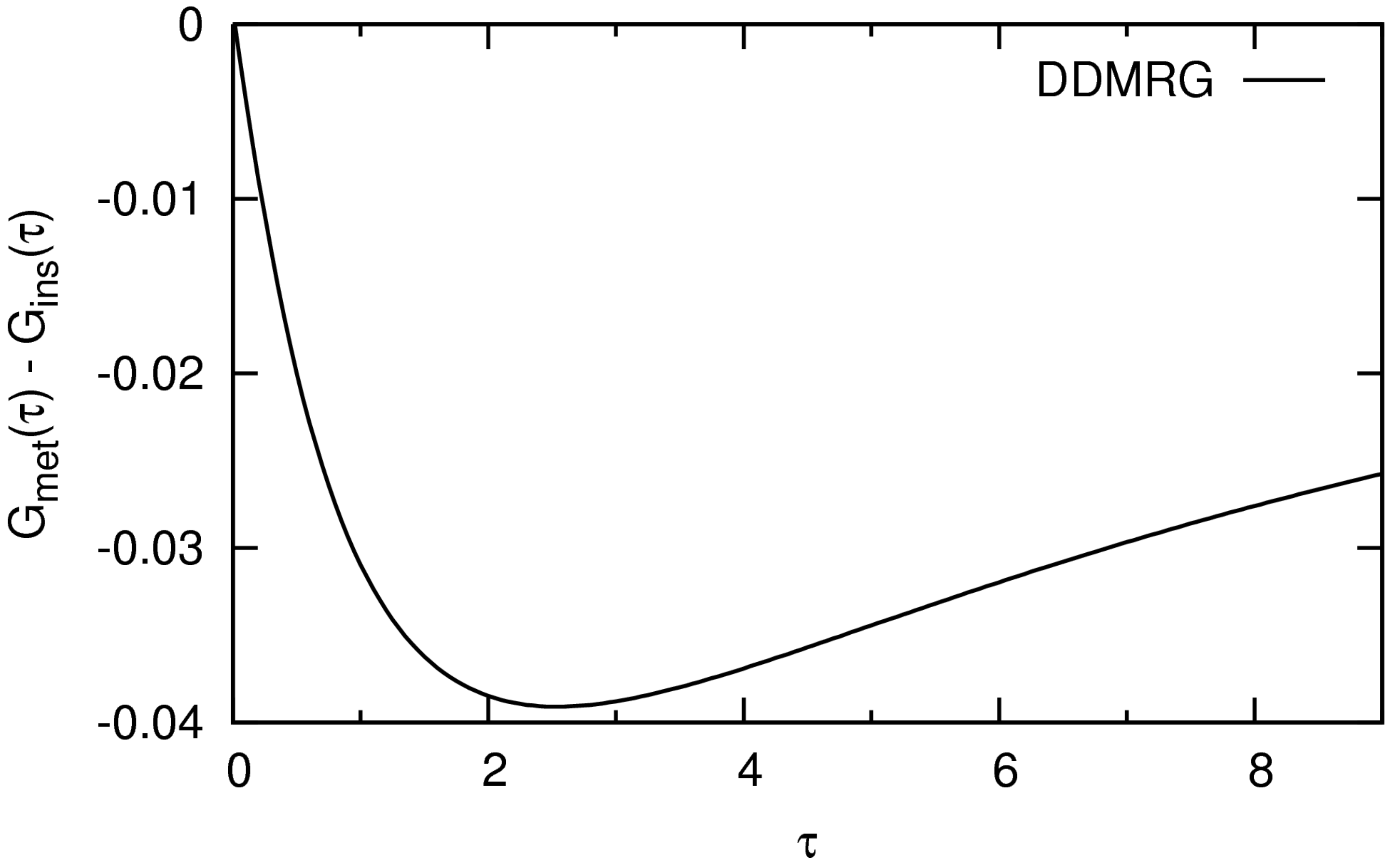

Difference Green functions in imaginary time

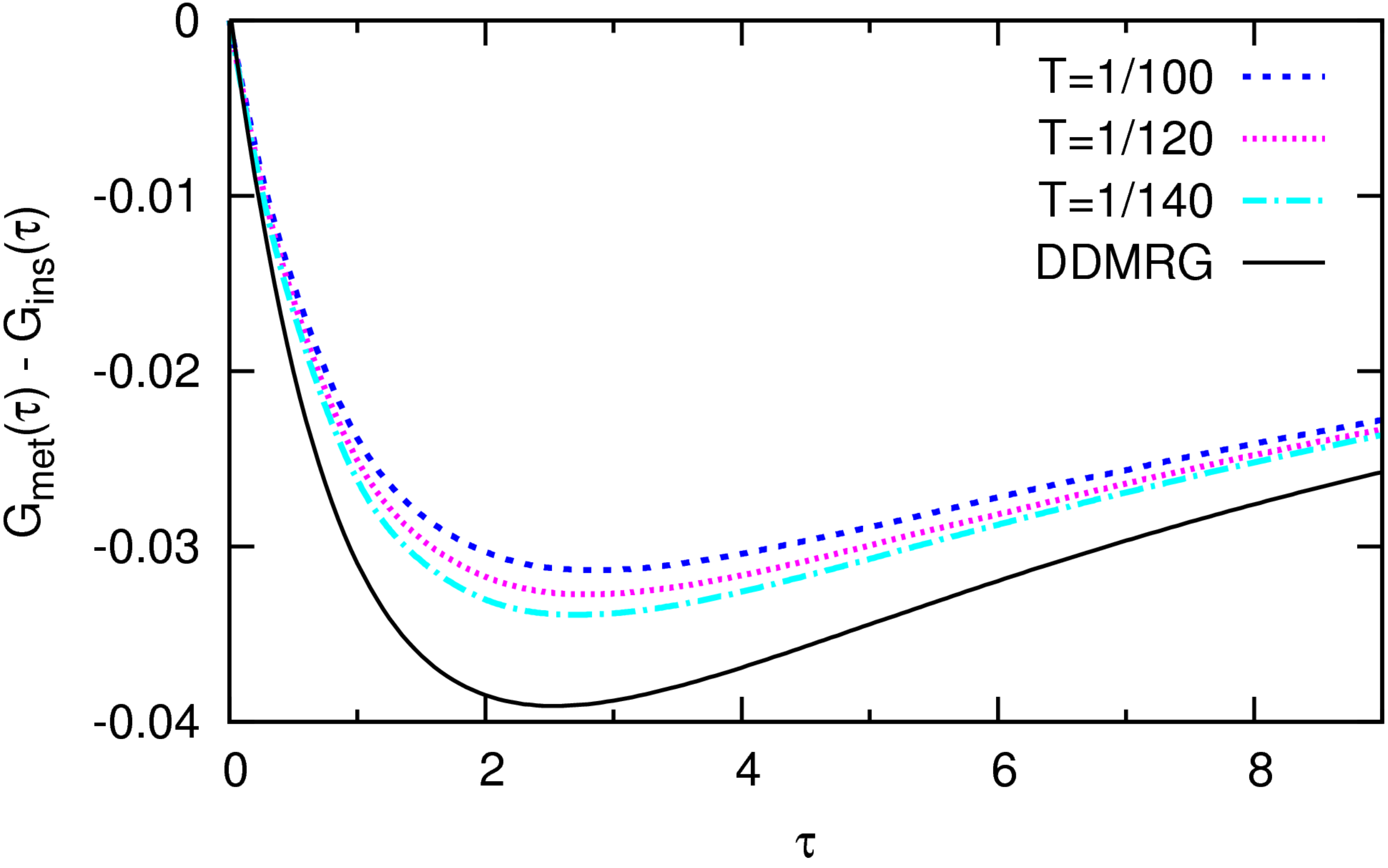

Difference Green functions in imaginary time

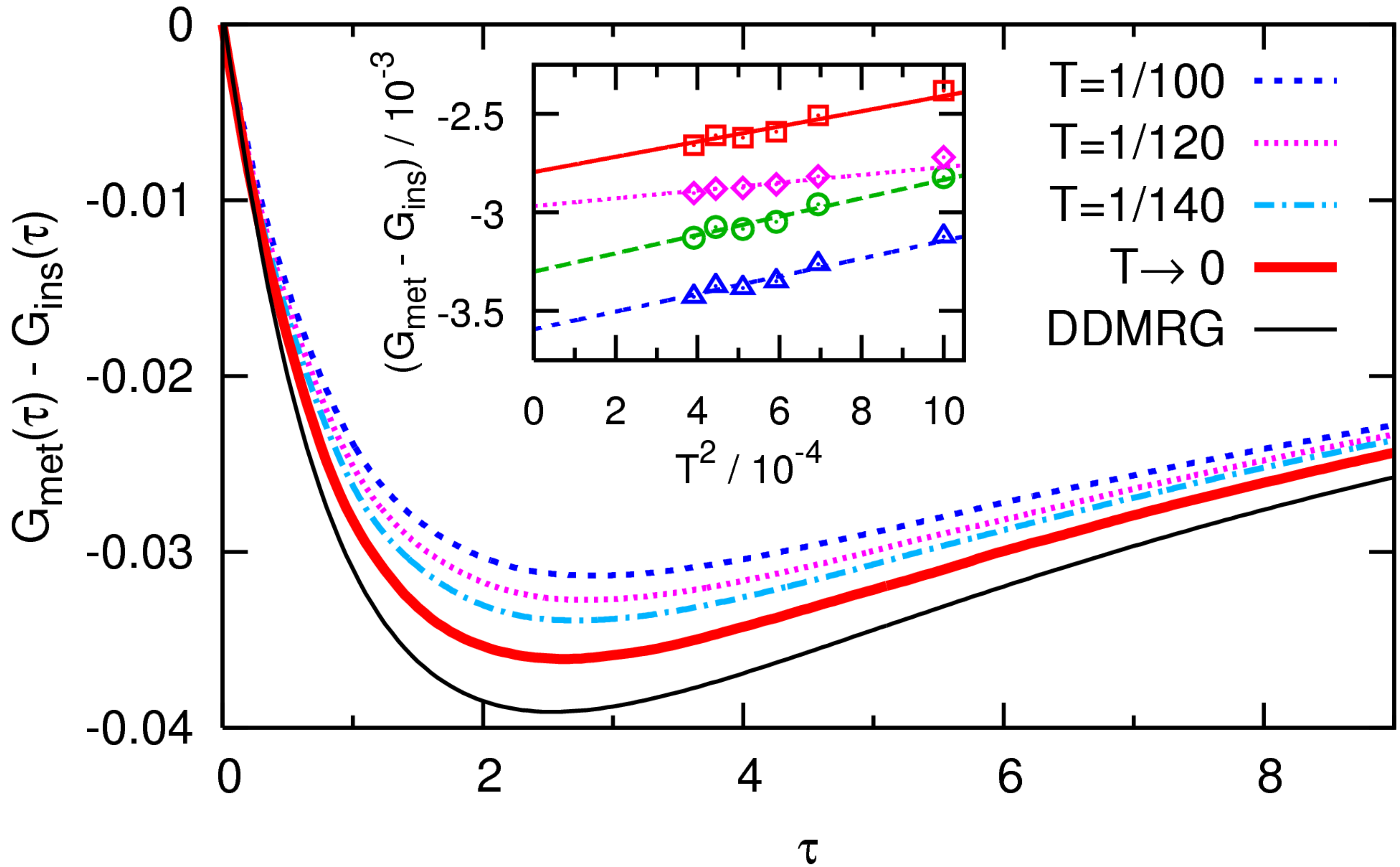

Multigrid HF-QMC data precise within linewidths [NB, arXiv:0801.1222]

DDMRG overestimates spectral weight transfer at $U = 5.2$ by about 10%!

Difference spectra

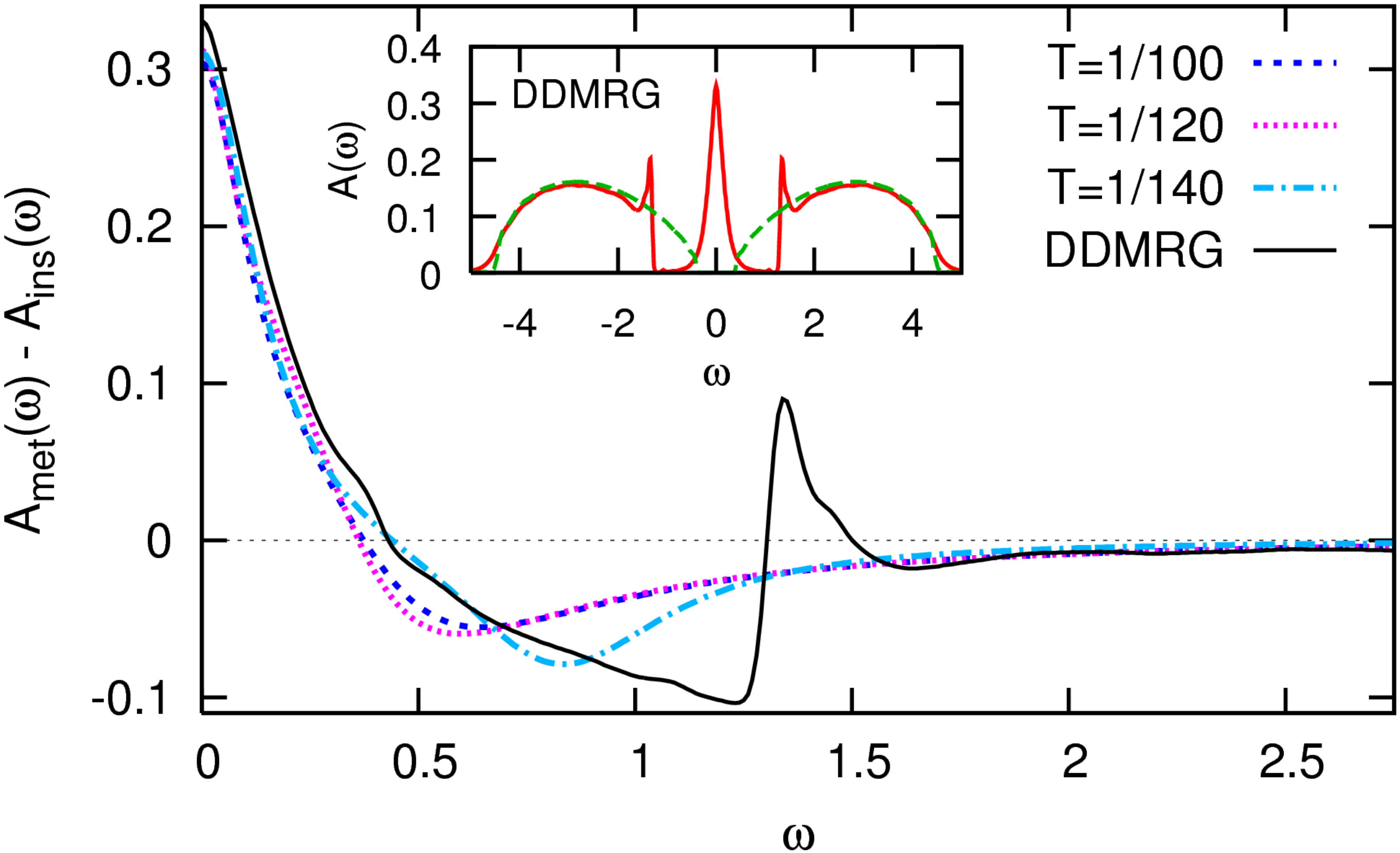

Similarities, but no indication for feature at $\omega = 1.3$ in QMC data

QMC spectral data via Padé interpolation, may be overly smooth [NB, arXiv:0801.1222]

Multigrid HF-QMC in multiband case

Test case: SU(4) symmetric 2-band model ($U = V$, $J = 0$)

Multigrid HF-QMC in multiband case

Test case: SU(4) symmetric 2-band model ($U = V$, $J = 0$)

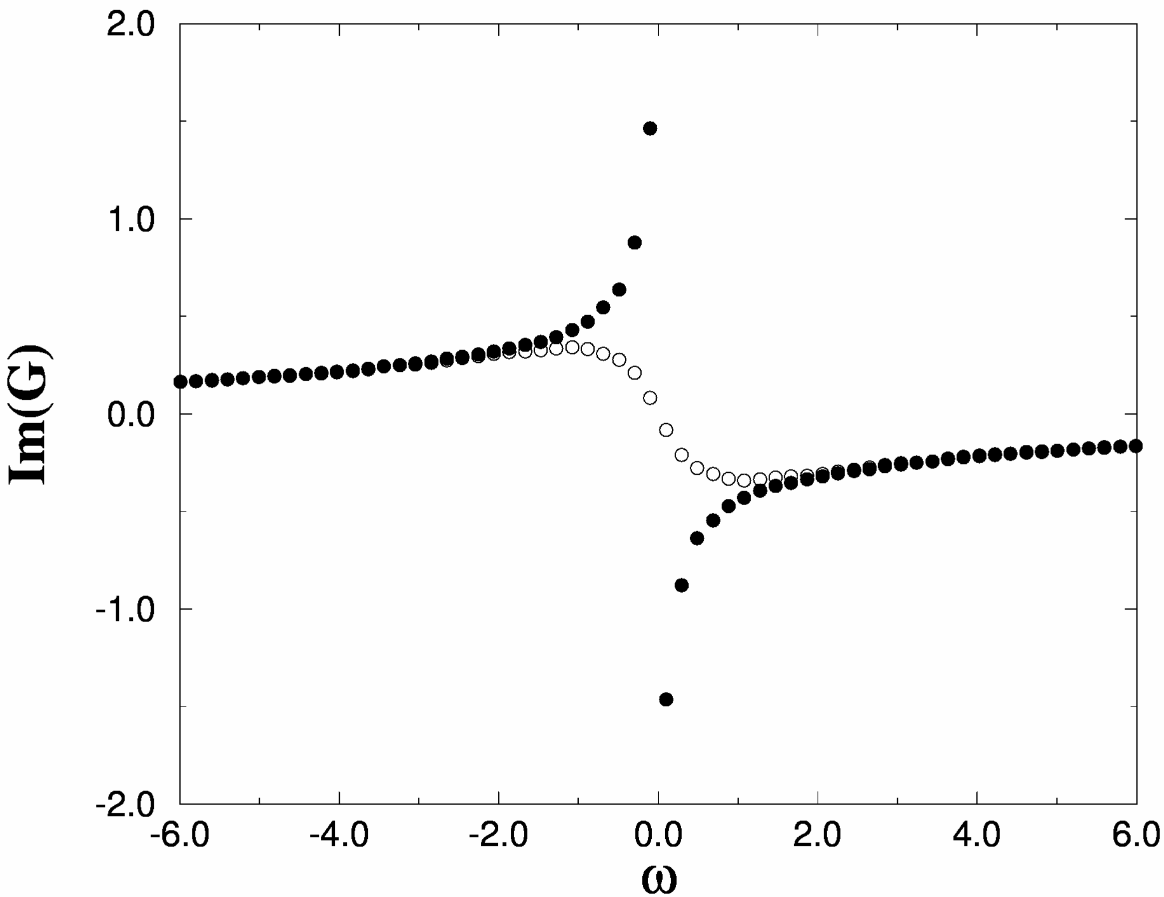

Bethe DOS

$W = 2$

$U = V = 3.4$

$T = 1/32$

[Rozenberg, Phys. Rev. B **55**, R4855 (1997)]

Discrepancies with CT-QMC (Fuchs/Pruschke) and HF-QMC (Nekrasov)

Imaginary-frequency Green function for metallic phase

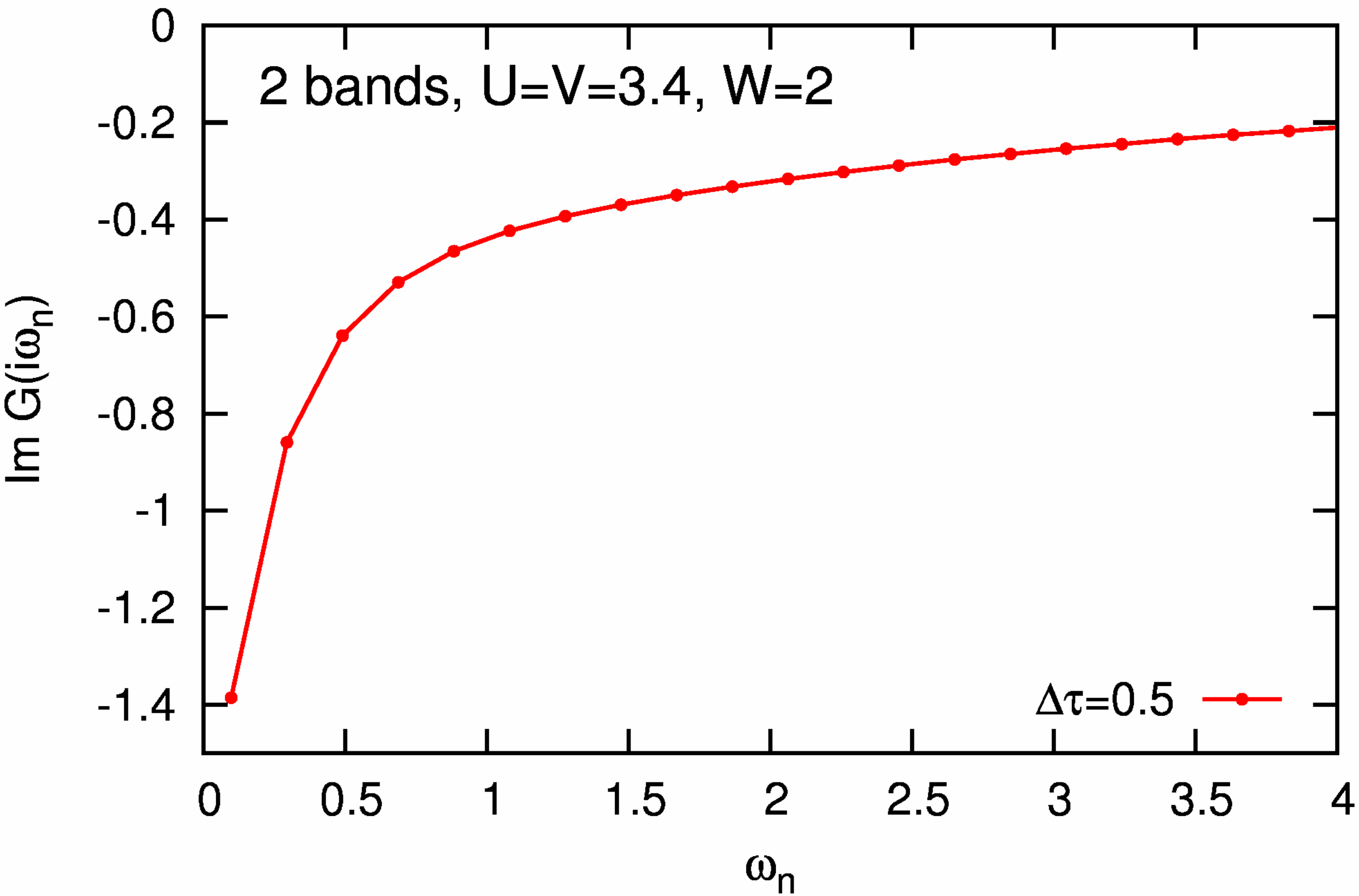

Imaginary-frequency Green function for metallic phase

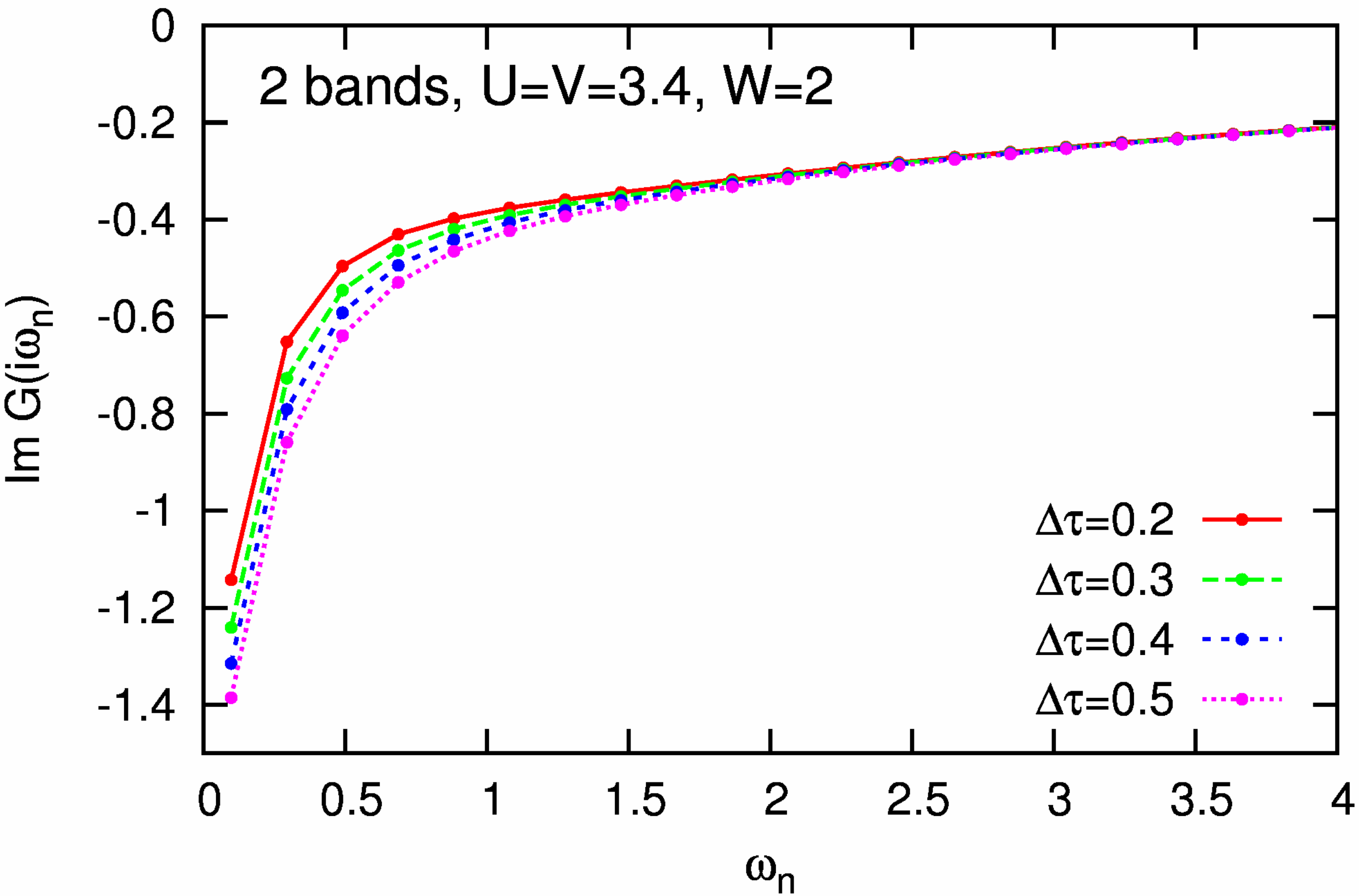

Imaginary-frequency Green function for metallic phase

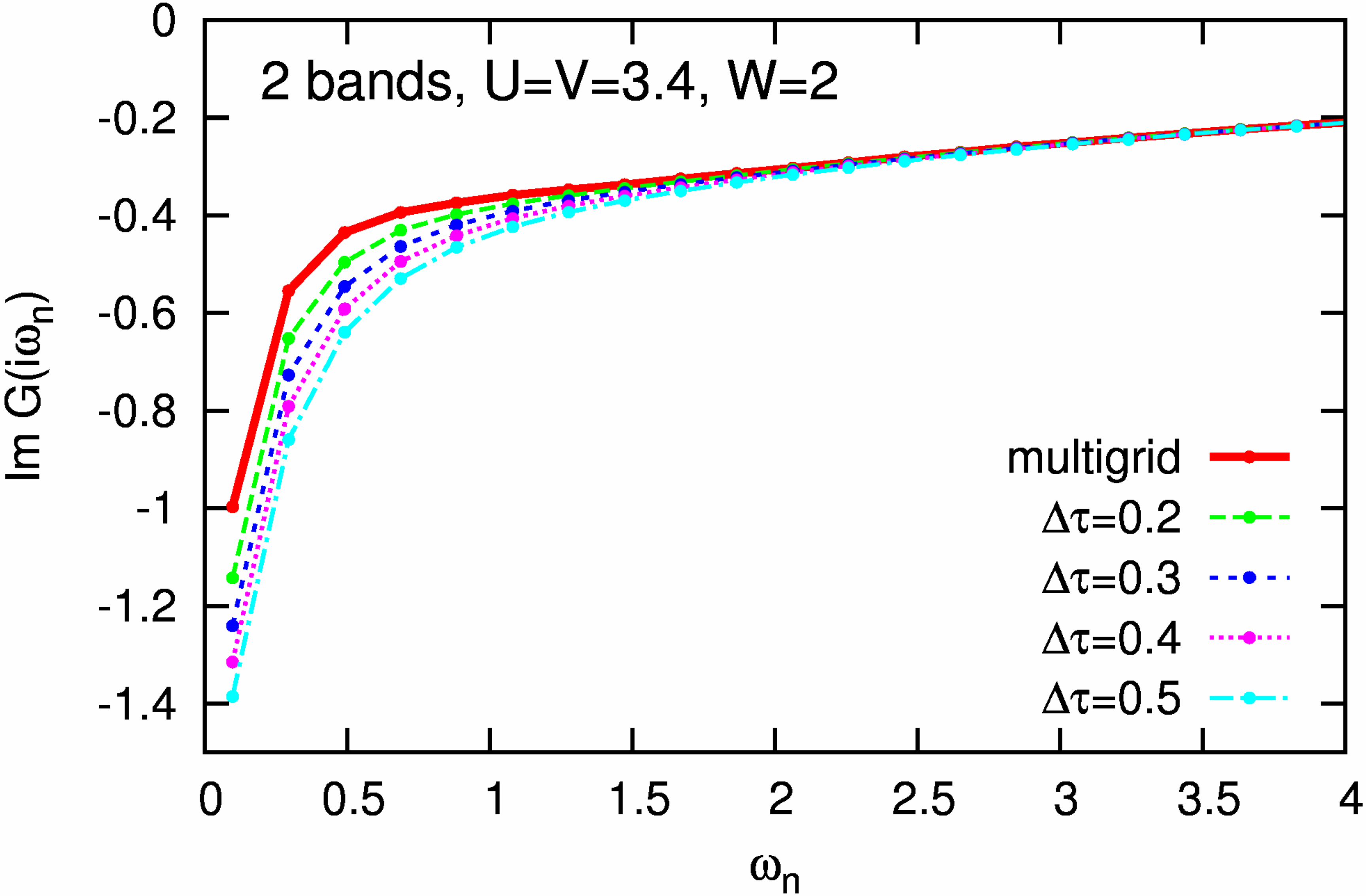

Multigrid algorithm essential for reliable results!

Thermal breakdown of a Fermi liquid

Fermi liquid theory:	linear specific heat	$c_V = \gamma T$	
	linear entropy	$S = \gamma T$	
	quadratic resistivity	$\rho \propto T^2$	for "low enough" T

When/how do these laws break down?

Thermal breakdown of a Fermi liquid

Fermi liquid theory: linear specific heat $c_V = \gamma T$

linear entropy $S = \gamma T$

quadratic resistivity $\rho \propto T^2$ for “low enough” T

When/how do these laws break down?

Exact diagonalization study (8 sites) for 1-band Hubbard model

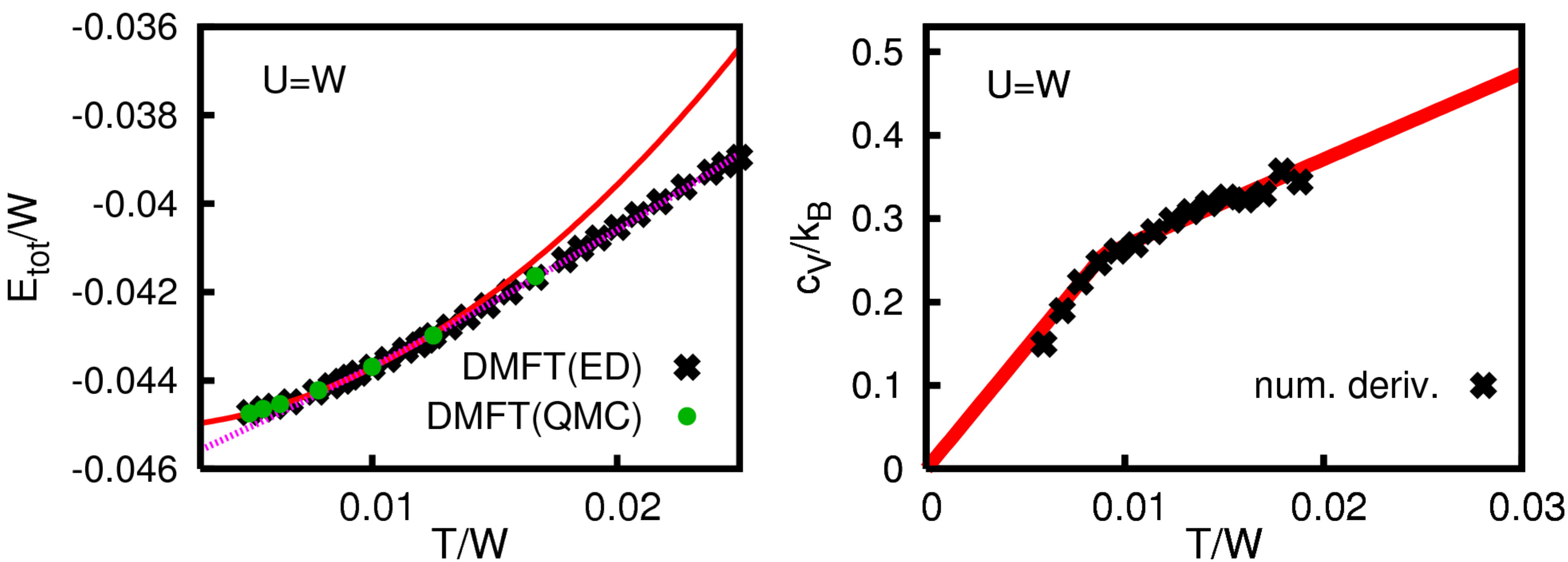

Distinct kink in c_V! [A. Toschi, M. Capone, C. Castellani, K. Held, arXiv:0712.3723]

Theoretical explanation: kink in self-energy ⇝ kink in c_V

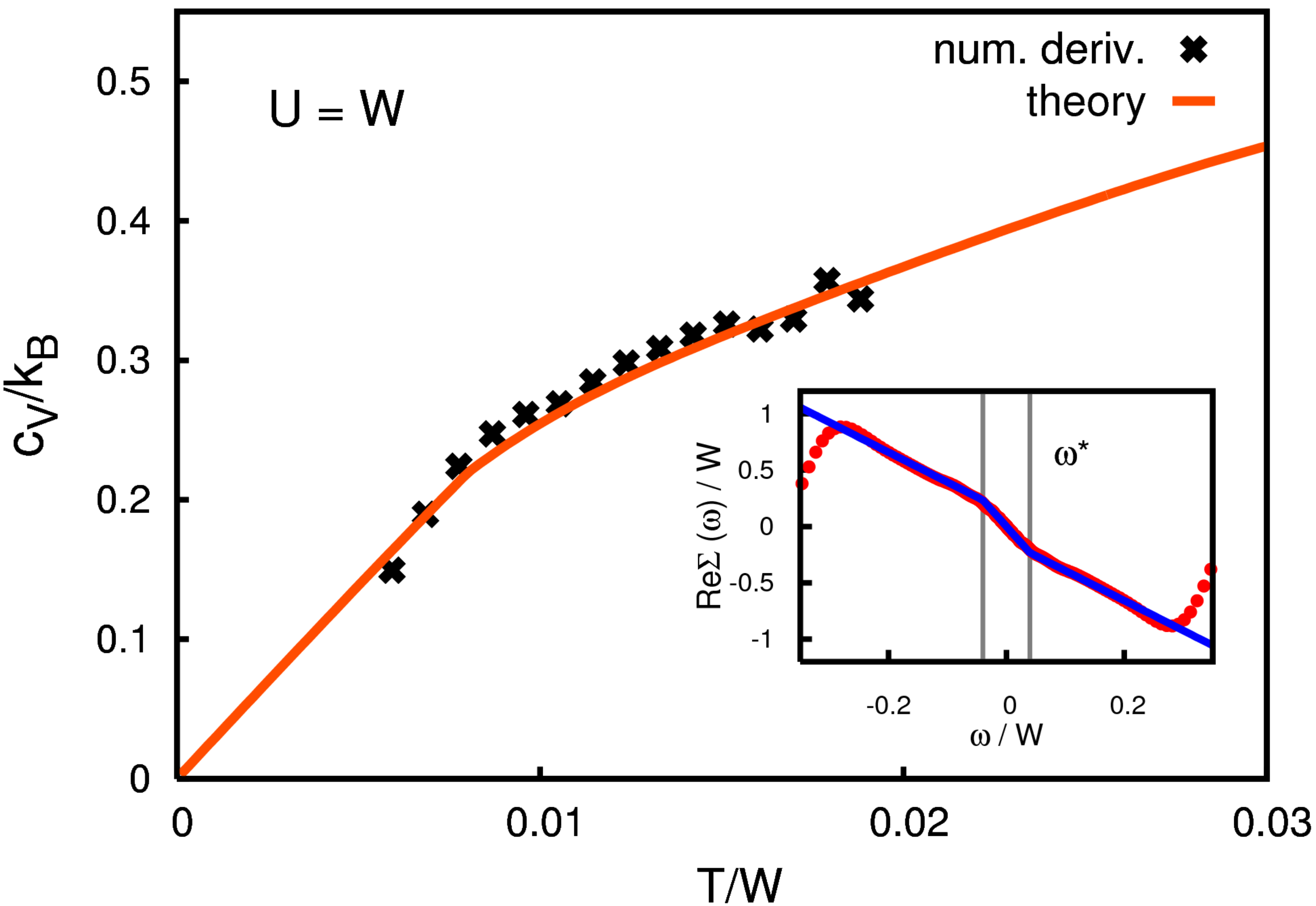

[A. Toschi, M. Capone, C. Castellani, K. Held, arXiv:0712.3723]

Kink feature visible in specific heat of heavy fermion LiV_2O_4?

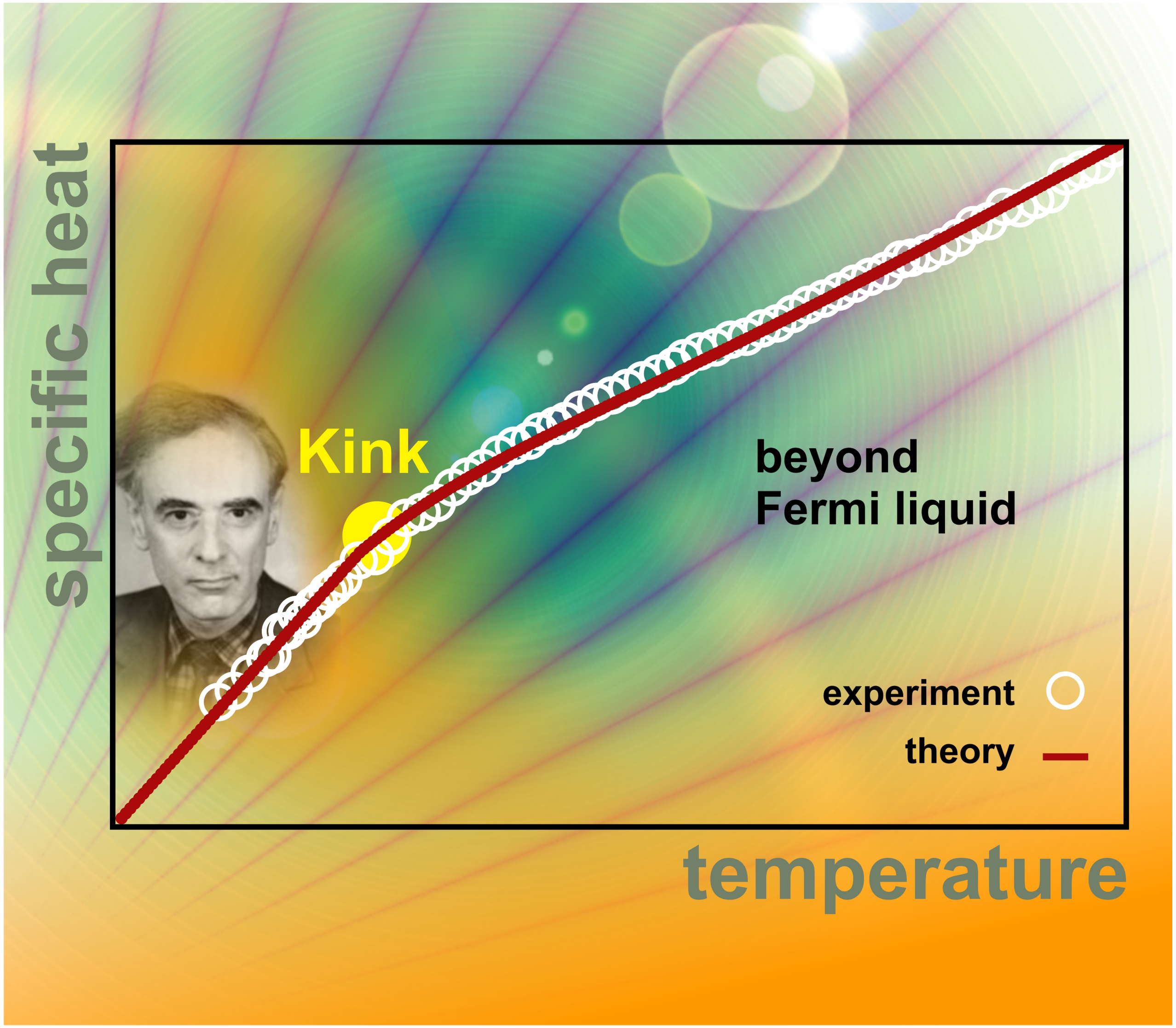

[A. Toschi, M. Capone, C. Castellani, K. Held, arXiv:0712.3723]

back to the model . . .

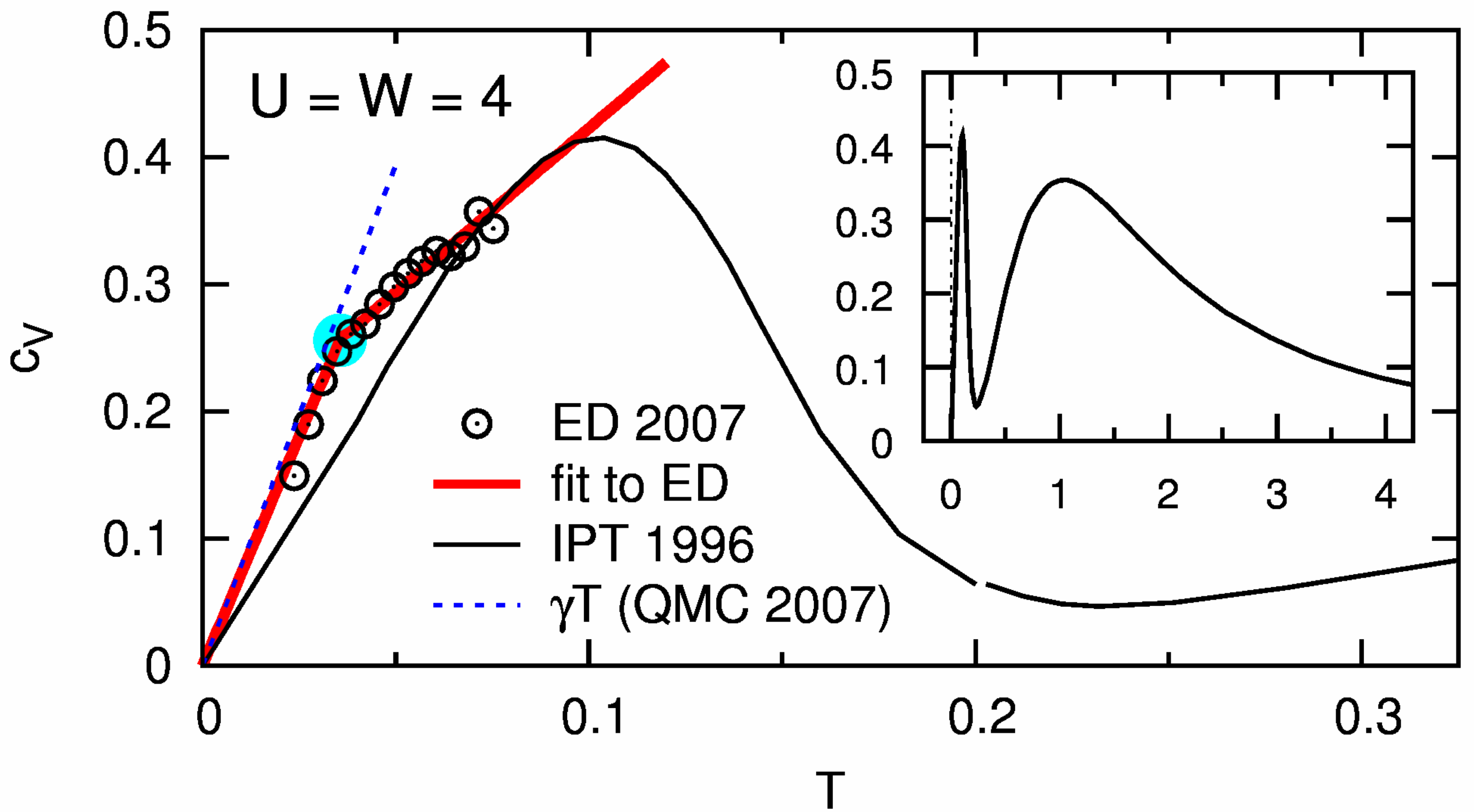

Significant discrepancies

Check using QMC. . .

Short version

Long version

First shot: conventional HF-QMC at constant discretization $\Delta\tau$, numerical derivatives from parabolic interpolation of tripels

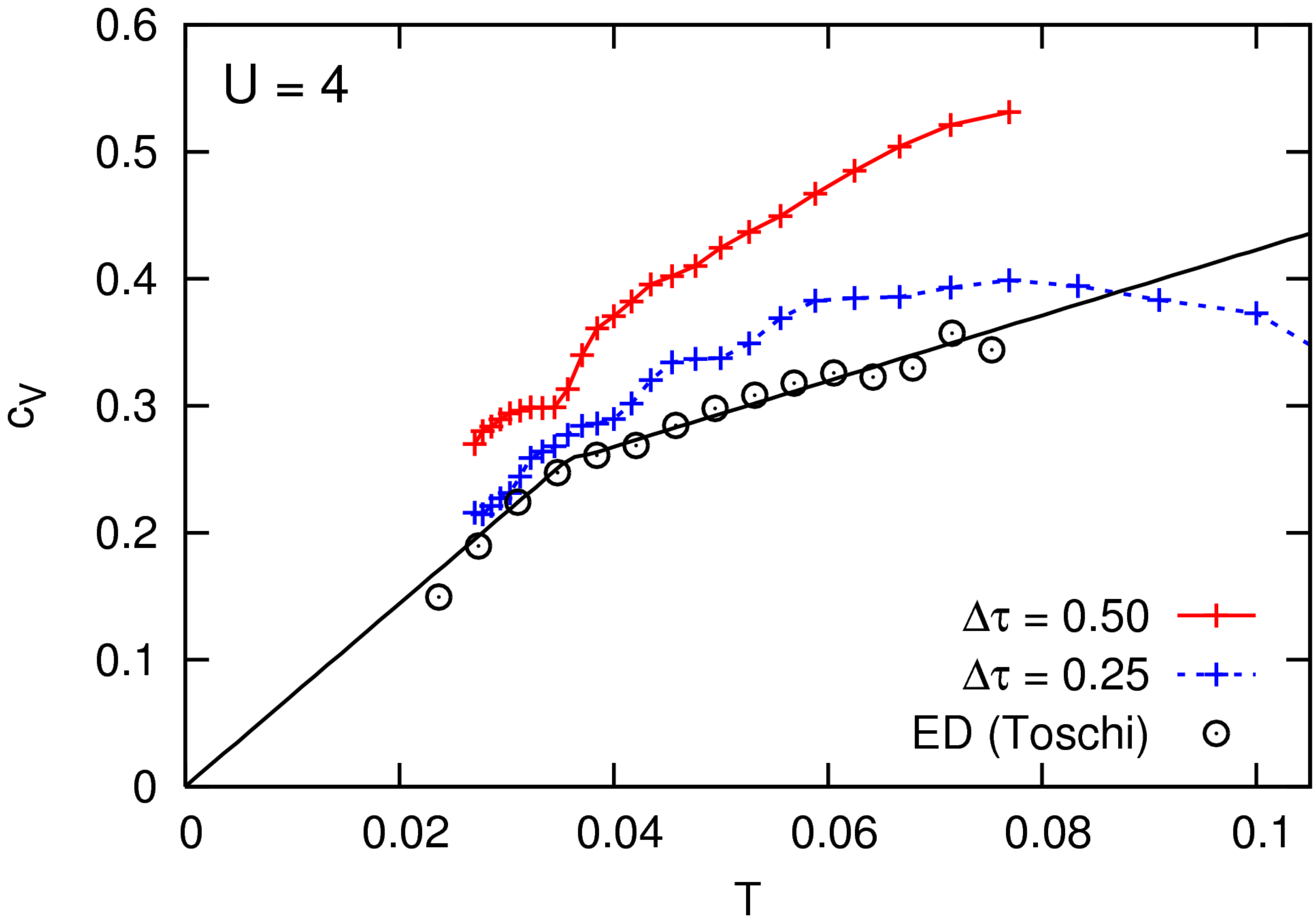

Roughly consistent with ED, but: no significant kinks, maximum at $T \approx 0.08$?

Best (only?) way to exclude kink: rescale data to straight line!

Best (only?) way to exclude kink: rescale data to straight line!

(i) consider c_V/T

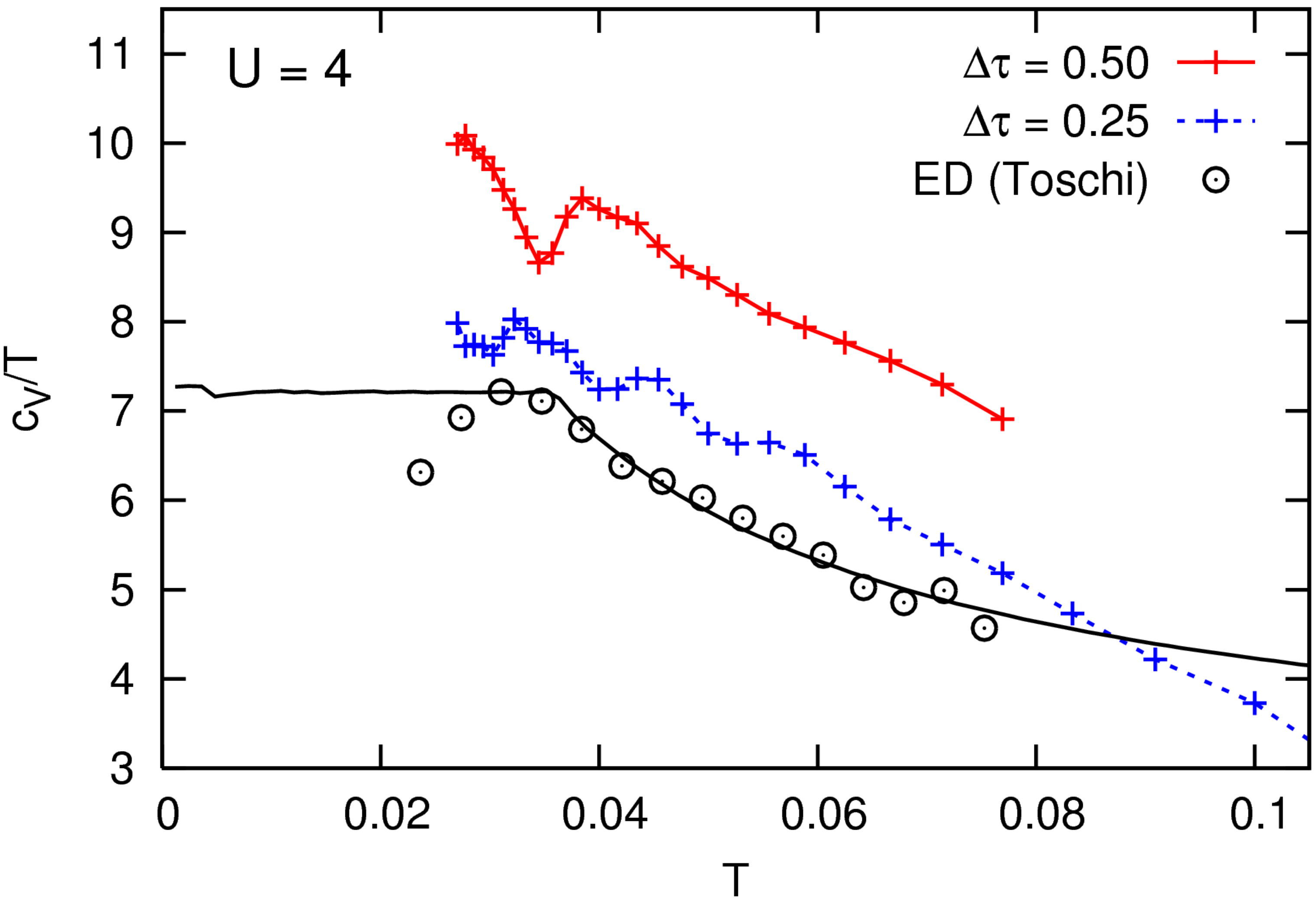

Best (only?) way to exclude kink: rescale data to straight line!

(i) consider c_V/T (ii) $T \longrightarrow T^2$

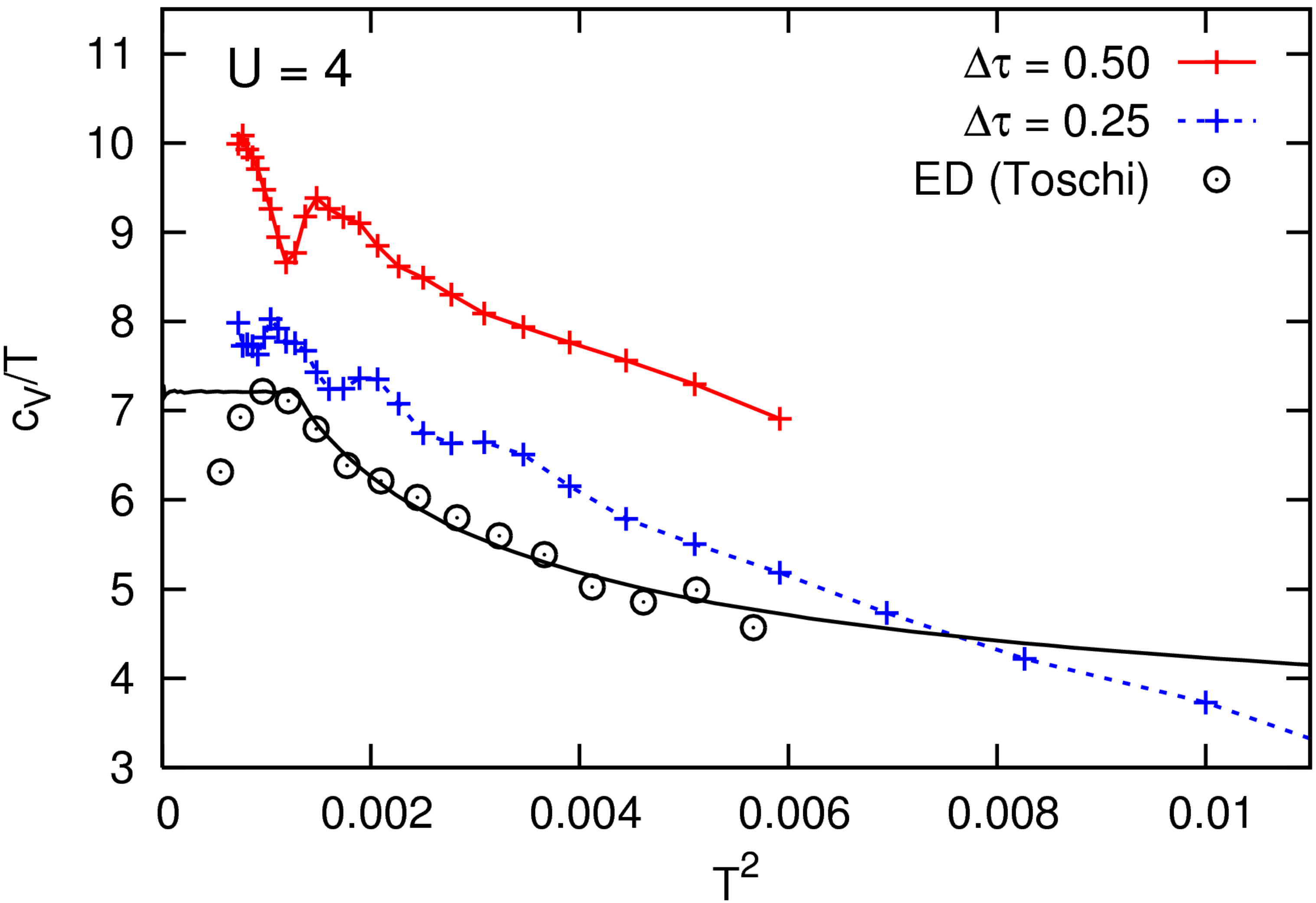

Best (only?) way to exclude kink: rescale data to straight line!

(i) consider c_V/T (ii) $T \longrightarrow T^2$ (iii) logarithmic scale

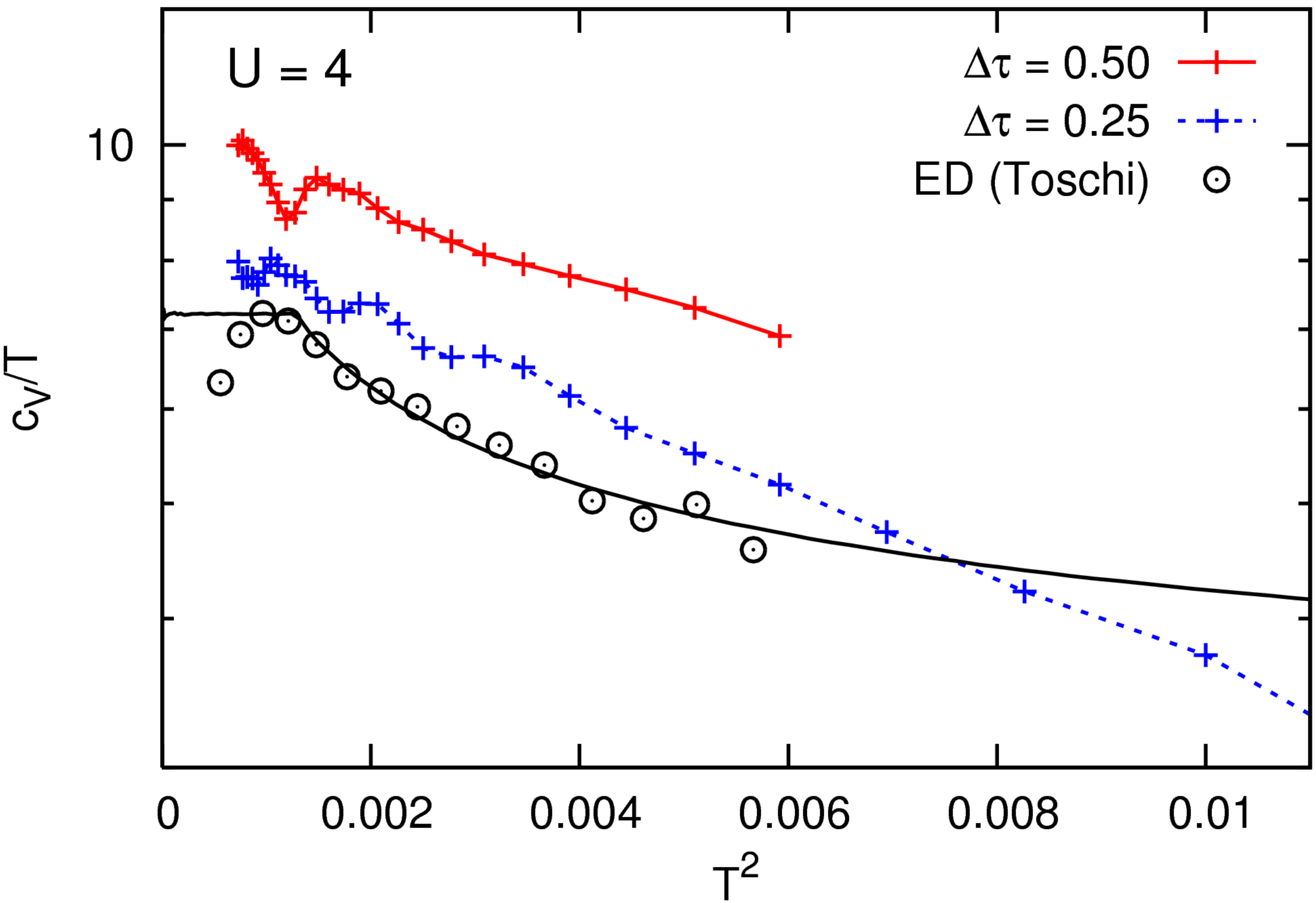

New hypothesis (for quasiparticle contribution): $c_V(T) \approx \gamma T\, e^{-aT^2}$

Now: more QMC sweeps + iterations, extended T range, smaller $\Delta\tau$

derivatives with error bars (via parabolic least-squares fits to 5-tupels)

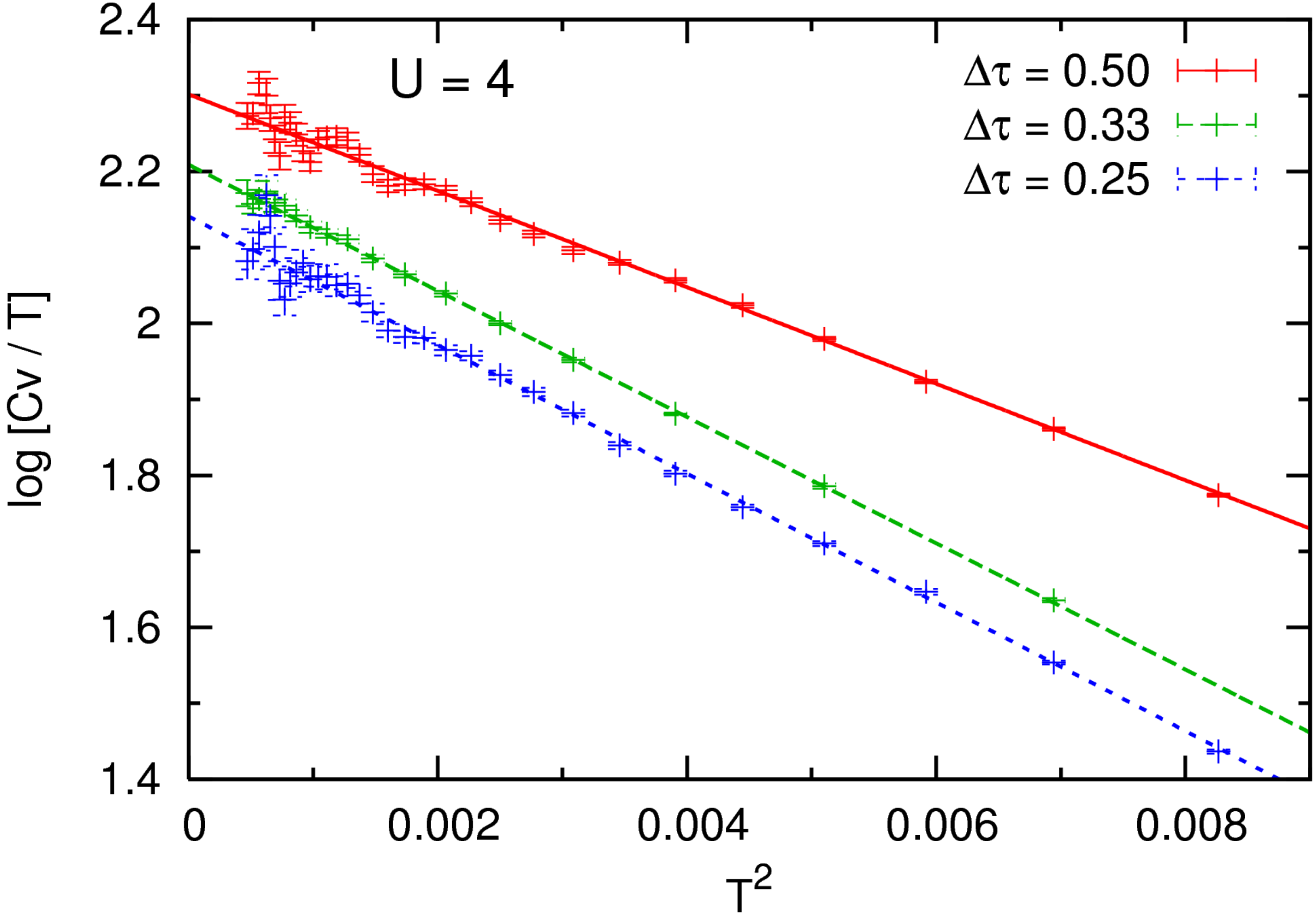

Now: more QMC sweeps + iterations, extended T range, smaller $\Delta\tau$

derivatives with error bars (via parabolic least-squares fits to 5-tupels)

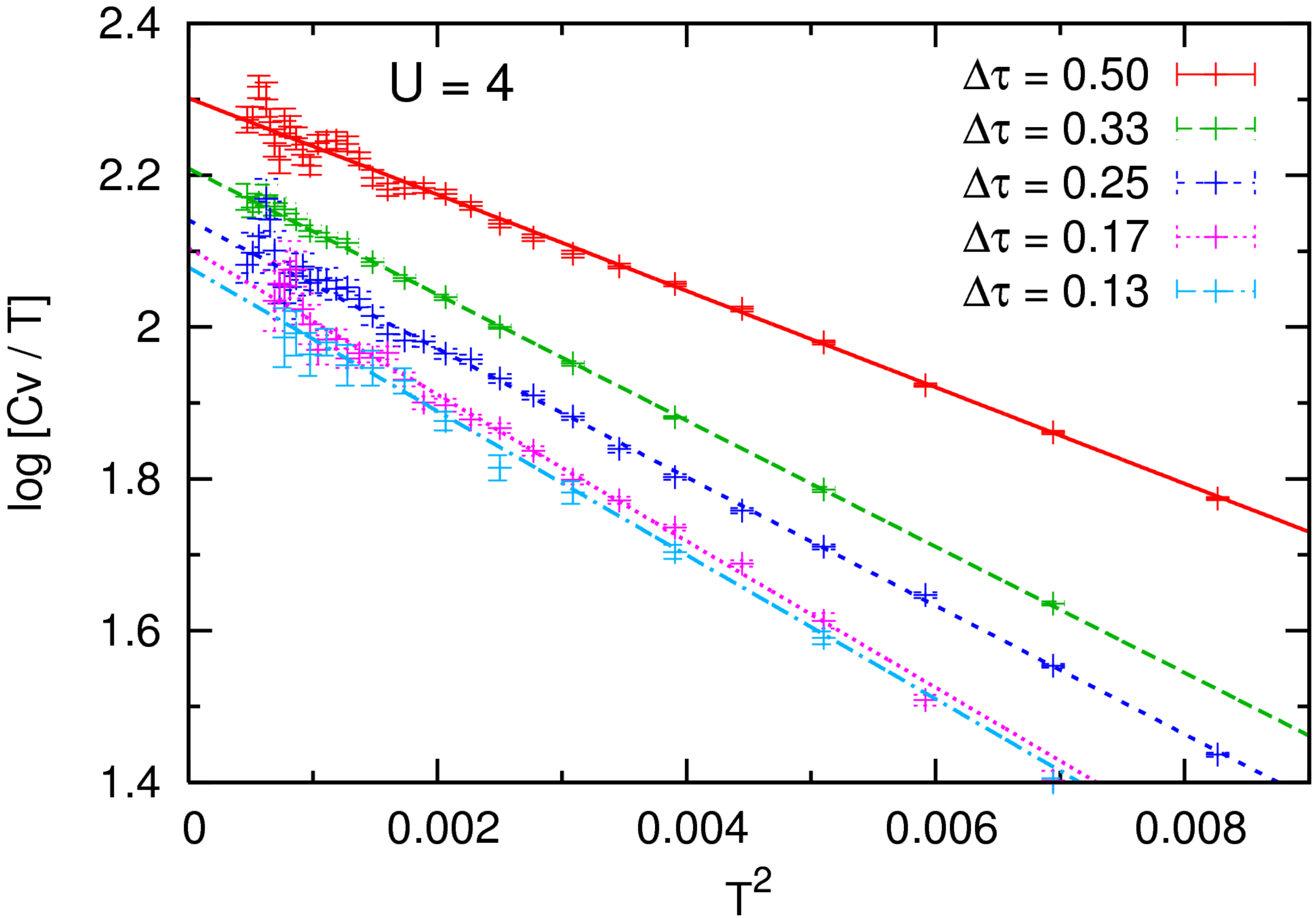

Now: more QMC sweeps + iterations, extended T range, smaller $\Delta\tau$

derivatives with error bars (via parabolic least-squares fits to 5-tupels)

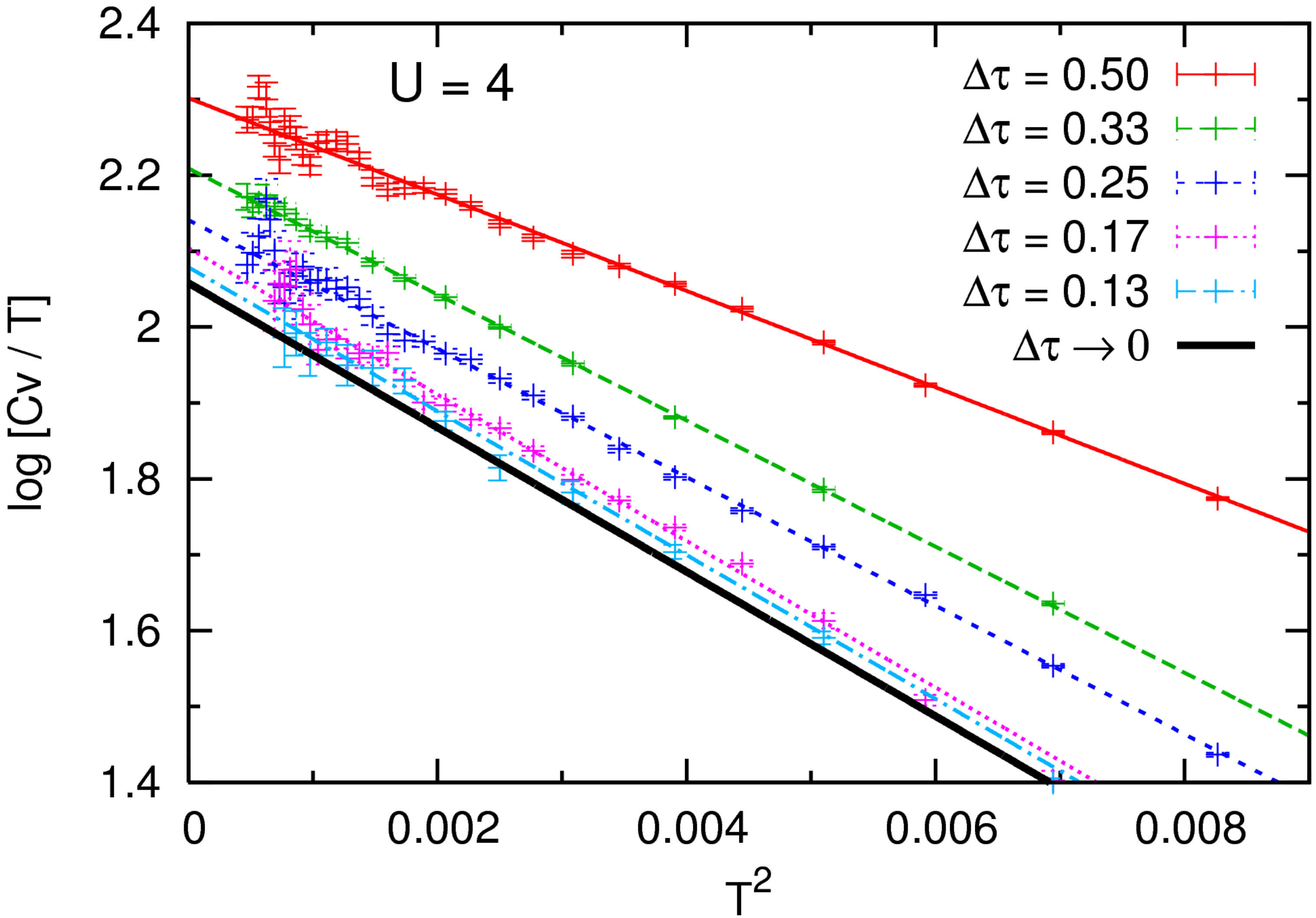

Parametric extrapolation $\Delta\tau \to 0$ is reliable

Independent check of γ via quasiparticle weight (from self-energy)

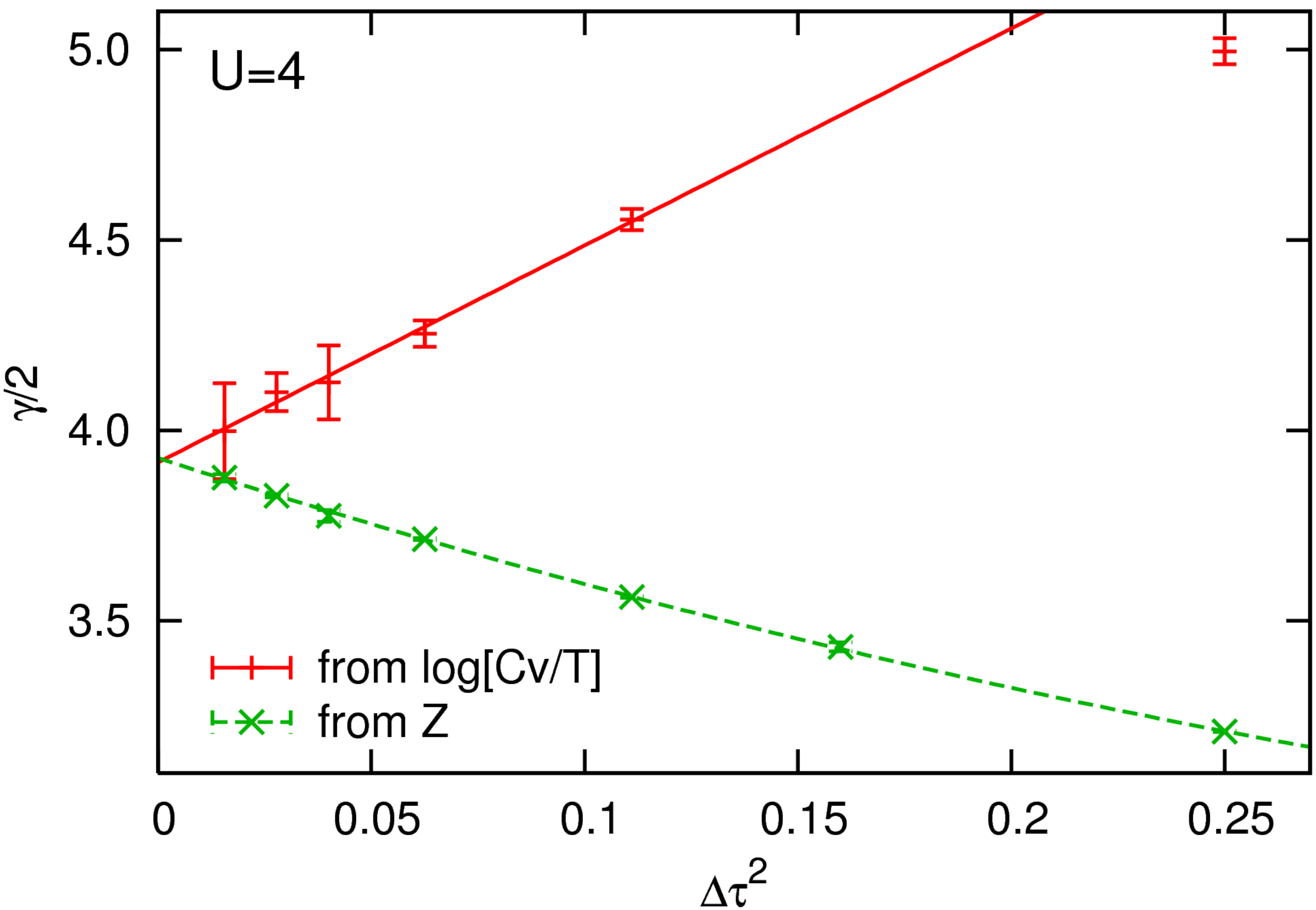

Perfect agreement (also with PRB **56**, 205120 (2007))

Now back to unscaled specific heat

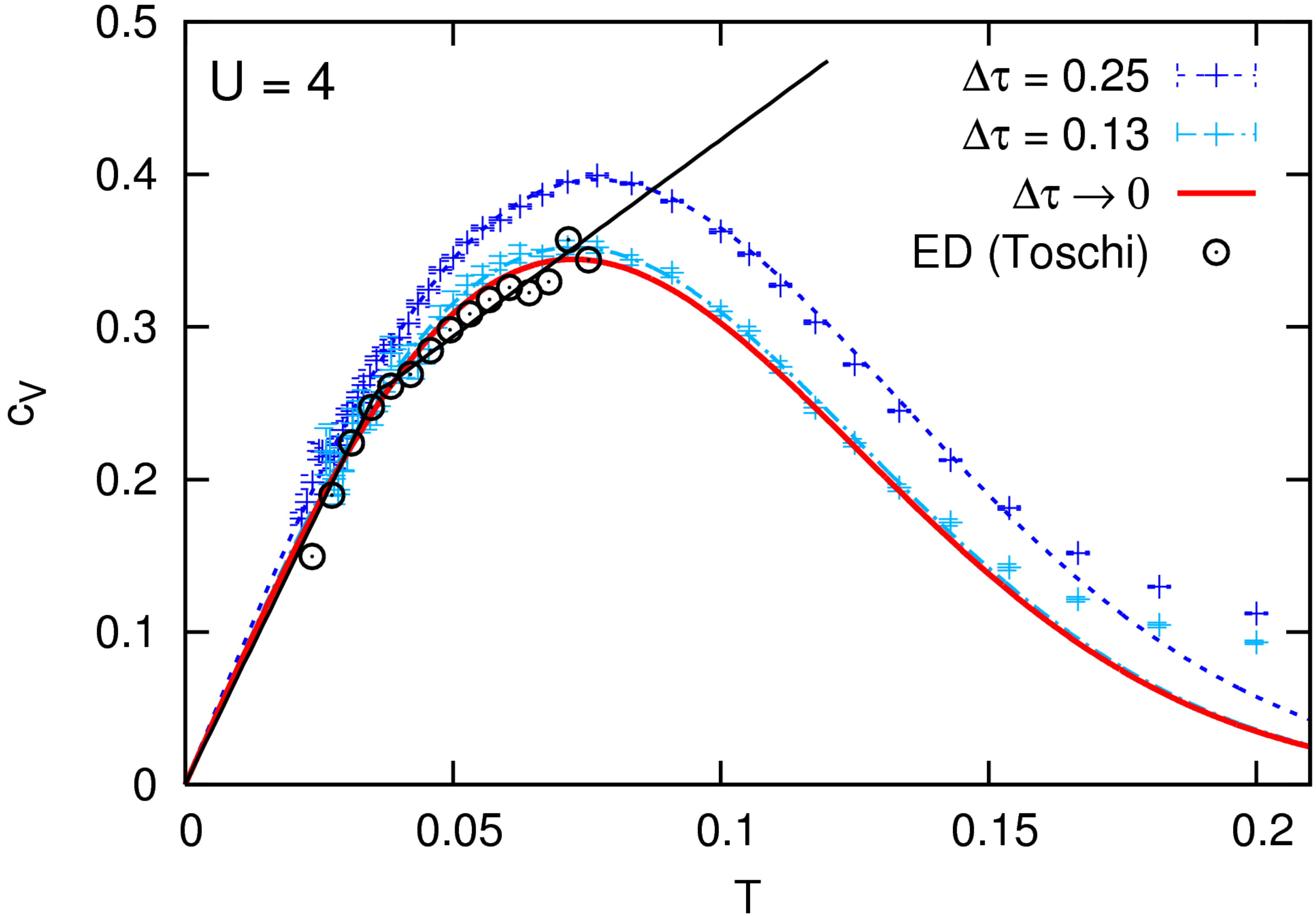

Exponential law valid far beyond fit range ($T \leq 0.084$)

ED raw data has reasonable accuracy, but fit lines are incorrect

Is entropy consistent? Yes!

$$S(T) = \int_0^T dT' \, \frac{c_V(T')}{T'} = \int_0^T dT' \, 7.83 \, T' e^{-95.14 \, T'^2} \stackrel{T \to \infty}{\longrightarrow} 0.711 \approx 0.693 \approx \log(2)$$

Interpretation: free spins at $T \gtrsim 0.2$ (in subspace without double occupancies)

Is entropy consistent? Yes!

$$S(T) = \int_0^T dT' \, \frac{c_V(T')}{T'} = \int_0^T dT' \, 7.83 \, T' e^{-95.14 \, T'^2} \stackrel{T \to \infty}{\longrightarrow} 0.711 \approx 0.693 \approx \log(2)$$

Interpretation: free spins at $T \gtrsim 0.2$ (in subspace without double occupancies)

Generalized Fermi liquid law for quasiparticle contribution to specific heat

$$c_V(T) = \frac{2\pi}{3Z} T \exp\left[-(T/T_0)^2 \right]; \quad T_0 = \frac{3\log(2)}{\pi^{3/2}} Z \qquad \text{(Bethe DOS)}$$

Single (low-frequency) qp weight $Z = \left.\frac{d\Sigma(\omega)}{d\omega}\right|_{\omega=0}$ governs c_V!

Prediction with no free parameters, to be tested at smaller/larger U.

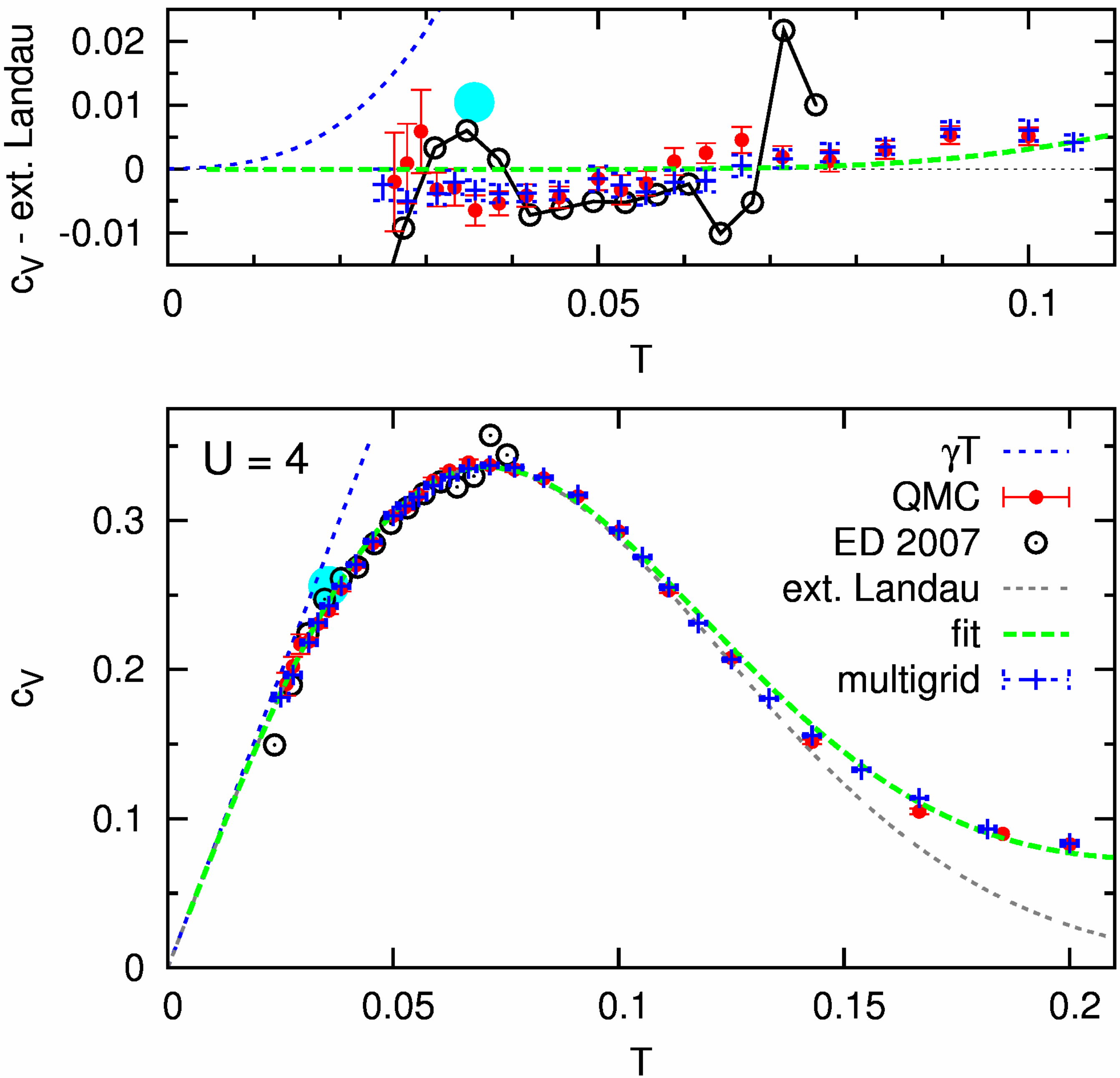

0.02
0.01
0
-0.01
c_V - ext. Landau
0
0.05
0.1
T
U = 4
γT
QMC
ED 2007
ext. Landau
fit
multigrid
0.3
0.2
0.1
0
c_V
0
0.05
0.1
0.15
0.2
T

Direct measure of "kinkiness": energy curvature

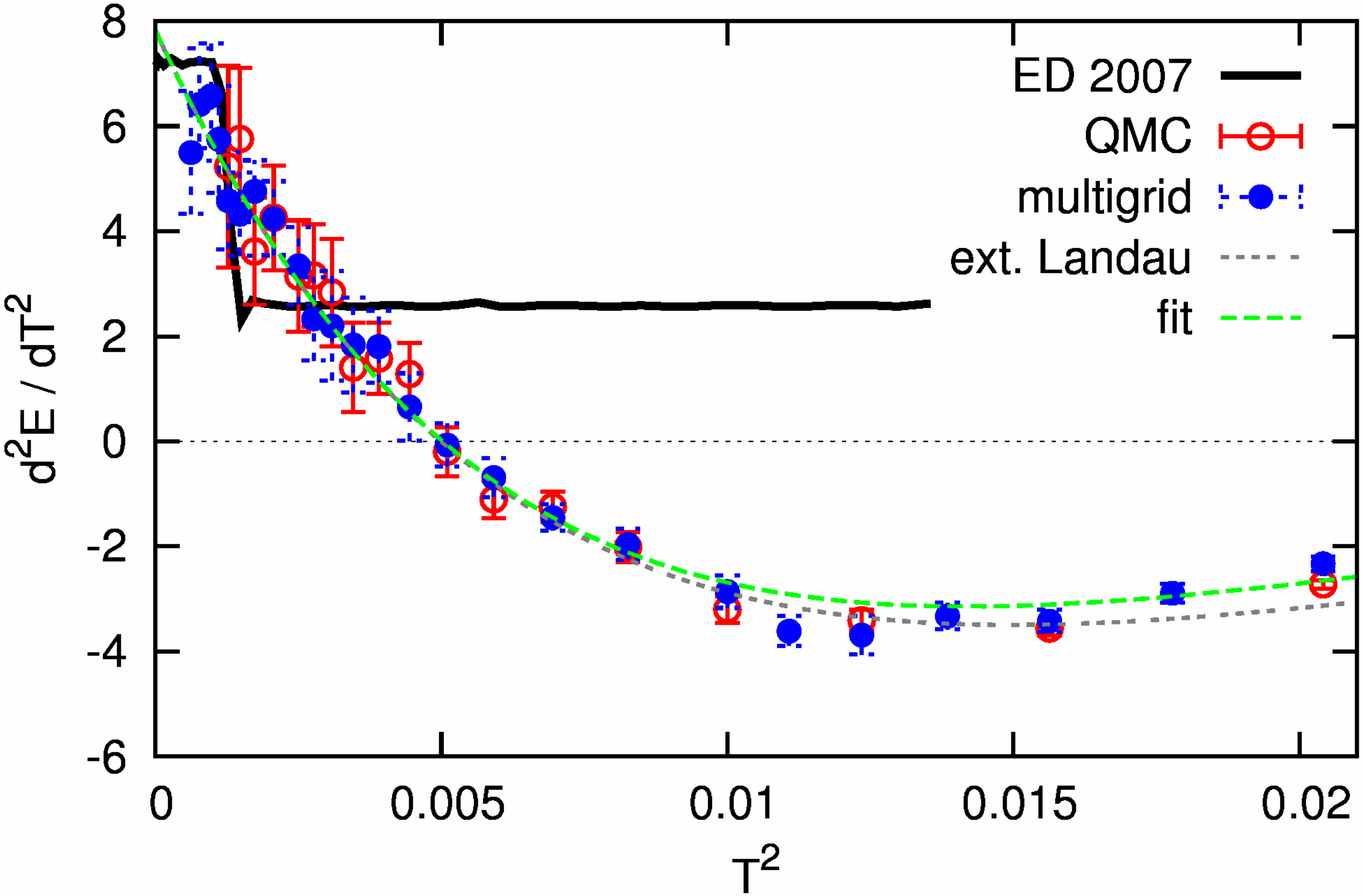

Full agreement of (multigrid) HF-QMC with extended Landau theory (parameter: Z)

Initial slope: contributions from Sommerfeld expansion + T-dependence of $\Sigma(\omega)$

Generalized Fermi liquid law for quasiparticle contribution to specific heat

$$c_V(T) = \frac{2\pi}{3Z} T \exp\left[-(T/T_0)^2 \right]; \quad T_0 = \frac{3\log(2)}{\pi^{3/2}} Z \qquad \text{(Bethe DOS)}$$

Single (low-frequency) qp weight $Z = \left.\frac{d\Sigma(\omega)}{d\omega}\right|_{\omega=0}$ governs c_V!

Prediction with no free parameters, to be tested at smaller/larger U.

Specific heat over full temperature range

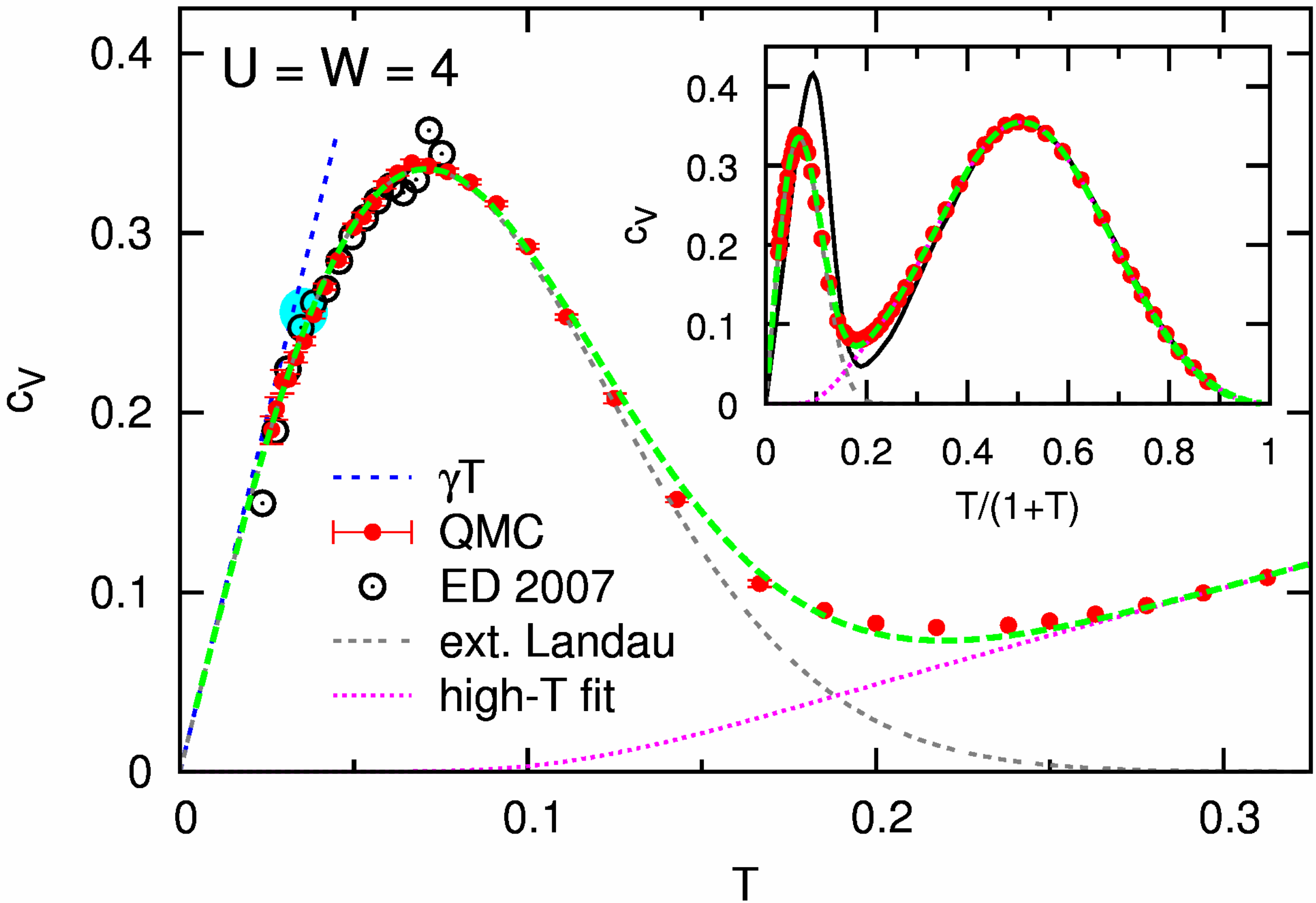

Entropy, different couplings

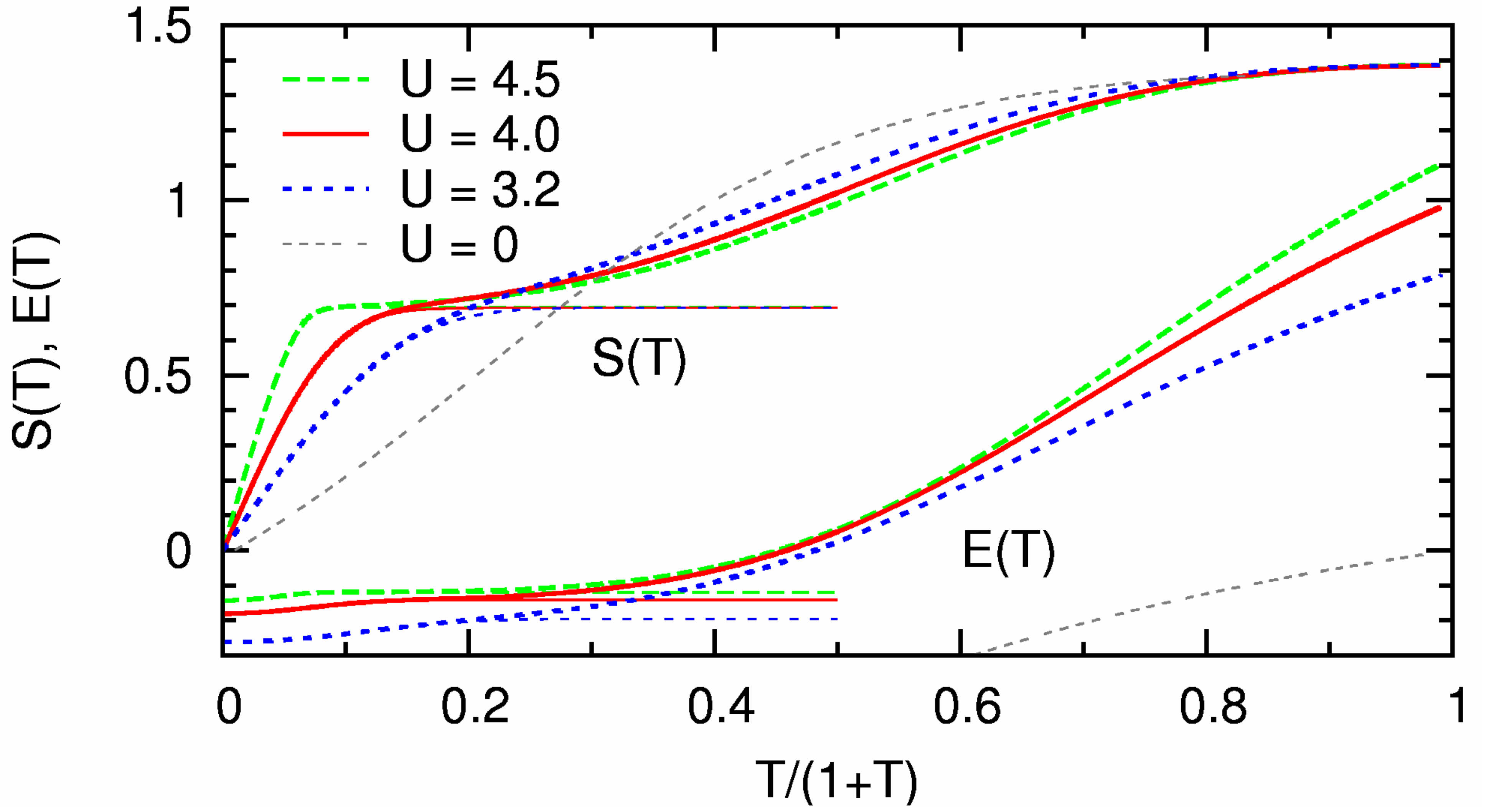

Summary

Efficiency of QMC DMFT solvers: HF-QMC competitive (for not too low T)

Unbiased Green functions and spectra from HF-QMC

Multigrid Hirsch-Fye quantum Monte Carlo algorithm

- Quasi continuous time $\rightsquigarrow$ strictly "numerically exact"
- Stable and precise even at phase boundaries
- More efficient, lower T

Spectral weight transfer at the Mott transition

Breakdown of a Fermi liquid and low-T specific heat

Summary

Efficiency of QMC DMFT solvers: HF-QMC competitive (for not too low T)

Unbiased Green functions and spectra from HF-QMC

Multigrid Hirsch-Fye quantum Monte Carlo algorithm

- Quasi continuous time $\rightsquigarrow$ strictly "numerically exact"
- Stable and precise even at phase boundaries
- More efficient, lower T

Spectral weight transfer at the Mott transition

Breakdown of a Fermi liquid and low-T specific heat

Outlook

Flavor-selective Mott transitions in ultracold quantum gases (SFB/TR 49)

Material-specific multiband calculations in context of LDA+DMFT

Summary

Efficiency of QMC DMFT solvers: HF-QMC competitive (for not too low T)

Unbiased Green functions and spectra from HF-QMC

Multigrid Hirsch-Fye quantum Monte Carlo algorithm

- Quasi continuous time $\rightsquigarrow$ strictly "numerically exact"
- Stable and precise even at phase boundaries
- More efficient, lower T

Spectral weight transfer at the Mott transition

Breakdown of a Fermi liquid and low-T specific heat

Outlook

Flavor-selective Mott transitions in ultracold quantum gases (SFB/TR 49)

Material-specific multiband calculations in context of LDA+DMFT

New: hybrid parallelization (MPI and OpenMP) . . .

Benchmarks

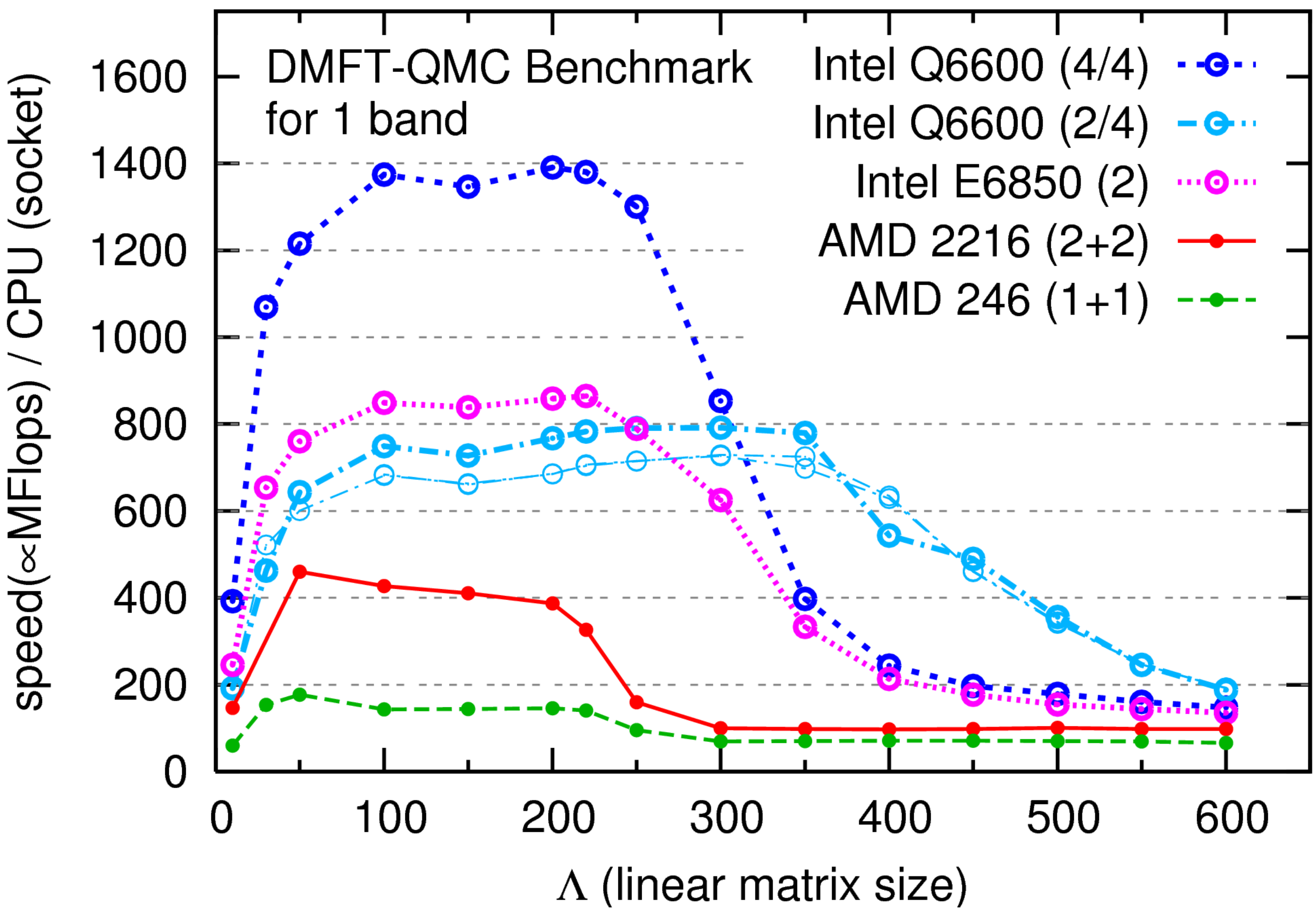

HF-QMC profits strongly from modern large-cache architectures

New (4/2008): hybrid parallelization (MPI + OpenMP)

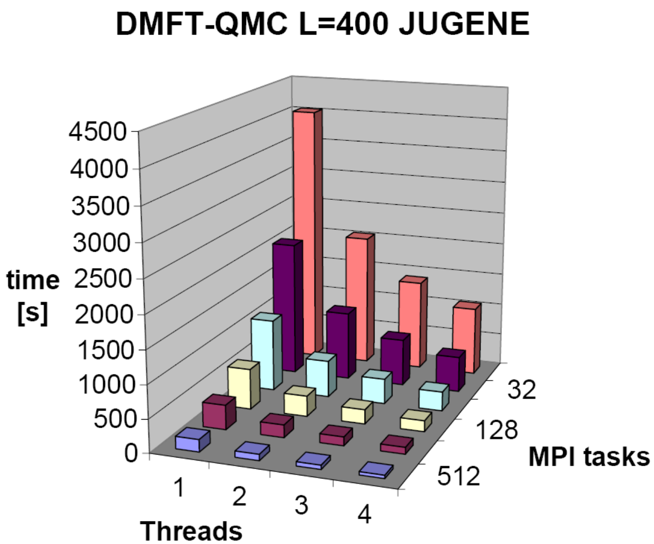

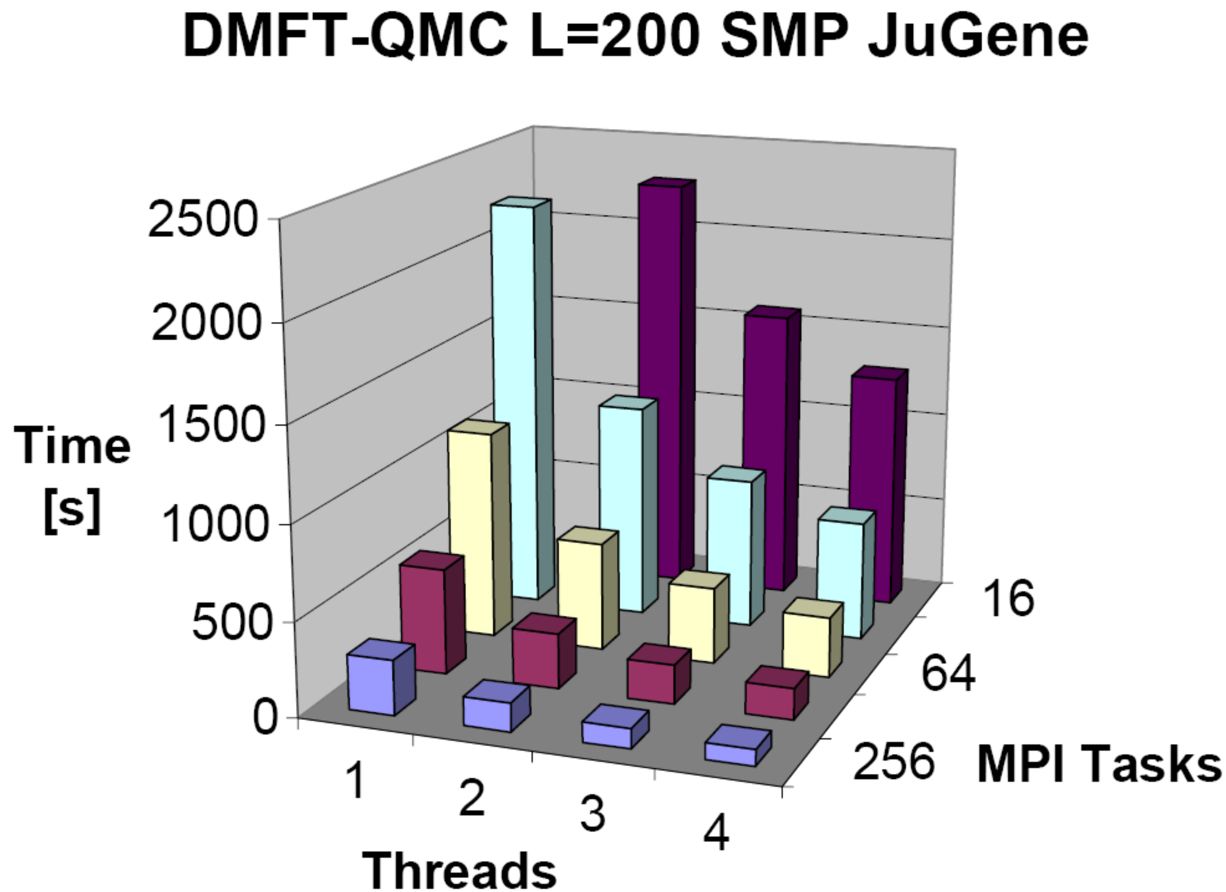

Very good scaling: speed roughly linear with number of CPU cores

Superlinear scaling on JUMP